PAUL SCHERRER INSTITUT

PSI

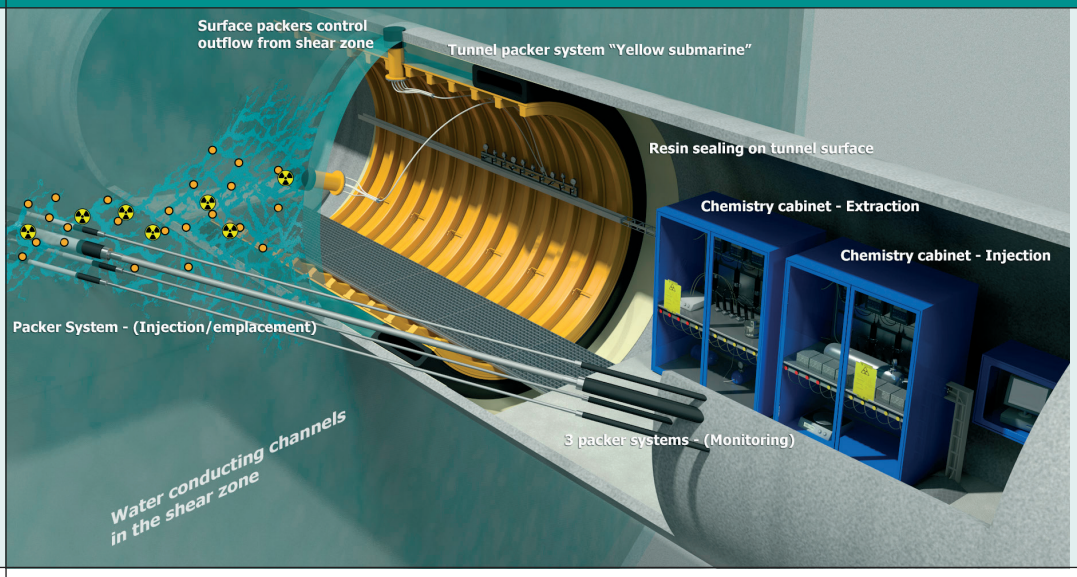

Progress Report 2012

Laboratory for Waste Management

Nuclear Energy and Safety Research Department

Cover photo
Schematic illustration of the Colloid Formation and Migration field test zone and instrumentation at the Grimsel Test Site.

Radionuclides
Colloids

3D Graphic: D. McKie, Nagra

PAUL SCHERRER INSTITUT

Progress Report 2012

Laboratory for Waste Management

Nuclear Energy and Safety Research Department

Preface

The main task of the Laboratory for Waste Management (LES) is to carry out an R&D programme to strengthen the scientific basis for radioactive waste management.

The Laboratory serves an important national role by supporting the Swiss Federal Government and Nagra in their tasks to safely dispose of radioactive wastes from medical, industrial and research applications as well as from nuclear power plants. The activities are in fundamental repository geochemistry, chemistry and physics of radionuclides at geological interfaces and radionuclide transport and retardation in geological media and man-made repository barriers. The work performed is a balanced combination of experimental activities in dedicated laboratories for handling radioactive elements, field experiments and modelling. The work is directed towards repository projects and the results find their application in comprehensive performance assessments carried out by Nagra. In particular, a major priority for LES over the next decade or so will be to contribute to the Sachplan Geologische Tiefenlagerung ("Sectoral Plan").

This report summarises the activities and results achieved in the reporting period. It is organised as an overview followed by individual reports on the six waste management group/sub-programme activities.

We gratefully acknowledge the help of the institute's management and of Nagra in our work.

Table of Contents

1 OVERVIEW

M.H. Bradbury

1.1 Introduction

The progress made in the Laboratory for Waste Management (LES) over the period from January 1, 2012 to December 31, 2012 is summarised in the first part of the report. The activities carried out in the individual groups are described in chapters 2 to 7 and are either predominantly "experimental" or predominantly "modelling" in their nature. However, there are strong interactions between groups, and between experimentalists and modellers.

1.2 General

On the 30th November 2011 the Swiss Federal Council confirmed the 6 geological siting regions proposed by Nagra in October 2008. With this decision, Stage 1 of the Sectoral Plan for Deep Geological Disposal (SGT-E1) was completed, and Stage 2 could officially begin (SGT-E2). Preparations for the Provisional Safety Analyses (PSAs) required in Stage 2 to select at least two sites each for high-level (SF/HLW) and low- and intermediate-level (L/ILW) radioactive waste repositories began already in the autumn of 2008. This selection process is anticipated to take approximately 4 years i.e. until 2016.

Over the last 2 years or so the Lab has been involved in the preparation of the data bases and scientific reports for the PSAs. The breadth and content of these reports evolved over this time period. This implied that they generally involved much more work than was anticipated at the outset. Nevertheless, the tight deadlines were met, and the reports were finished, at least as advanced drafts, before the end of 2012.

The Lab is involved in two projects in the 7th EU Framework Programme: "Processes of Cation Diffusion in Clay Rocks", (CatClay) and "Slow Processes in Close-to-Equilibrium Conditions for Radionuclides in Water/Solid Systems of Relevance to Nuclear Waste Management" (SKIN). Two further projects finished in 2012, namely, "Redox Phenomena Controlling Systems", ReCosy, and ACTINET I3, in March and September respectively. The joint programme of work with the KFKI Atomic Energy Research Institute in connection with the Schweizer Erweiterungsbeitrag DEZA/SECO agreement is still ongoing.

The main multi- and bi-lateral co-operations with external institutions and universities are summarized in Table 1.1.

Table 1.1: *National and international co-operations.*

Co-operations
Nagra Major financial contribution Various technical working groups
Multinational **7th EU FP (CatClay, SKIN)** **Mont Terri Project (Diffusion Retardation, Cement Interaction experiments)** **Grimsel Test Site (Colloid Formation Migration)**
Universities **Bern**, Switzerland (mineralogy, petrography, water chemistry, **C-14 AMS**) **Surrey, United Kingdom; EPFL, Switzerland (cement systems, molecular modelling)** UC London, United Kingdom (molecular modelling) Mainz, Germany (cement, montmorillonite) **Strasbourg, France (glass)** **Tübingen, Germany (geosphere transport)** **ETH, Zürich, Switzerland (GEMS)** **FHNW Muttenz, Switzerland (gas phase analytics)**
Research Centres CEA*, France (near- and far-field) **CIEMAT, Spain (colloids)** **EMPA*, Switzerland (cement)** IFR, HZDR*, Germany (XAS, TRLFS) **INE, KIT*, Germany (near- and far-field; TRLFS)** SCK/CEN, Belgium (clays) **UFZ*, Germany (reactive transport)** *formal co-operation agreements

Those organisations/universities with which the Lab has direct collaborative activities are marked in bold type.

Current PhD and postdoc projects being carried out in LES are listed below:

M. Bestel (PhD): "Water dynamics in compacted clay systems." Start date: September 2009. (Funding: SNF) LES participation.

B. Dilnesa (PhD): "The fate of iron during the hydration of cement". Start date: February 2008. (Funding: SNF) LES participation.

J. Poonoosamy (PhD): "Experimental benchmarks for verification and validation of reactive transport codes." Start date: October 2012. (Funding: Nagra/PSI)

A. Shafizadeh (PhD): "Porosity and structural changes at clay-cement interfaces and their relations to transport properties." Start date: September 2012 (Funding: Nagra/PSI Cross proposal, in collaboration with the Neutron Activation and Imaging Group (NUM)).

D. Soltermann (PhD): "The influence of Fe(II) on clay properties, the sorption of Fe(II) on clays and competitive sorption investigations: a combined macroscopic and microscopic study." Start date: August 2010. (Funding: SNF)

H. Wang (PhD): "A novel Micro Beam Analysis Alliance (MBA2) strategy for micro-heterogeneous systems." Start date: September 2009. (Funding: SNF) LES participation.

Dr. L. Pegado (postdoc): "Stable phase composition in cementitious systems: C-A-S-H." Start date: November 2010. (Funding: SNF-Sinergia project)

Dr. Ph. Schaub (postdoc): "Application and development of a micro diffraction synchrotron-based approach for the characterization of complex materials in radioactive waste management." Start date: September 2011. (Funding: PSI)

Dr. J. Schenzel (postdoc): "Development of C-14 AMS-based analytical methods for the identification and quantification of C-14 labeled dissolved and volatile organic compounds." Start date: July 2012. (Funding: Swissnuclear)

Dr. B. Thien (postdoc): "Development of new theoretical approaches to geochemical modelling of slow, kinetically controlled radionuclide uptake by (re)crystallizing host minerals." Start date: February 2011. (Funding: 7th EU Framework Programme, SKIN project)

Further, 1 PhD and 1 postdoc are jointly supervised by Dr. Faux (Physics Dep., Uni. Surrey, UK) and S. Churakov (LES) within an international project on: "Water transport in cements: A bottom – up approach based on NMR relaxation and imaging analysis and numerical modelling". Co-ordinator: Prof. P. McDonald, Uni. Surrey, UK.

Dr. M. del Henar Rojo-Sanz (Guest Scientist): "The fate of selenium and technetium in a cementitious repository near-field under reducing conditions." Start date: November 2012. (Funding: Verbund-projekt: Grundlegende Untersuchungen zur Immobilisierung langlebiger Radionuklide durch die Wechselwirkung mit endlagerrelevanten Sekundär-phasen. Bundesministerium für Bildung und Forschung)

N. Ver (Guest Scientist): "Experimental investi-gations of Cs, Ni, Co, Eu, Th and U sorption on Boda Claystone and Opalinus Clay." March to October 2012 (Funding: Schweizer Erweiterungsbeitrag DEZA/SECO)

As indicated above, but still worth noting, is that the majority of the funding for postdocs and PhDs comes from additional (non Nagra) external sources.

Dr. M. Tyagi completed his postdoc work in LES and is now working as a development engineer for thermodynamic software applications in the turbine division at Alstom, Baden, Switzerland. Drs. L. Aimoz and F. Hingerl were awarded their PhDs in April and July 2012 respectively. Dr. Aimoz is currently working in the instrumentation and international customer support branch with Olympus, Paris, France. Dr. Hingerl has a postdoc position at Stanford University, USA.

The refurbishment of all of the inert gas glove boxes was completed in 2012. This involved the installation of automatic visual and audio warning systems for gas pressure within the glove boxes and the replacement of the re-circulating gas purification systems. This was an expensive exercise demanded

for safety reasons. No further such refurbishments are anticipated for at least the next decade(s).

A member of LES, together with 28 other experts, was invited to participate in an "Intermediate-Evaluation of the Helmholtz-Zentrum Dresden-Rossendorf" on October 4th and 5th in Rossendorf. The evaluation was done by the Scientific Advisory Board, complemented with experts from various fields. Three topics were evaluated: Energy, Health, and Matter. LES participated in the former group.

During 2012 members of LES continued to participate in international technical review groups: (i) "SARG (SFR extension, Application Review Group)", SKB, Sweden (ii) "Expert Panel on Radionuclide Migration in Plastic Clay", Ondraf/Niras and SCK-CEN, Belgium (iii) "Near surface disposal of Category A waste at Dessel", Ondraf/Niras, Belgium (iv) International Review Group, Posiva, Finland (v) "Review panel of the Belgian programme on the behaviour of spent fuel in a cementitious environment", Ondraf/Niras, Belgium (vi) "Advisory Group for the BIGRAD Consortium: Biogeochemical gradients and radionuclide transport", Research Center for Radwaste and Decommissioning, University of Manchester, UK.

Although participation in these activities is time intensive, they are seen as an important part of LES's international co-operations and obligations.

On February 28/29, 2012, the Waste Management Program Committee met for their annual meeting. The work performed within LES and the future plans were discussed, as usual. The valuable help and advice from the members of the committee, both at the meeting, and throughout the year, are appreciated by the whole Laboratory.

1.3 Sachplan Geologische Tiefenlager, SGT (Sectoral Plan)

The major part of the work carried out in LES during 2012 was directly associated with the Sectoral Plan and the Provisional Safety Analyses (PSAs) planned by Nagra for completion in the autumn of 2013.

A relatively new methodology was used to derive sorption data bases for the four potential repository host rock types selected by Nagra i.e. Opalinus Clay (SF/HLW), and 'Brauner Dogger', Effingen Member and Helvetic Marl (L/ILW), plus the compacted bentonite backfill in a SF/HLW repository, and finally, for the lower confining units situated below the Opalinus Clay. Taking into account the combinations of different mineralogies and water chemistries resulted in a total of 84 individual SDBs being produced. Each SDB consisted of 32 radionuclides. Without the new SDB methodology, such an exercise would not have been possible.

Because of the "newness" of the SDB derivation procedure, the robustness and reliability of the sorption values chosen needed to be demonstrated. An extensive exercise was carried out in which blind predictions of sorption values were made and compared with measured ones. A total of 37 isotherm data sets were measured on the selected host rocks and MX-80 bentonite for metals with valences from I to VI, i.e. Cs(I), Co(II), Ni(II), Eu(III), Th(IV) and U(VI). The results of the comparisons were very satisfactory.

Model calculations have been carried out to define the composition and characteristics of inter-particle porewaters in compacted bentonite in the parameter range (ε_{bulk} = 36% to 48% and I ~ 0.3-0.8 M). The bulk porosity is the total volume of water incorporated in bentonite (including interlayer, diffuse double layer and inter-particle water) divided by the total volume of the bentonite. The anion accessible porosity (ε_{anion}) defines the volume of inter-particle water i.e. "free" water that is not subject to electrostatic forces in the model. ε_{anion} defines the fraction of water in which aqueous-solid chemical reactions obey classical mass action laws. Because of the soluble minor minerals present in bentonite (e.g. NaCl, gypsum), and the complex equilibria involved, variations of ε_{anion} may have a potentially significant impact on the porewater composition.

In the development of the updated SDBs for cement, particular emphasis was placed on assessments of the influence of processes such as: carbonation caused by the generation of CO_2 during the degradation of organic waste materials, the dissolution of metallic waste materials, cement degradation, and the complexation of radionuclides with isosaccharinic (ISA) and gluconic (GLU) acids. Twenty four separate sorption data bases were produced taking the above processes into account.

Maximum solubilities for ~30 radionuclides have been evaluated for the reference compacted MX-80 and concrete porewaters defined for Stage 2 of the Sectoral Plan using the PSI/Nagra 07/12 Thermodynamic Data Base (TDB). The compacted bentonite porewater used was that calculated to prevail after 10'000 years of contact time between the bentonite barrier material and the Opalinus Clay host rock. The concrete porewater was a high pH solution (pH 12.5) characteristic for a situation in which portlandite is still the dominating solid phase.

Since the extended Archie's relationship (e-Archie) is used extensively to compile diffusion data for the PSAs, there is an ongoing activity designed to establish a wide experimental basis justifying its application. To this end, new diffusion measurements on fresh samples of Opalinus Clay and "Brauner Dogger" from the deep borehole in Schlattingen using HTO and $^{36}Cl^-$ as tracers were completed. The measured diffusion coefficients were in good agreement with those estimated using e-Archie, providing additional confidence in its use. The results from all of the diffusion measurements carried out so far have been summarised in a report together with a compilation of effective diffusion coefficients for the potential Swiss host rocks.

Reactive transport simulations with the coupled code OpenGeoSys-GEMS have been used extensively to model the in situ conditions in the near-field of SF/HLW and L/ILW repositories and their evolution in time and space. For example, a sensitivity study was performed to understand the influence of an optional low pH concrete liner on the SF/HLW near-field. Reactive transport simulations, which included kinetically controlled precipitation/dissolution reactions, have also been applied to simulate the geochemical evolution at interfaces in the Engineered Gas Transport System (EGTS).

Under the assumptions used in the calculations, it was found that the concrete layer associated with the EGTS would degrade completely in a few thousand years due to the alkali-silicate-aggregate reactions (ASR). These ASR reactions resulted in the dissolution of cement minerals, the re-crystallization of C-S-H phases with low Ca/Si ratios, the neo-formation of clay minerals and a strong decrease in pH to values of around 10. An alternative scenario in which the reactive quartz in the concrete was replaced by carbonates (calcite), effectively prevented the ASR reactions, and most of the concrete was still buffered by portlandite (pH = 12.5) after more than three thousand years.

Some 3D simulations on the disposal of high burn up fuel were carried out using the Comsol-Multiphysics code. With the constraints that temperatures should remain below 100°C in the bentonite buffer and below 85°C in the Opalinus Clay, the calculations showed that, independent of the water content and density of the bentonite, the heat released from canisters must be below 1500 W/canister in order to avoid detrimental effects on the clay barrier system.

1.4 Foundations of repository chemistry

Most of the experimental data in the PSI/Nagra chemical thermodynamic data bases were obtained at room temperature, whereas the ambient temperature of the host rock around a SF/HLW repository is expected to be ~50°C, and the maximum temperature at the surface of a waste container may be as high as 160°C. An isocoulombic extrapolation method is being developed based on the observation that reactions comprising of equal numbers of like-charged aqueous ions on both sides of the reaction have negligible entropy and heat capacity effects. As a consequence, extrapolations to higher temperatures can be simply made using only the equilibrium constants of such isocoulombic reactions measured at room temperature. The programming language Python was used to create a set of modules to extract those reactions in the PHREEQC version of the PSI/Nagra 07/12 TDB for which enough data are known for extrapolation to higher temperatures. The method appears to be promising, and provides an efficient tool for assessing the potential of the isocoulombic approach to extrapolate thermodynamic data to higher temperatures.

Newly developed porewater chemistry models for compacted bentonite include the montmorillonite in mineral dissolution and transformation processes. (A similar model is under development for Opalinus Clay based on illite.) A literature review focused on the question of the extent to which clay mineral dissolution – precipitation processes can be reliably described by thermodynamic equilibrium models. While the situation for kaolinite is clear, there still

remains a question mark surrounding the "equilibrium thermodynamic values" published for illite, smectite and illite-smectite interstratifications.

The sorption of Se(IV,VI) on natural pyrite over time periods of up to 8 months under anaerobic conditions was investigated using μ-XRF and μ-XANES techniques at the SLS, and EXAFS at the DUBBLE beamline (ESRF). This study showed that pyrite can readily take up and reduce dissolved Se(IV) and Se(VI). The complete conversion to sparingly soluble Se(0) requires a few months ageing time at room temperature.

The work on the uptake mechanisms of iodide (I^-) by a cement mineral (AFm-SO_4, "monosulphate") was completed. This study provided thermodynamic data which could be used to model the fate of ^{129}I in the cementitious near-field of a radioactive waste repository. An important conclusion drawn was that although the AFm-SO_4 end-member is much more stable than the AFm-I_2 end-member, nevertheless AFm-SO_4 can act as a sink for ^{129}I, even at very low iodide concentrations.

The irreversible uptake of trace elements by minerals is a potentially important consideration in the safety assessment of radioactive waste repositories. Two models describing trace element uptake in growing minerals from an aqueous solution were unified into a "merged" model and included in the GEM-Selektor v.3 code. The "merged" model can be used to describe the trace element uptake during mineral precipitation in aqueous solutions with changing composition, and fully accounts for the aqueous solution speciation, as well as for depletion effects which may occur on long time scales. Further improvement will account for tracer in-diffusion, the effects of specific surface area and surface roughness.

1.5 Repository near-field

1.5.1 Clay systems

In the compacted bentonite the porewater will contain dissolved impurities from many sources, as well as mixtures of radionuclides. Competition between the dissolved elements/radionuclides can potentially result in a reduction in sorption values. An estimate of the extent to which sorption values may be reduced was examined in a case study using the 2SPNE SC/CE sorption model and solubility data in a bentonite porewater. The sorption model calculations indicated that the influence of competition on trace element sorption values was to reduce them by approximately one order of magnitude for bi- and trivalent elements, and two orders of magnitude (max.) for tetravalent elements. In almost all cases the sorption remained significant due to uptake on the montmorillonite "weak sites" which have a high capacity for the bivalent and trivalent elements, and, because the low solubilities ($< 10^{-6}$ M) of tetravalent elements does not lead to sorption saturation of strong sites.

There are large quantities of iron in a SF/HLW repository, and it is important to know how this iron behaves, and what the influence on PA may be. As part of a PhD study the sorption of Fe on montmorillonite under reducing conditions is being studied. EXAFS and Mössbauer spectroscopy, combined with macroscopic sorption experiments and modelling, were applied to investigate the sorption mechanism of Fe(II) on a homo-ionic Na synthetic iron free montmorillonite (Na-IFM) i.e. a montmorillonite without any structural iron. (Structural Fe in a natural montmorillonite interferes strongly with EXAFS measurements.) The Fe(II) uptake at trace concentration ($\sim 10^{-7}$ M) as a function of pH is typical for bivalent transition metals. Sorption edges and isotherms could be modelled with the 2SPNE SC/CE sorption model. The EXAFS measurements were consistent with the strong/weak site hypothesis in that the iron surface complexes at the high loadings (weak sites) exhibit a stronger structural disorder and are less well crystalographically defined than iron sorbed at low loadings (strong sites). Mössbauer spectroscopy measurements confirmed that Fe is predominantly present as Fe(II) at the Na-IFM surface.

In the TRAPHICCS programme on pure clay minerals the in-diffusion of U(VI) in compacted montmorillonite was studied with the aim of investigating the influence of speciation on radionuclide transport. Discrepancies between the experimental results and the modelling were in evidence.

For the diffusion measurements foreseen in the future for ^{60}Co(II), ^{65}Zn(II) and ^{152}Eu(III) on compacted illite, a new type of diffusion cell was developed and tested. The problems of tracer sorption on filters, and the diffusive resistance of the filters, were avoided. The mechanical confinement of the small compacted illite sample was provided by an organic polymeric membrane with a thickness of ~100 µm.

Repository systems have several interfaces where there are strong chemical gradients e.g. particularly the cement-clay interface. Due to dissolution-precipitation reactions occurring at these interfaces, porosity changes can result in changes in the transport properties of solutes and gases. In order to achieve a better understanding of dissolution-precipitation reactions, and their effect on solute transport, two new PhD projects were started in 2012. The first aims at investigating the relationship between porosity, structural changes and transport properties, and the second aims at providing experimental benchmarks for the verification and validation of reactive transport codes.

1.5.2 Cement

Low molecular weight (LMW) organic compounds containing ^{14}C may be formed during the anaerobic corrosion of steel in a cementitious near-field. In order to properly define the ^{14}C source term, information is required on the chemical nature and long-term chemical stability of such organic compounds.

Analytical techniques such as gas chromatography coupled with ion mass spectrometry for the volatile LMW organics, and high performance ion exclusion chromatography coupled with ion mass spectrometry and conductivity detection for oxidized hydrocarbons, are under development.

Anoxic corrosion tests were carried out by immersing iron powder in either acidic (pH 3) or alkaline (pH 13) solutions and showed that volatile hydrocarbons do form. Further, a first series of batch-type corrosion experiments using different types of iron powders were performed with the aim of determining the identity of the oxidized LMW hydrocarbons produced. Quantification of the selected carboxylic acids was achieved by applying deuterated forms of the compound being analysed as internal standards. The high initial concentrations of acetic- and formic acid, along with the presence of other carboxylic acids at trace concentrations, was tentatively assigned to the oxidative pre-treatment of the iron powders using HCl in which the carbon released due to iron dissolution was oxidized. Pre-treatments with HCl will not be used further.

Future studies will focus on corrosion experiments in hyperalkaline cement porewaters, bentonite pore-water and Opalinus Clay groundwater.

The uptake of Np(IV) and Np(V) by hardened cement paste (HCP) was found to exhibit fast kinetics, to be high (R_d values ranging between 7×10^4 and 2×10^6 L kg^{-1}) and very similar to that previously observed on calcium silicate hydrate (C-S-H) phases with high C:S ratios under the same conditions. The wet chemistry data agree with the conclusions drawn from earlier EXAFS studies in that the C-S-H phases are the component in HCP controlling the Np(IV/V) uptake.

The luminescence spectroscopy investigations on U(VI) uptake by cementitious materials were continued in 2012 on U(VI) loaded C-S-H phases and HCP using direct laser excitation at cryogenic temperatures (~20 K) instead of broadband laser excitation. It could be shown that U(VI) loaded HCP exhibited two sets of emission bands very similar to those found for C-S-H phases, indicating the presence of two types of U(VI) sorbed species in HCP. The current interpretation is that one corresponds to a U(VI) surface complex, whereas the other is indicative of U(VI) incorporated into the C-S-H structure.

Alkali-silicate-aggregate reactions (ASR) are one of the most important deterioration mechanisms in concrete systems all over the world. Micro-XRD studies were carried out with the aim of identifying the product(s) formed during the course of ASR in concrete. Powder patterns from different points along reaction veins, and in different veins, were found to be identical. However, finger-print-matching using crystallographic databases did not succeed in identifying the phase, indicating that the structure had not yet been determined. Several possible structural models of the ASR phase were developed, but need to be confirmed.

On the molecular modelling side, the influence of aluminium substitutions on alkali and alkali earth ion sorption by C-S-H is being investigated. The mechanism of aluminium incorporation into the surface of C-S-H phases is being studied with periodic Density Functional Theory (DFT) calculations. The C-S-H phase is modelled based on a single structural layer-module of the natural mineral tobermorite with so-called silicate "dreierketten" chains of alternating one bridging and two pairing tetrahedra on both surfaces. There is strong computational evidence that Al in C-S-H sits preferentially in bridging positions, in agreement with experimental information.

1.6 Repository far-field

Diffusion measurements with ^{60}Co(II), ^{65}Zn(II) and ^{152}Eu(III) on OPA were performed after a 6-month pre-equilibration time with the appropriate porewater using a filter-free in-diffusion technique. These newly measured diffusion profiles did not exhibit the "two slope" shape measured earlier in samples for which only a short pre-equilibration phase of few weeks was used. In order to help in the interpretation of the experimental results, and to devise an improved protocol for forthcoming experiments, generic modelling studies were performed taking into account potential experimental uncertainties. Special attention was paid to estimating the effects of sorption competition (Co(II), Zn(II), Fe(II), Mn(II)), possible gradients between the diffusion cell reservoir water composition and the "expected" clay porewater composition (e.g., pH, Fe), the duration of the pre-equilibration phase and the influence of concentration (carrier concentrations in the tracer source).

The ionic strength of the saturating/contacting solutions (1, 0.3 and 0.03 M NaCl) in diffusion experiments was varied in order to test whether surface enhanced diffusion is an important process or not. The measurements showed a slightly reduced in-diffusion tracer profile at higher ionic strengths for both ^{65}Zn(II) and ^{60}Co(II), possibly indicating that sorption enhanced diffusion might play a role. Modelling carried out with MCOTAC using two activity coefficient models, Davis and SIT, predicted different penetration profiles already at an ionic strength of 0.3 M. For a given set of transport parameters, both activity coefficient models predicted a deeper penetration of the tracers into the sample at higher ionic strengths, contrary to the experimental observations.

The "bottom-up" modelling approach, based on the premise that radionuclide uptake in complex mineral/groundwater systems can be quantitatively predicted from a knowledge and understanding of the mechanistic sorption processes on clay minerals, and the models developed to describe them, has been successfully applied to Opalinus Clay and MX-80 bentonite. It is intrinsically desirable to test this approach on other argillaceous rocks. As part of the Schweizer Erweiterungsbeitrag DEZA/SECO agreement with Hungary (co-operation between PSI/LES and KFKI Atomic Energy Research Institute), sorption isotherms for Cs, Ni, Co, Eu, Th and U were measured on Boda Claystone (Boda) samples in a synthetic porewater. Blind predictions of the isotherms were made using the 2SPNE SC/CE model and the PSI/Nagra 07/12 thermodynamic data base. The predictions of the sorption model were generally good, and in those cases where there were discrepancies, plausible explanations could be found and improved modelling procedures suggested.

One of the main aims of the DR field experiment carried out at the Mont Terri Rock Laboratory was to derive anisotropy ratios from the diffusion profiles measured in the over-cored samples. The results obtained so far indicate slightly larger anisotropy factors for HTO and ^{22}Na (~5) compared with anions (~4 for I and ~3 for Br). Such differences were not seen in earlier laboratory studies where values of ~4 were measured for both HTO and ^{36}Cl. Interestingly, recent pore-scale modelling studies indicate lower anisotropy ratios for anions compared to water tracers which is consistent with the field results.

In the DR-A field experiment, started in November 2011, the intention is to measure the effects of a change in the ionic strength of the artificial porewater in a packed-off borehole interval on the transport of various ions, and whether these effects can be modelled. The initial part of the DR-A experiment was very similar to previous experiments i.e. an artificial porewater matching as closely as possible the in situ porewater, was spiked with several tracers. LES is the co-ordinator of the modelling work in which several modelling groups will first try to

model the diffusion of non-sorbing and linearly sorbing tracers as well as Cs which undergoes multi-site cation exchange. The outcome of these modelling tasks will be used to compare the ability of the different models to cope with the various aspects of the experiment for given sets of generic parameters and processes. The next tasks will include modelling the effects of the perturbation: a doubling of the ionic strength of the artificial porewater was involved in this experiment.

The activities within the Grimsel Long Term Cement Studies involve the cross-benchmarking of geochemical setups and reactive transport simulation approaches against experimental data and other transport codes. Several modelling teams are applying state-of-the-art geochemical models to re-appraise the earlier simulations on the long term changes occurring in rocks in contact with a hyperalkaline solution at the Maqarin natural analogue.

Within the co-operation agreement between UFZ, Leipzig, Germany, and LES, the Richards flow module has been added into OpenGeoSys-GEMS coupling. With this module it has become possible to simulate geochemical reactions in partially saturated media. Furthermore, the coupled OpenGeoSys-GEMS version was parallelized with a hybrid algorithm based on MPI and OMP threads. This enables a much more effective simulation of 2D/3D systems on high performance computers.

Table 1.2: *LES Organigram, December 2012*

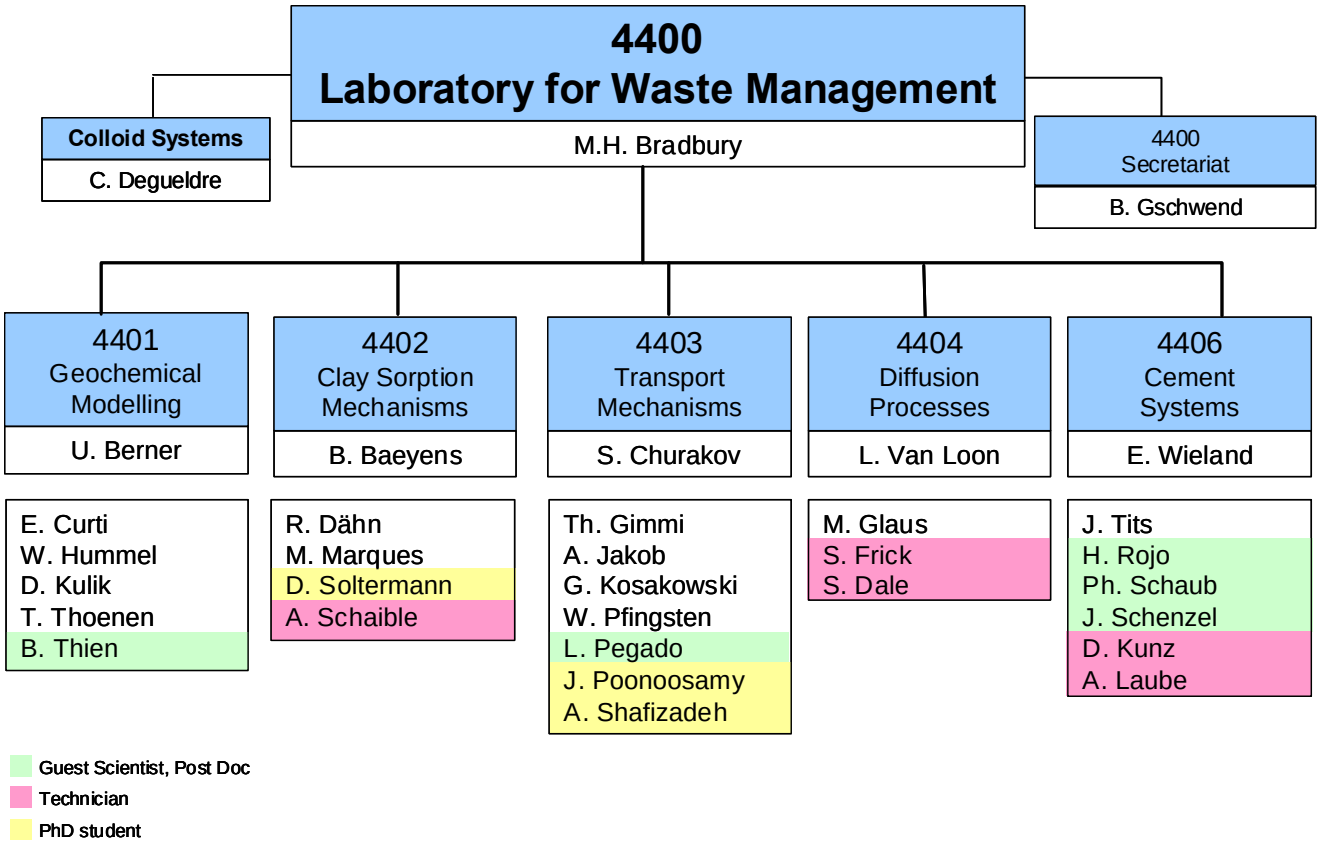

2 GEOCHEMICAL MODELLING

W. Hummel, U. Berner, E. Curti, D. Kulik, T. Thoenen, L. Aimoz (PhD), B. Thien (postdoc)

2.1 Overview

A large part of the Geochemical Modelling Group's work in 2012 was related to the Swiss Sectoral Plan for deep geological disposal. This work comprised of model calculations for radionuclide solubilities and contributions to two Nagra Technical Reports on the geochemical evolution of the near-field of planned geological repositories for spent fuel / high level waste and intermediate level waste. Further topics related to the Swiss Sectoral Plan explicitly mentioned here are:

- A new tool for extrapolating thermodynamic data to elevated temperatures via isocoulombic reactions.
- First results of an ongoing literature review on the status of the thermodynamic data for clay minerals.
- Bentonite porewater calculations for varying porosities and salinities.

Progress in the field of trace element behaviour was made in the framework of a now completed PhD work and a post doc project (L. Aimoz and B. Thien respectively) and an investigation into the behaviour of the dose determining element selenium.

- Thermodynamic properties of AFm-I_2 and of its solid solution with AFm-SO_4 were evaluated based on solubility and sorption experiments in aqueous solutions and modelled using GEMS.
- A kinetic model of trace element uptake in host minerals was implemented in GEMS and tested with experimental data on Sr, Cd, Co and Mn co-precipitation with calcite.
- Evidence for reductive sorption of Se(IV/VI) by natural pyrite was obtained from XAS/XRF investigations.

2.2 Work related to the Sectoral Plan

2.2.1 Evaluation of maximum radionuclide solubilities and comparison with recommendations given in earlier studies

Maximum solubilities for about 30 different radionuclides have been evaluated for the reference compacted MX-80 and concrete porewaters defined for Stage 2 of the Sectoral Plan (BERNER, 2009; 2011; BERNER & KOSAKOWSKI, 2011; 2011a) using an updated version of the PSI/Nagra 07/12 Thermodynamic Data Base (TDB) (THOENEN, 2012). The MX-80 porewater composition used was that calculated after 10'000 years contact time between the bentonite barrier material and the Opalinus Clay host rock (BERNER & KOSAKOWSKI 2011). The concrete porewater is a high pH solution (pH 12.5) characteristic of a situation in which portlandite is still dominating the porewater (BERNER & KOSAKOWSKI, 2011a; KOSAKOWSKI & BERNER, 2011).

A similar evaluation was made some 10 years ago for the corresponding reference porewater compositions at that time (BERNER, 2002; 2003).

Comparison of solubilities in compacted MX-80 porewater:

- Similar solubilities, within a factor of 10, were evaluated for

Co, Ni, Se, Sr, Nb, Mo, Tc, Pd, Ag, Sm, Eu, Ho, Pb, Ac, Pa, Np, Am and Cm

- A factor between 10 and 100 times higher solubilities were evaluated for

Zr, Sn, Ra and U

- A factor between 10 and 100 times lower solubilities were evaluated for

I, Po, Th and Pu

Comparison of solubilities in concrete porewater: (several nuclides were not included in the earlier study)

- Similar solubilities, within a factor of 10, were evaluated for

Co, Ni, Se, Sr, Mo, Sn, Sm, Eu, Ho, Ac, Th, U, Np, Pu, Am and Cm

- A factor between 10 and 100 times higher solubilities were evaluated for

Pa

- A factor between 10 and 100 times lower solubilities were evaluated for

Zr, Tc, I, Po and Ra

For the majority of nuclides the evaluated solubilities were similar to within a factor of 10, which in most cases is within the uncertainty band related to such evaluations. For a few nuclides, particularly in the MX-80 porewater, the application of the up-dated data base led to higher solubilities, but for several nuclides we were able to establish significantly lower solubilities, particularly in the concrete porewater.

2.2.2 Bentonite porewater calculations

Over the past two years, model calculations have been carried out in the framework of the Sectoral Plan to define the composition and characteristics of inter-particle porewaters in compacted bentonite. In the first series of calculations a high degree of compaction was assumed, corresponding to a bulk porosity (ε_{bulk}) of 36%. This degree of compaction must be regarded as an upper limit of what is technically feasible, and lower degrees of compaction (up to a bulk porosity of 48 %) need to be considered for realistic calculations.

The bulk porosity is equivalent to the total volume of water incorporated in the bentonite (interlayer, diffuse double layer and inter-particle water) divided by the total volume of the bentonite. The anion accessible porosity (ε_{anion}) defines the volume of inter-particle water. This is “free” water that is not subject to electrostatic forces in the model. Conventional complexation and saturation equilibria can be applied only in such anion accessible water. Therefore, ε_{anion} defines the fraction of water where aqueous-solid chemical reactions obeying classical mass action laws apply. However, ε_{anion} depends both on the clay compaction and the ionic strength of the reacting porewater, and may vary considerably in the parameter space of interest (ε_{bulk} 36% to 48% and I ~ 0.3-0.8 m). The sensitivity of anion accessible porosity to ionic strength is due to the decrease in the thickness of the diffuse double layer (DDL) with increasing electrolyte concentration. At high ionic strengths the volume of charge balanced inter-particle solution (and thus ε_{anion}) increases due to the reduction in the extent of the DDL. Because of the soluble minor minerals present in bentonite (e.g. NaCl, gypsum), and the complex equilibria involved, variations of ε_{anion} may have a potentially significant impact on the porewater composition.

In a second series of bentonite porewater calculations, the combined effect of compaction and ionic strength was explored. A series of calculations were carried out to model the interaction of MX-80 bentonite (compacted to 48% bulk porosity) with either a low-salinity or a high-salinity Opalinus Clay porewater (OPAw) and then compared with the results previously obtained assuming 36% bulk porosity. In these calculations, an empirical relation describing the dependence of anion accessible porosity on bentonite compaction and ionic strength (VAN LOON, 2012) was used iteratively in conjunction with the PSI/Nagra 07/12 TDB (THOENEN, 2012). An increase in the bulk porosity from 36% to 48% was found to result in considerably higher anion accessible porosities (from 5% to 11% for low salinity OPAw; from 5% to 14.5% for high salinity OPAw), which implies a two- to three-fold larger water volume available for the dissolution of the NaCl inventory. However, the resulting decrease in ionic strength was predicted to be only 3% - 5% due to the relatively high initial salinity of the reacting OPAw.

Another effect identified was related to ion exchange equilibria. Because dissolved Na^+ concentrations are lower in the 48% porosity system, more exchanged Na^+ is released from the bentonite interlayer, compared to the original calculation at 36% porosity. This implies that more Ca^{2+} enters the interlayer, resulting in lower final Ca concentrations in the inter-particle solution. This mechanism causes a slight increase in sulphate concentrations due to the imposed gypsum equilibrium constraint. Overall, the

changes in aqueous chemistry caused by variations in bentonite compaction were found to be minor.

2.2.3 The thermodynamic status of clay minerals

In conventional geochemical models, illite and smectites are considered as chemically non-reactive "pin-boards" where ion exchange is described via simple ion exchange equilibria. A new model concept (BERNER et al., 2012) assumes that montmorillonite is an ideal solid solution with end members which only differ in the nature of the charge compensating cation. This solid solution model allows the montmorillonite to participate in mineral dissolution and transformation processes. As a result of the application of the new model in coupled transport calculations, the question arose concerning the extent to which clay mineral dissolution/precipitation processes can be reliably described by thermodynamic equilibrium models.

A literature review revealed that this can be done with the clay mineral kaolinite. The thermodynamic constant in the PSI/Nagra 07/12 TDB (THOENEN, 2012) is derived from reversible dissolution/ precipitation experiments which reached chemical equilibrium, and it has been shown that kaolinite crystals precipitate from aqueous solutions under ambient conditions. Furthermore, kaolinite is most probably the thermodynamically most stable phase of all of the $Al_2Si_2O_5(OH)_4$ polymorphs of the kaolin group.

The situation is quite different for illite, smectites and illite-smectite interstratifications. Long-term solubility experiments with natural samples of illite and montmorillonte have been inconclusive, and the results have evoked much debate in the open literature. The interpretation of calorimetric data needs dehydration models. Whereas kaolinite crystals are known on the millimetre scale, illite and smectite particles never exceed the micrometre scale, and hence experimental discrimination between interlayer and inter-particle water in dehydration experiments is far from straightforward. Whether the thermodynamic data published for illite, smectites and illite-smectite interstratifications are "equilibrium values" is currently unclear.

2.2.4 Thermodynamic data at elevated temperatures

The ambient temperature of a potential underground repository for SF/HLW is expected to be approximately 50°C, while the maximum temperature at the surface of a waste container may be as high as 160°C. Since most of the experimental data considered in the PSI/Nagra TDB were obtained at room temperature, and since it cannot be realistically expected that experimental data will be produced at higher temperatures in the near future (or ever), methods must be found that reliably extrapolate room temperature data to the temperatures of interest. For this purpose, the isocoulombic extrapolation method shows some promise. The isocoulombic extrapolation method is based on the observation that reactions comprising of equal numbers of like-charged aqueous ions on both sides of a reaction have negligible entropy and heat capacity effects. As a consequence, extrapolations to higher temperatures can be simply made using only the equilibrium constants of such isocoulombic reactions measured at room temperature. Reactions that are not isocoulombic can often be brought into an isocoulombic form by the appropriate addition of another reaction.

Within the framework of an internship, the programming language Python was used to create a set of programming modules that operate on the PHREEEQC version of the PSI/Nagra TDB. The modules can be used to extract those reactions (called model reactions) in the database for which enough data are available for extrapolation to higher temperatures. For every non-isocoulombic reaction in the database, the modules can find all possible isocoulombic formulations that can be obtained from the addition of model reactions.

This set of Python modules provides an efficient tool for assessing the potential of the isocoulombic approach to extrapolate data in the PSI/Nagra TDB to higher temperatures.

2.3 Trace element behaviour

2.3.1 Thermodynamics of AFm-(I_2, SO_4) solid solution in aqueous media

Cement minerals carrying positively-charged surfaces may potentially reduce the mobility of long-lived anionic radionuclides such as ^{129}I, ^{79}Se, and ^{99}Tc in the near-field of a cement-based repository. In the context of a completed PhD project (L. Aimoz), the uptake mechanisms of iodide (I^-) by a cement mineral (AFm-SO_4, "monosulphate") were investigated. This study provided thermodynamic data which could be used to model the fate of ^{129}I in the cementitious near-field of a radioactive waste repository.

AFm-SO_4 belongs to the layered double hydroxides family and is composed of positively charged Ca^{2+}-Al^{3+} hydroxide layers, with charge compensating SO_4^{2-} anions in their interlayers. Different ratios of SO_4^{2-} and I^- were co-precipitated as AFm compounds under ambient conditions (23 ± 2°C), and characterized by X-ray diffraction (Fig. 2.1). A solid solution was found to form between the sulphate and the iodide end-members in which the interlayer distance between the two adjacent hydroxide layers continuously increased from one end-member to the other, Fig. 2.1(b).

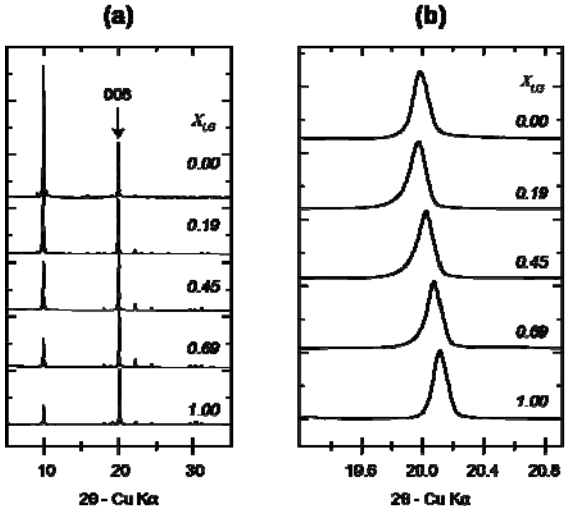

Fig. 2.1: *For 5 different I/SO_4 molar ratios ($X_{I,G}$); (a) X-ray diffractograms of AFm phases (b) evolution of the position of the 006 line, which is representative of the increasing interlayer distance between AFm-I_2 and AFm-SO_4 end-members.*

The thermodynamic properties of AFm-I_2, and its solid solution with AFm-SO_4, were evaluated based on solubility and sorption experiments in aqueous solutions and modelled using GEM-Selektor.

The Gibbs energy of formation at standard state (1 bar, 25°C) of AFm-I_2 ($Ca_4Al_2(OH)_{12}I_2{\cdot}2H_2O$) and AFm-$SO_4$ ($Ca_4Al_2(OH)_{12}SO_4{\cdot}6H_2O$) were assessed to be -6650.0 ± 4.8 (2σ) kJ·mol^{-1} and -7781.4 ± 4.6 (2σ) kJ·mol^{-1}, respectively. Thus, the AFm-SO_4 end-member was found to be significantly more stable than the AFm-I_2 end-member.

The complexity of this solid solution system resides in the heterovalent nature of the mixing, i.e. the fact that the substituting ions have different valences, (-1) for I^- and (-2) for SO_4^{2-}. As a consequence, the definition of mole fraction depends on the exchange model. Two approaches have been investigated: (i) GAPON (1933) defines the exchange as a partial substitution on equal number of sites, i.e. a single divalent SO_4^{2-} anion is substituted by two monovalent I^- ions, whereas (ii) the ion exchange hypothesis of VANSELOW (1932) assumes the substitution of one mole of an ion by one mole of another ion, irrespective of the different valences, i.e. one mole of I^- is substituted by one mole of SO_4^{2-}, still maintaining the charge balance in the solid solution phase.

Lippmann diagrams were constructed in a mol fraction concentration scale for the experimental solubility points following both conventions. Fig. 2.2 shows that the experimental solidus data match the ideal Vanselow model more closely than the Gapon model.

In addition, sorption experiments with small I^- concentrations (10^{-11} to 10^{-3} M) enabled data to be obtained in the region closer to the AFm-SO_4 end-member, which were missing in the co-precipitation experiments due to the much larger stability of AFm-SO_4. A linear isotherm was found for the uptake of iodide onto AFm-SO_4 (Fig. 2.3) with a selectivity coefficient ${}_{SO4}^{I}K_v = 1.0\times10^{-4}$ (Vanselow convention).

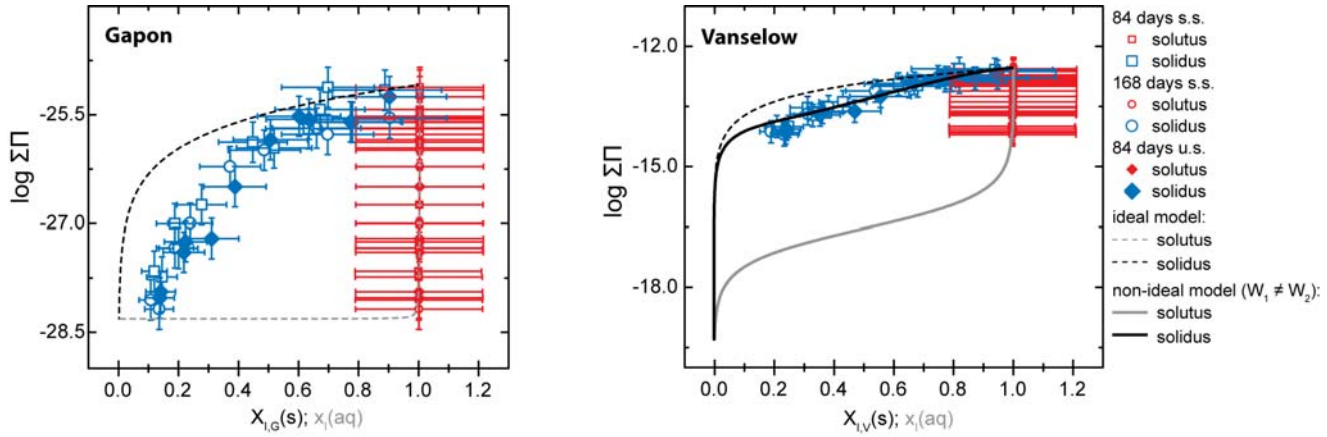

Fig. 2.2: *Lippmann diagrams of the solid solution between AFm-I_2 and AFm-SO_4 using (a) the Gapon and (b) the Vanselow conventions. The solid black line in (b) represents the best fit obtained with a sub-regular non-ideal model setting W_{SO4} = -1.0 kJ·mol^{-1} and W_I = -8.0 kJ·mol^{-1}.*

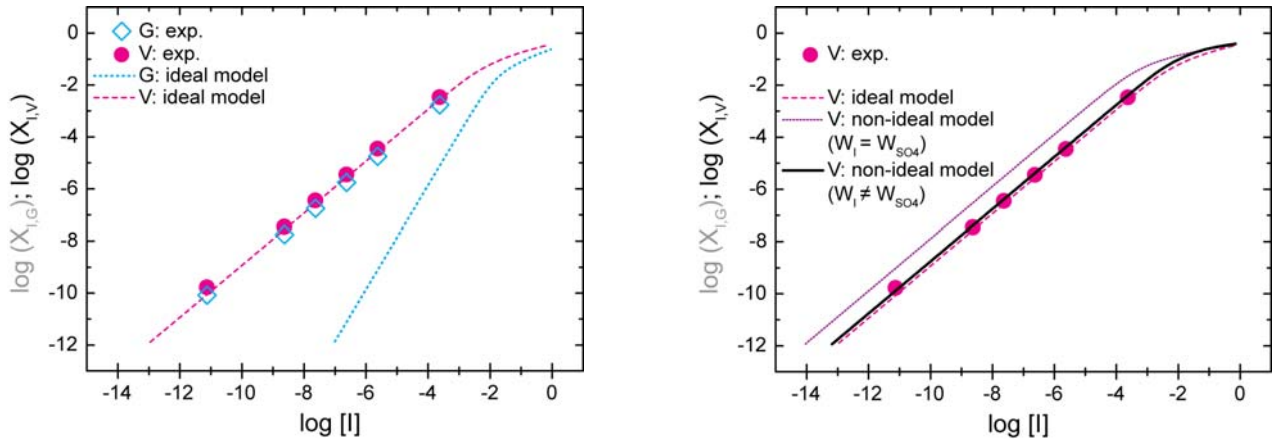

Fig. 2.3: *Theoretical and experimental sorption isotherms of I^- uptake by AFm-SO_4. (left) Experimental data compared to ideal solid solutions following the Vanselow (V) and the Gapon (G) conventions. (right) Refinement showing the best fit (solid black line, represents the sub-regular non-ideal model with W_{SO4} = -1.0 kJ·mol^{-1} and W_I = -8.0 kJ·mol^{-1}).*

This low coefficient indicates a strong selectivity for SO_4^{2-} ions. The Gapon-type model predicted that I^- would remain in solution below I^- ~10^{-7} M, with an isotherm slope that does not correspond to the experimental data. However, a measurable uptake was obtained down to ~10^{-11} M iodide in solution, which is well modelled by the Vanselow-type model (Fig. 2.3).

Using iterative adjustments of the Lippmann diagrams (Fig. 2.2), and of the sorption isotherm (Fig. 2.3), the thermodynamic model indicates the formation of a sub-regular solid solution between AFm-I_2 and AFm-SO_4, using negative asymmetric Margules interaction parameters with $W_I << W_{SO4}$. The substitution of a divalent anion into a sub-lattice filled with monovalent anions thus seems to be energetically less favoured than the substitution of a monovalent anion into a sublattice filled with divalent anions. Although the AFm-SO_4 end-member is much more stable than the AFm-I_2 end-member, the strongly negative interaction parameter W_I implies that AFm-SO_4 can act as a sink for ^{129}I, even at very low iodide concentrations.

2.3.2 Reductive sorption of Se(IV/VI) by natural pyrite: XAS/XRF evidence

^{79}Se is a major dose determining redox sensitive nuclide. Under oxidizing conditions, selenium forms soluble anionic species ($Se^{IV}O_3^{2-}$ and $Se^{VI}O_4^{2-}$) which hardly sorb at all on the negatively charged surfaces of common host-rock minerals. However, Se is known to have a strong affinity for sulphides such as pyrite, a common minor mineral in the argillaceous rocks being considered as host formations for radioactive waste repositories.

The uptake of Se(IV,VI) on natural pyrite was investigated by X-ray spectroscopy. µ-XRF and µ-XANES data were acquired under an inert gas flux at the µ-XAS beamline (SLS) on polished pyrite samples previously exposed to aqueous solutions of $Na_2Se^{IV}O_3$ or $Na_2Se^{VI}O_4$ at 80°C under anoxic conditions during a period of 15 days to 2 months. Bulk Se EXAFS data were collected at the DUBBLE beam line (ESRF) on a powdered pyrite sample aged for 8 months.

The µ-XRF data showed that the Se uptake process was highly heterogeneous. Micrometer-sized Se-rich clusters were formed, which were surrounded by areas of low and uniform distributions of Se (see Fig. 2.8 in LES progress report, 2009). The µ-XANES data revealed that most of the Se taken up by pyrite from Se(IV) or Se(VI) solutions was progressively reduced on the mineral surface, mostly to Se(0) (Fig. 2.4). The XANES data did not always allow a distinction to be made between Se(0) and Se(-II).

A pyrite powdered sample (Se-21) was treated with a Se(IV) solution and studied over a period of 8 months. Fig. 2.5 shows the bulk XANES spectra, which indicate a mixture of about 50% Se(IV) and 50% Se(0) after a 2 month ageing time. After an additional 6 months at room temperature in a glove box flushed with N_2, reduction to Se(0) was found to be complete. The EXAFS spectrum of the 8 month old sample shows a coordination environment practically identical to that of crystalline grey Se(0) (Fig. 2.6).

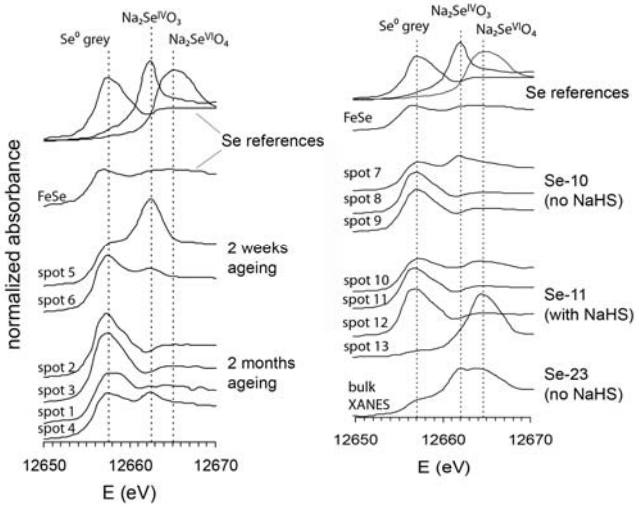

Fig. 2.4: *µ-XANES Se K-edge of selected spots from pyrite chips and a powder (Se-23) treated with (a) $Na_2Se^{IV}O_3$ or (b) $Na_2Se^{VI}O_4$ solutions, compared to the XANES spectra of reference compounds.*

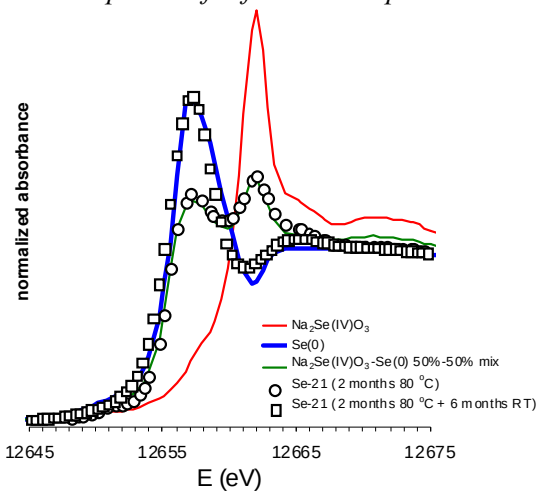

Fig 2.5: *Bulk XANES spectra of a pyrite powdered sample (sample Se-21) treated with Na_2SeO_3 solution for 2 months at 80°C and after an additional 6 months ageing period at room temperature (RT). The spectra of Se^0, Na_2SeO_3 and of an equimolar mixture of both compounds are superimposed.*

In conclusion, this study showed that pyrite can readily take up and reduce dissolved Se(IV) and Se(VI). The reduction kinetics are relatively slow, and the complete conversion to sparingly soluble Se(0) requires a few months ageing time at room temperature. The results of this project are reported in a recent publication (CURTI et al., 2012).

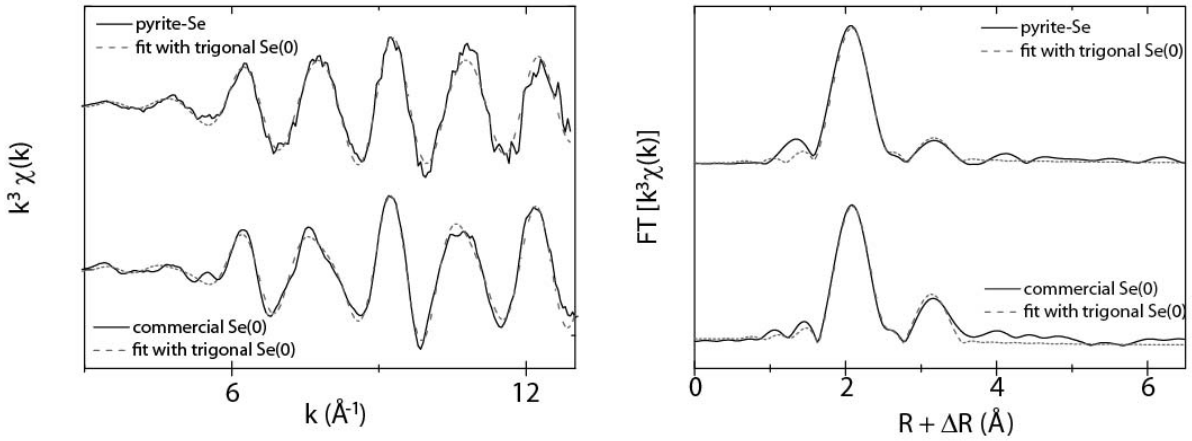

Sample	$N_{Se\text{-}Se1}$	$R_{Se\text{-}Se1}$(Å)	$N_{Se\text{-}Se2}$	$R_{Se\text{-}Se2}$(Å)
Se^0 (grey)	2.1 ± 0.2	2.39 ± 0.01	2.6 ± 0.3	3.41 ± 0.01
Se -21	3.2 ± 0.3	2.38 ± 0.01	1.3 ± 0.4	3.41 ± 0.02

Fig. 2.6: *Se K-edge EXAFS of a crystalline grey Se^0 reference sample and of Se sorbed onto pyrite (sample Se-21) after 8 months ageing time: k^3-weighted normalized spectra (top left), the corresponding Fourier Transforms (top right) and the fit results (bottom).*

2.3.3 Modelling kinetics of trace element uptake in host minerals

Equilibrium aqueous-solid-solution-sorption thermodynamic models are usually not capable of predicting trace element uptake in growing minerals from the experimentally measured trace element (*Tr*) partitioning between a host mineral (*Hc*) and the aqueous solution (e.g. fractionation coefficient, $\Delta_{Tr,Hc}$). Hence, within the framework of the SKIN project, the work focused on the growth-rate dependency of $\Delta_{Tr,Hc}$. For elements which can hardly be incorporated into the mineral lattice (designated "incompatible", e.g. Sr^{2+} in calcite), $\Delta_{Tr,Hc}$ increases with growth rate, whereas the opposite trend is observed for elements which can easily be incorporated (designated "compatible", e.g. Ni^{2+} in calcite). Two existing uptake kinetics models were investigated (WATSON, 2004; DE PAOLO, 2011) which seemed to be promising in terms of their scientific value and the potential for inclusion in geochemical modelling codes. These models were found to be complementary, and were unified into a "merged" model implemented in the GEM-Selektor v.3 code (THIEN et al., 2012):

$$\Delta_{Tr,Hc} = \frac{F \cdot \Delta_{Tr,Hc,eq}}{1 + \frac{(D_s / ml)}{(D_s / ml) + V}(F - 1)} \qquad \text{(Eq. 1)}$$

where F is the surface enrichment factor, V the linear mineral growth rate, D_s the surface diffusivity coefficient, and ml the thickness of the surface layer in which surface diffusion occurs.

The "merged" model equation was provisionally implemented in a script in the GEM-Selektor "process simulator" module. In such simulations, the time evolution of a geochemical thermodynamic system can be represented as a sequence of "partial equilibrium" states. In such a state, at least one phase is kept out of equilibrium with the rest of the system by additional "metastability constraints" (KARPOV et al., 2001; KULIK et al., 2012). For instance, precipitation of calcite can be simulated over time steps as a sequence of partial equilibrium states, each with a metastability constraint from above on the mole amount of calcite. With time, this upper constraint increases according to a kinetic rate law (e.g. WOLTHERS et al., 2012) that involves the saturation index and the surface area of the mineral.

Because the fractionation of *Tr* depends on the host mineral growth rate (see Eq. 1), it becomes possible to calculate $\Delta_{Tr,Hc}$ and the metastability constraints on the amount of trace end member ($SrCO_3$) from the current aqueous speciation and the increase of mole amount of the host end member (calcite) at a given time step.

The results of such GEM-Selektor calculations involving the merged uptake kinetics model (Eq. 1) were compared against the experimental data on Sr, Cd, Co, and Mn coprecipitation with calcite (LORENS, 1981). Fig. 2.7 shows that this "merged" model is able to describe the growth-rate dependency of the measured $\Delta_{Tr,Hc}$ value.

In comparison with existing models, the currently developed model fully accounts for the aqueous solution speciation, as well as for depletion effects, which may occur on long time scales. Actually, solution depletion can reduce both the *Tr* aqueous activity and host mineral growth rate, and thus modify $\Delta_{Tr,Hc}$ (Fig. 2.8).

The "merged" model can be used to describe the trace element uptake during mineral precipitation in aqueous solutions with changing composition provided that a few parameters regarding the trace element/host mineral couples are known. In the framework of the SKIN project, a further improvement will be to account for Tr in-diffusion, which can influence $\Delta_{Tr,Hc}$ especially on long time scales. In addition, the effect of specific surface area and surface roughness on $\Delta_{Tr,Hc}$ needs to be included and requires investigation. It is planned to "hard-code" the "merged" uptake model to make it usable in geochemical reactive-transport codes coupled with the GEMS3K kernel (KULIK et al., 2012) of the GEM-Selektor package.

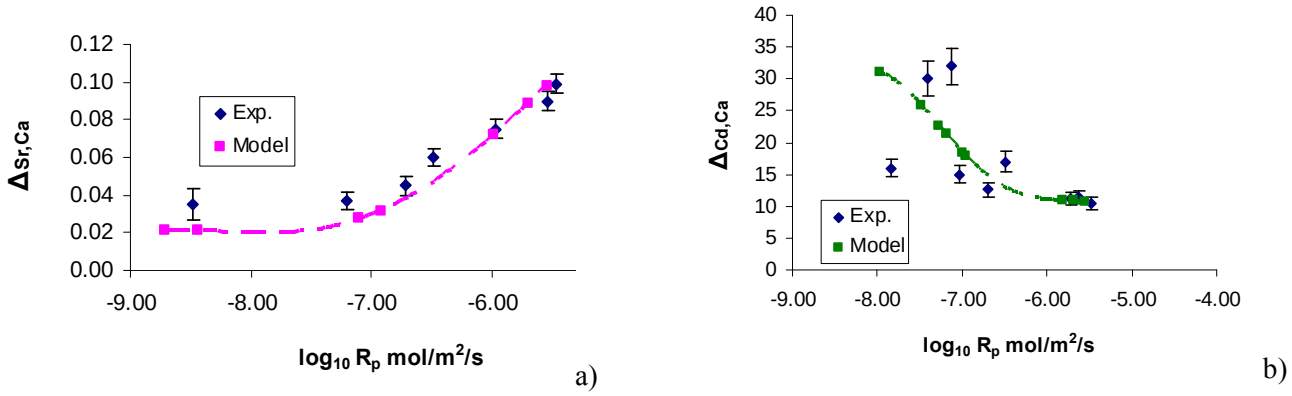

Fig. 2.7: *Fractionation coefficient as a function of growth rate for (a) Sr in calcite and (b) Cd in calcite.*

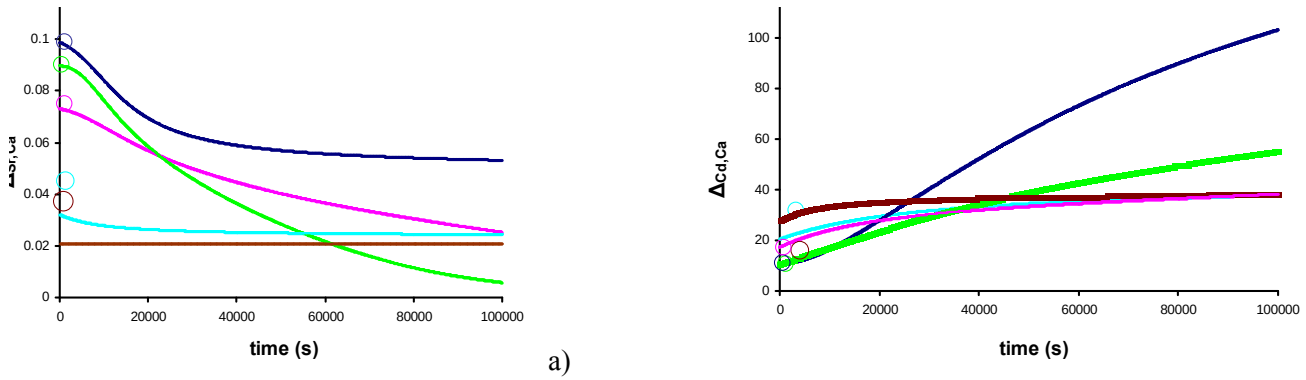

Fig. 2.8: *$\Delta_{Tr,Hc}$ variations as a function of time for (a) the calcite-strontianite and (b) the calcite-otavite systems. Circles correspond to the experimental results shown in Fig. 2.7.*

2.4 Teaching activities

The teaching duties of W. Hummel as Privatdozent (PD) for "Nuclear Environmental Chemistry" at ETH Zurich included lectures and exercises on nuclear waste management within the scope of the course "Nuclear Energy Systems" (Spring Semester 2012).

2.5 References

BERNER, U. (2002)
Project Opalinus Clay: Radionuclide concentration limits in the near-field of a repository for spent fuel and vitrified high-level waste. PSI Bericht Nr. 02-22, and Nagra Technical Report NTB 02-10.

BERNER, U. (2003)
Project Opalinus Clay: Radionuclide concentration limits in the cementitious near-field of an ILW repository. PSI Bericht Nr. 02-26, and Nagra Technical Report NTB 02-22.

BERNER, U. (2009)
Modelling hydrated HTS cement and its porewater. PSI Internal Report AN-44-09-10.

BERNER, U. (2011)
Setting up bentonite porewater composition. PSI Internal Report AN-44-10-04-Rev1.

BERNER, U. & KOSAKOWSKI, G. (2011)
Freigabe Bentonitporenwässer. PSI Internal Report AN-44-11-12.

BERNER, U. & KOSAKOWSKI, G. (2011a)
Freigabe Bentonitporenwasser. PSI Internal Report AN-44-11-21.

BERNER, U., KULIK, D.A., KOSAKOWSKI, G. (2012)
Influence of a low-pH cement liner on the near-field of a repository for spent fuel and high-level radioactive waste. Phys. Chem. Earth (submitted).

CURTI, E., AIMOZ, L. KITAMURA, A. (2012)
Selenium uptake onto natural pyrite. J. Radioanal. Nucl. Chem.
doi 10.1007/s10967-012-1966-9.

DE PAOLO, D.J. (2011)
Surface kinetic model for isotopic and trace element fractionation during precipitation of calcite from aqueous solutions. Geochim. Cosmochim. Acta 75, 1039-1056.

GAPON, E.N. (1933)
On the theory of exchange adsorption in soils. USSR J. Gen. Chemistry 3, 144.

KARPOV, I.K., CHUDNENKO, K.V., KULIK, D.A., AVCHENKO, O.V., BYCHINSKII, V.A. (2001)
Minimization of Gibbs free energy in geochemical systems by convex programming. Geochem. Int. 39, 1108-1119.

KOSAKOWSKI, G. & BERNER, U. (2011)
Reactive transport calculations on the evolution of a cementitious repository. PSI Internal Report AN-44-11-09.

KULIK, D.A., WAGNER, T., DMYTRIEVA, S.V., KOSAKOWSKI, G., HINGERL, F., CHUDNENKO, K.V., BERNER, U. (2012)
GEM-Selektor geochemical modeling package: Numerical kernel GEMS3K for coupled simulation codes. Comput. Geosci. (in press).

LORENS, R.B. (1981)
Sr, Cd, Mn and Co distribution coefficients in calcite as a function of calcite precipitation rate. Geochim. Cosmochim. Acta 45, 553-561.

THIEN, B., KULIK, D.A., CURTI, E. (2012)
Preliminary review on modeling approaches and their implementation. Report from the collaborative project SKIN (Grant agreement N°269688), Work Package 4: Modeling, Theory.

THOENEN, T. (2012)
The PSI/Nagra Chemical Thermodynamic Data Base 12/07: Compilation of updated and new data with respect to the PSI/Nagra Chemical Thermodynamic Data Base 01/01. PSI Technical Report TM-44-12-06.

VAN LOON, L.R. (2012)
Estimation of anion accessible porosities of compacted bentonite to be used in performance assessment calculations. PSI Internal Report AN-44-12-01.

VANSELOW, A.P. (1932)
Equilibria of the base-exchange reactions of bentonites, permutites, soil colloids and zeolites. Soil Sci. 33, 95-113.

WATSON, E.B. (2004)
A conceptual model for near-surface kinetic controls on the trace-element and stable isotope composition of abiogenic calcite crystals. Geochim. Cosmochim. Acta 68, 1473-1488.

WOLTHERS, M., NEHRKE, G., GUSTAFSSON, J.P., VAN CAPPELLEN, P. (2012)
Calcite growth kinetics: Modeling the effect of solution stoichiometry. Geochim. Cosmochim. Acta 77, 121-134.

3 TRANSPORT MODELLING

S.V. Churakov, Th. Gimmi, A. Jakob, G. Kosakowski, W. Pfingsten, M. Tyagi (postdoc), L. Pegado (postdoc), F. Hingerl (PhD), J. Poonoosamy (PhD), A. Shafizadeh (PhD)

3.1 Overview

Reactive transport simulations with the coupled code OpenGeoSys-GEMS have become a standard approach in LES for modelling the in situ conditions in the near-field of SF/HLW and L/ILW repositories and their evolution in time and space (section 3.2.1). Thanks to the further development of GEMS, and the strong co-operation with the Geochemical Modelling Group, the geochemical setup applied in the simulations is being continuously improved. Recently, kinetic controlled mineral precipitation/ dissolution reactions have been applied to simulate the evolution of the Engineered Gas Transport System (EGTS).

In 2012 the group participated further in the modelling of data from the DR-experiment and in the co-ordination of the modelling activities in the DR-A experiment at Mont Terri (section 3.2.4). Field experiments provide input data for modelling, and are used for the validation of conceptual transport models. Inverse modelling of conventional diffusion experiments provides the radionuclide transport parameters needed in performance assessment studies (section 3.3). Two new PhD projects (sections 3.4.1 and 3.5.2) have been started which are aimed at addressing high priority issues concerning clogging and repository re-saturation.

The simulations carried out for PA studies span time frames of a million years and therefore have to be conceptually simple and numerically robust. Numerical codes are benchmarked, and modelling competences have been extended to maintain state-of-the-art capabilities and the conceptual quality of the system descriptions (section 3.5). Teaching, supervision of PhD students and postdocs, are an integral part of the group's activities which contribute to knowledge transfer and the visibility of the research.

3.2 Activities in support of the Sectorial Plan

3.2.1 Geochemical evolution of the repository near-field

In the past few years numerous reactive transport simulations have been carried out in support of the reports on the geochemical evolution of the SF/HLW and L/ILW near-fields. The results of these studies were summarized in two publications which were submitted to the Journal of Physics and Chemistry of the Earth (BERNER et al., 2012; KOSAKOWSKI & BERNER, 2012). The geochemical system set-up, and the process coupling used for various transport scenarios, was developed in close co-operation with the Geochemical Modelling Group. In order to understand the influence of an optional low pH concrete liner on the SF/HLW near-field, a sensitivity study was performed in which the influence of kinetically controlled precipitation/dissolution reactions was included. It was found that a kinetics based system description did not change the general evolution of the reaction fronts and porosity clogging because the dominant mineral precipitation/-dissolution reactions were controlled by the availability of reactants diffusing across material interfaces, and not by the reaction kinetics themselves.

Recently, reactive transport simulations have been applied to simulate the geochemical evolution of interfaces in the EGTS. Several potential design options are currently being investigated. The geochemical setup for these simulations was identical to the one used in BERNER et al. (2012) and KOSAKOWSKI & BERNER (2012), except that kinetically controlled precipitation/dissolution reactions were introduced. Fig. 3.1 shows the mineralogical profiles across a simplified plug/seal layout for a simulated evolution time of 1500 years. The plug/seal layout comprised of (from left to right) a sand/bentonite backfill in the access tunnels, a transition layer of gravel to separate the clay and cement materials, and the concrete backfill in the

emplacement tunnels. In the reference layout a quartz sand/gravel aggregate was used in the sand/bentonite mixtures, the transitional layers and in the concrete. No significant mineralogical and porosity changes were observed in the sand/bentonite mixtures and transition layers. Only minor quantities of precipitates of cement minerals (C-S-H with low Ca/Si ratio) were formed. In contrast, the concrete layer degraded completely due to alkali-silicate-aggregate reactions (ASR), which are a consequence of the thermodynamic instability of silicate aggregates embedded in a cementitious matrix. These ASR reactions resulted in the dissolution of cement minerals, a re-crystallization of C-S-H phases with low Ca/Si ratios, the neo-formation of clay minerals and a strong decrease in pH to values around 10. The dissolution kinetics of quartz was modelled assuming that the quartz grains had a spherical form with a 2.8 mm diameter. It should be noted, however, that the effective time evolution of ASR is very uncertain since the development of reaction rims around the quartz grains may change the transport/reaction parameters which would most likely slow down the ASR reaction rates.

An alternative setup is shown in the lower part of Fig. 3.1. In this scenario the reactive quartz in the transitional layer and in the concrete is replaced by carbonates (calcite). This effectively prevents ASR reactions. After 1500 years most of concrete is still buffered by portlandite and the porewater pH is 12.5. The strong geochemical differences between concrete and the sand/bentonite backfill causes the diffusion of solutes across the transition layer and drives the advance of reaction fronts with accompanying mineral precipitation and dissolution. In the bentonite/sand backfill, the montmorillonite at the interface is dissolved and replaced by zeolites (phillipsite) and other clay minerals (illite, kaolinite). In the concrete compartment, ettringite precipitation, portlandite (hydrotalcite, monocarbonate) dissolution and a change in C-S-H composition were observed. The advance of these reaction fronts slows down with time since it is controlled by diffusion across the transition layer. Therefore, a 10 fold wider transition layer would decrease the concentration gradients by a factor of 10, and consequently also decrease the advance of reaction fronts by the same factor.

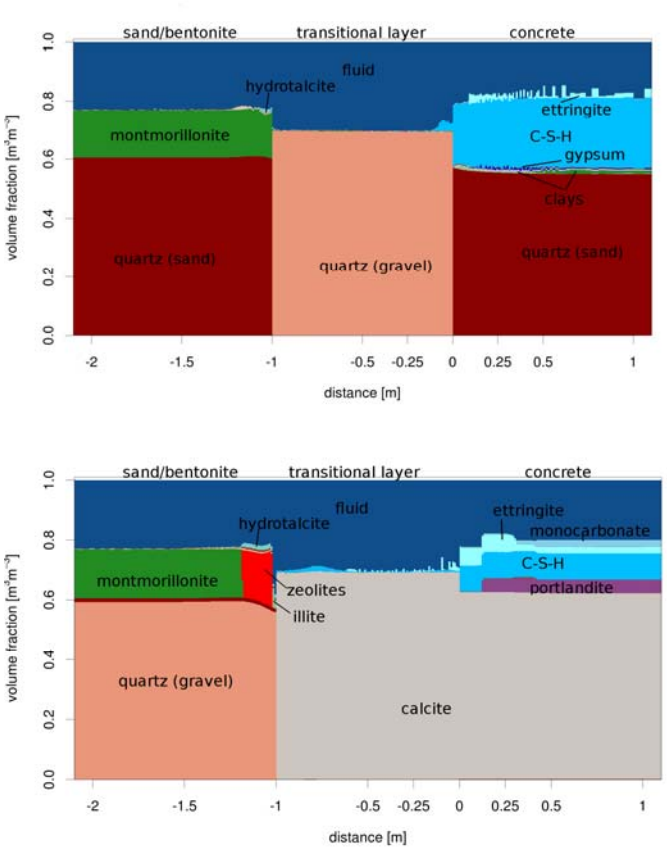

Fig. 3.1: *Simulated mineralogical profiles across the tunnel backfill, gravel filters and concrete after 1500 years for two different EGTS layouts (see text for details).*

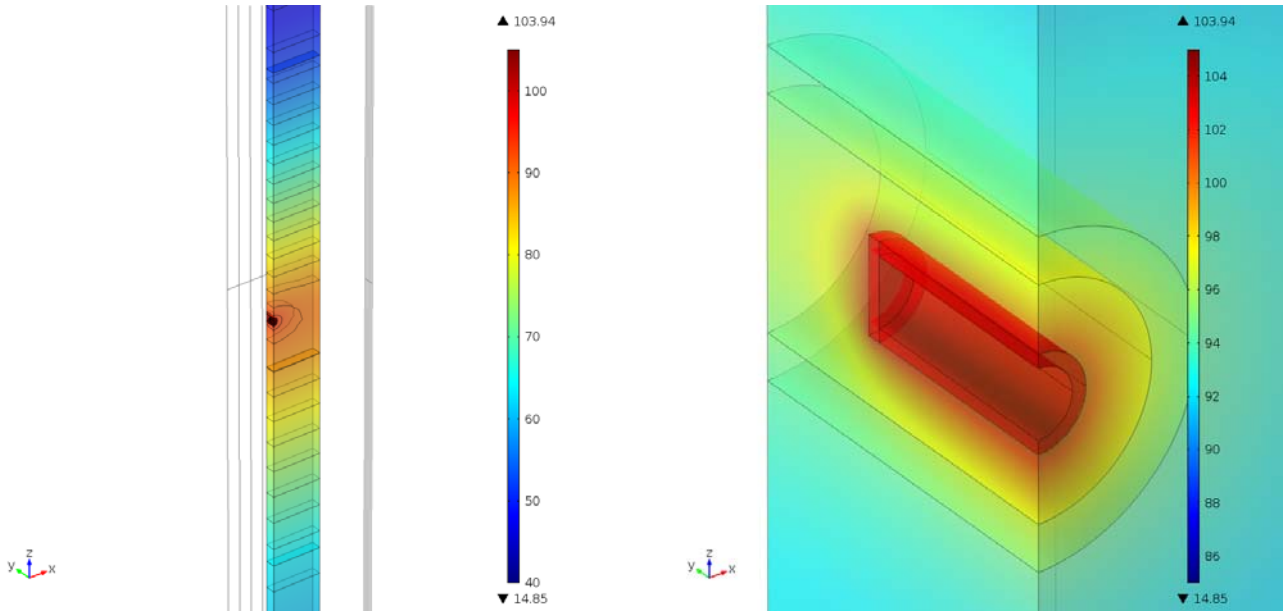

***Fig. 3.2**: The temperature distribution in the near- and far-fields 400 years after repository closure. For a heat production rate of 1500 W/canister, the highest temperature in the host rock is reached after 400 years. In the left sub-figure, the heat transport domain is shown on a larger scale. The temperatures lie between 40 (bluish parts) and 105°C (reddish parts). In addition, some iso-temperature lines are drawn. In the right sub-figure the temperature distribution (range: 85 – 105 °C) in the core zone is shown. The sequence from the inside to the outside of the cylindrical structure is: the canister walls, the bentonite backfill, the excavation disturbed zone and part of the host rock.*

3.2.2 Temperature effects of high burn up fuel on the integrity of the barrier system of a SF/HLW repository

Use of higher burn up fuel in nuclear power plants would allow, in principle, fewer shutdowns for refueling and eventually result in less spent fuel elements for disposal in a radioactive waste repository. However, the long-term heat emission due to the increased content of fission products, such as ^{137}Cs and ^{90}Sr, is a severe limiting factor for geological disposal of such high burn up fuel. At temperatures above 100°C, bentonite cannot swell sufficiently well to seal around the canisters. Moreover, elevated temperatures may result in unfavourable mineral transformation both in the near- and far-fields. An important requirement for the bentonite in the near-field is the efficient heat transfer between the canisters containing the highly radioactive waste and the surrounding Opalinus Clay host rock. Basically, temperatures should remain below 100°C in the bentonite buffer and below 85°C in the Opalinus Clay.

Since only the design of the near-field can be adjusted, it is important to understand and optimize the heat transfer through the bentonite. The results of numerous studies worldwide using all kinds of bentonite have demonstrated that two quantities strongly affect the thermal conduction of bentonite, namely, its water content and density. Mobile porewater has the potential to efficiently distribute heat to other compartments of the barrier system by convection. A high bentonite density increases heat transfer because the grain-grain contact is higher. Hence, the thermal conduction of bentonite increases with higher densities and higher water contents.

The 3D simulations carried out with the Comsol-Multiphysics code (Fig. 3.2) clearly showed that, independent of the water content and density of the bentonite, the heat released from canisters with a heat output above 1500 W/canister cannot be dissipated rapidly enough to the host rock to avoid detrimental effects on the clay barrier system. Only by reducing the heat output to less than 1500 W/canister can such unwanted effects be avoided.

3.2.3 DR experiment in the Mont Terri Rock Laboratory

In the Mont Terri DR field experiment, 13 different tracers were added in two injection intervals, from which they diffused into the surrounding rock. One of the aims of this experiment was to derive anisotropy ratios for diffusion from the final over-coring measurements. Fig. 3.3 displays tracer profiles for HTO, ^{22}Na, Br and I in the radial and axial directions. The profiles in the two directions were matched to each other by adjusting the scale of the radial axis. Anisotropy ratios of the diffusion coefficients were then obtained from the scaling factors needed to match the profiles. The data indicate slightly larger anisotropy factors for HTO and ^{22}Na (~5) compared to the anions (~4 for I and ~3 for Br). Such differences were not seen in earlier laboratory studies on Opalinus Clay from Mont Terri (VAN LOON et al., 2004), where values of ~4 were reported for both HTO and ^{36}Cl. Interestingly, however, lower anisotropy ratios for anions compared to water tracers were suggested recently by the pore-scale modelling of CHURAKOV & GIMMI (2011) which is consistent with the field observations.

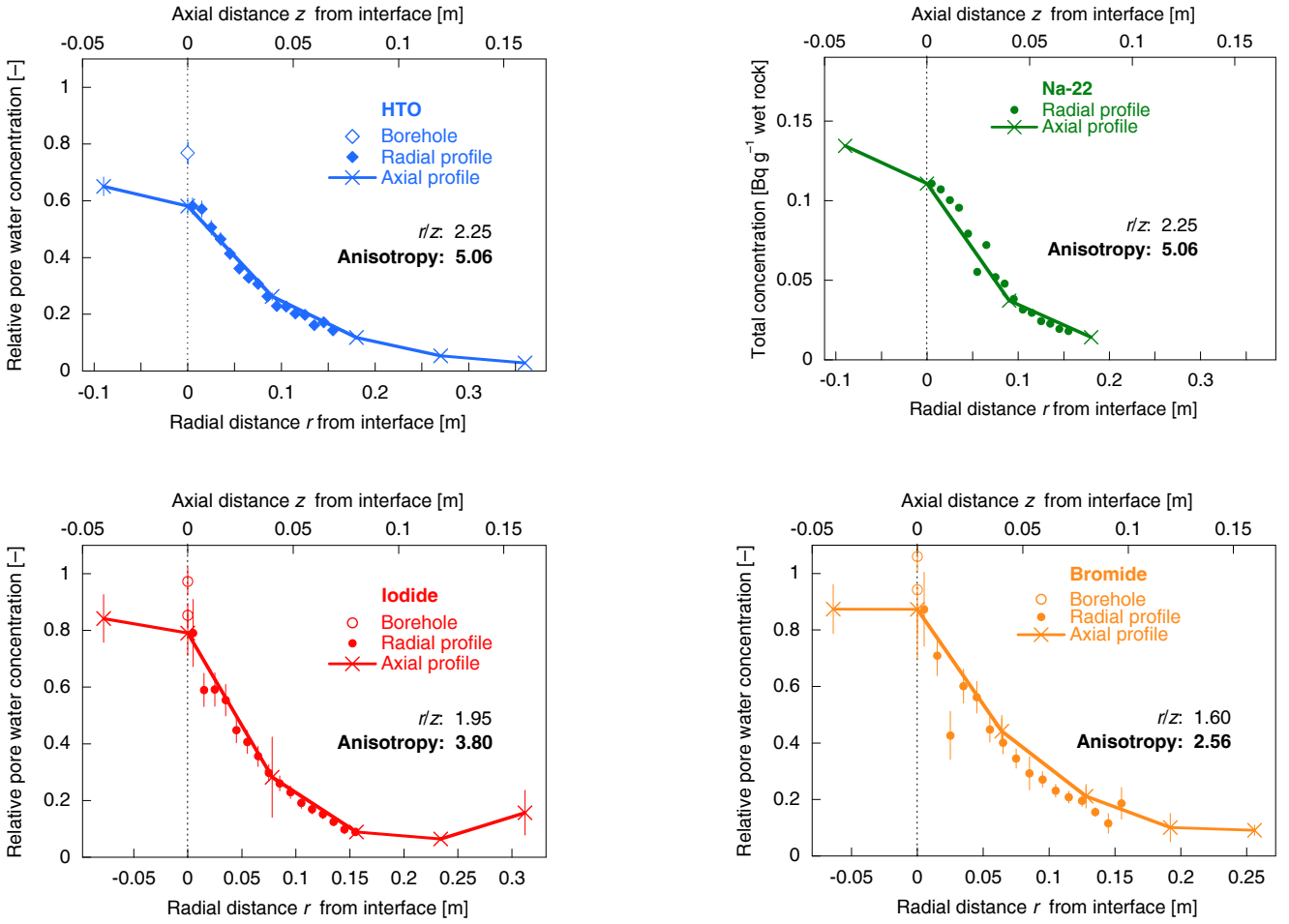

Fig. 3.3: *Comparison of radial and axial profiles of HTO, ^{22}Na, I and Br. To obtain the anisotropy ratio, the x-axis representing the radial distance was scaled such that the diffusion profiles in the radial and axial directions matched. All axial profiles were obtained at a radial distance of r = 0.015 m. "r/z" denotes the ratio of the scales of the r and z axes, from which the anisotropy ratios were estimated.*

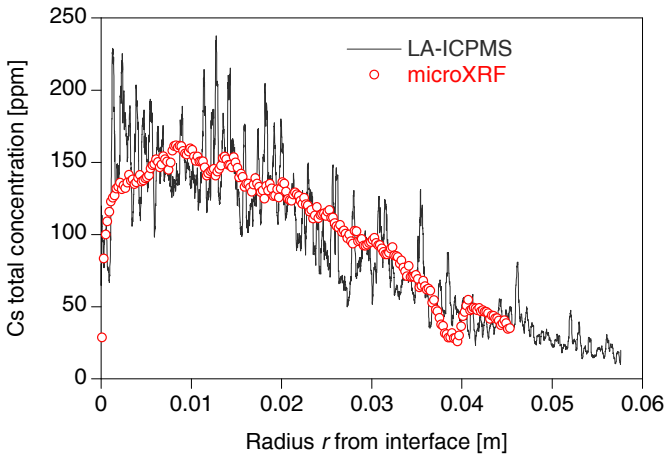

Fig. 3.4: *High-resolution profiles of total Cs concentrations obtained from laser ablation-ICPMS (lines) and from synchrotron-based micro X-ray fluorescence (points) on a sample from the DR experiment.*

New profile data (Fig. 3.4) for stable Cs were obtained in co-operation with H.A.O. Wang, D. Grolimund and C.N. Borca (SLS/microXAS Beamline, PSI). Stable Cs, added at a concentration of ~1.8×10^{-4} M, showed a larger penetration depth than ^{137}Cs which was added at trace concentrations. This is consistent with the non-linear nature of Cs sorption. The new data will be used to check the modelling concepts for Cs.

3.2.4 DR-A experiment in the Mont Terri Rock Laboratory

The DR-A field experiment in the Mont Terri Rock Laboratory started in November 2011. The aim is to test the effect of a change in the ionic strength of the artificial porewater in a packed-off borehole interval on the transport of various ions. The first part of the DR-A experiment was very similar to previous experiments i.e. an artificial porewater, which should match as closely as possible the in situ porewater, was spiked with several tracers. In a second part, the porewater chemistry was intentionally perturbed: additional KCl was added to double the ionic strength of the artificial porewater, and simultaneously some new tracers were added. Several modelling groups are involved in this experiment. As co-ordinators of the modelling study, LES defined a benchmark study with different modelling tasks of increasing complexity. The first tasks are focused on the initial, unperturbed part of the experiment, and include transport calculations for non-sorbing and linearly sorbing tracers as well as for Cs which undergoes multi-site cation exchange. The outcome of these modelling tasks will be used to compare the ability of the different models to cope with the various aspects of the experiment for given sets of generic parameters and processes. The next tasks will include modelling the effects of the perturbation, and finally the optimisation of parameters based on the measured data.

3.3 Interpretation of multi tracer (Co, Zn) diffusion experiments in OPA using a filter-free experimental setup

New experiments in which Zn and Co were simultaneously in-diffused into OPA samples pre-equilibrated with an artificial porewater for half a year, have been performed using a filter-free experimental setup. These newly measured diffusion profiles do not exhibit the “two slope” shape measured earlier in the samples for which only a short pre-equilibration phase of few weeks was used (LES progress report, 2011). The new data strongly suggest that subtle differences in the in situ porewater composition of the sample, and the artificial porewater used in the experiments, can have a significant effect on the measured diffusion profiles. Both Co and Zn are bi-valent under the experimental conditions used, and are thus expected to compete with one another for the available sorption sites and with any other aqueous bi-valent transition metals (e.g. Fe, Mn) in the porewater. In addition, the artificial porewater contains stable isotopes of Zn and Co at concentrations of about four orders of magnitude higher than that of the corresponding radionuclides (^{60}Co=4.24×10^{-10} and stable Co=5.1×10^{-6} mol/l; ^{65}Zn=5.5×10^{-11} and stable Zn=4.3×10^{-7} mol/l). Thus, the total concentrations of Co and Zn have to be considered when interpreting and modelling the measured radionuclide profiles.

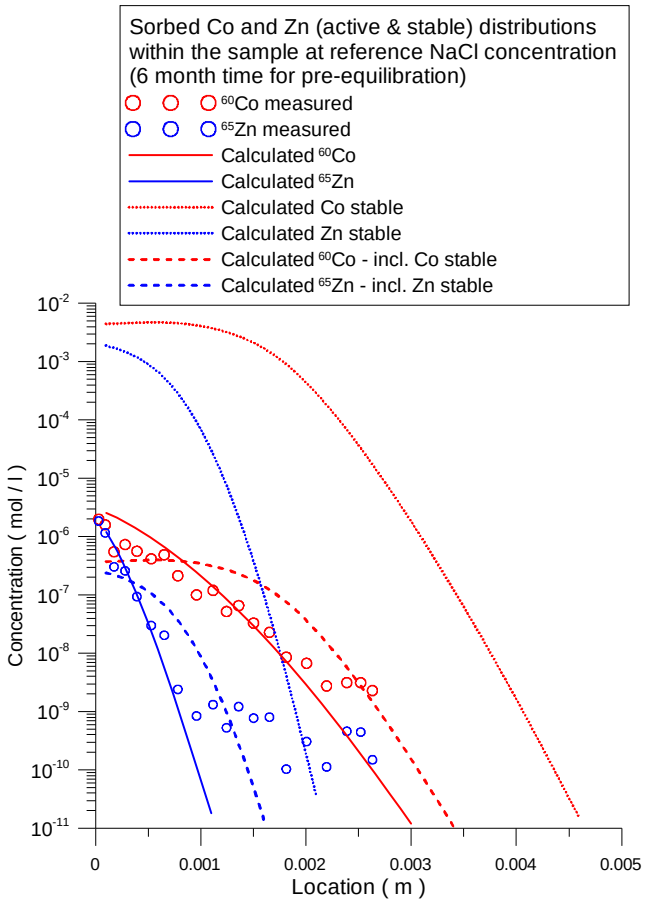

Fig. 3.5: *Calculated Co and Zn distributions in the sample. Solid lines: fits to experimental data taking into account only the active Co and Zn. The derived parameters were then used to model the simultaneous transport of the tracer and carrier. Tracer profiles (dashed lines) predicted in a later simulation setup, show different shapes and larger penetration depths.*

In order to help in the interpretation of the experimental results, and to devise an improved protocol for forthcoming experiments, a generic modelling study was performed taking into account potential experimental uncertainties. Special attention was paid to estimating the effects of sorption competition (Co(II), Zn(II), Fe(II), Mn(II)), possible gradients between the reservoir water composition and the "expected" clay porewater composition (e.g., pH, Fe), and the duration of the pre-equilibration phase.

Fig. 3.5 shows the influence of the carrier concentrations of Co and Zn on the diffusion of the radionuclides ^{65}Zn and ^{60}Co into the clay sample. The tracer distributions calculated in the presence and absence of the stable isotopes concentrations show different shapes indicating non-linear sorption effects attributed to the higher total Co and Zn concentrations. This example illustrates that all of the experiments with radionuclides should include information about carrier (stable isotope) concentrations in order to allow a correct evaluation of the transport parameters. Another aspect investigated was the effect of potential spatial heterogeneities in the samples (mineral zones with different transport and sorption properties) on the predicted Co and Zn profiles. One-dimensional transport modelling implies an averaging of mineral distribution and diffusion paths in the clay sample. To test such geometry effects at least a two-dimensional setup is necessary. Fig. 3.6 shows a 2D layered setup for areas of high and low sorption sites densities parallel and perpendicular to the tracer diffusion into the sample. This results in tracer accumulation where the sorption site density is high, and low tracer concentration where there are only few sites. The space averaged 1D tracer profiles, as measured in diffusion experiments, e.g. by abrasive peeling (total concentration), are shown in Fig. 3.6. In the setup where the layers with high and low sorption site densities are assumed to be perpendicular to the tracer diffusion direction, the Co profile looks like a monotonically decreasing saw tooth. In the setup with parallel distributions of sorption sites along the in-diffusion direction, a characteristic tailing in the diffusion profiles can be observed. It is unclear whether a tailing in the measured diffusion profiles is an indication of several diffusion pathways or an experimental artefact. Further experimental investigations are necessary to clarify this point.

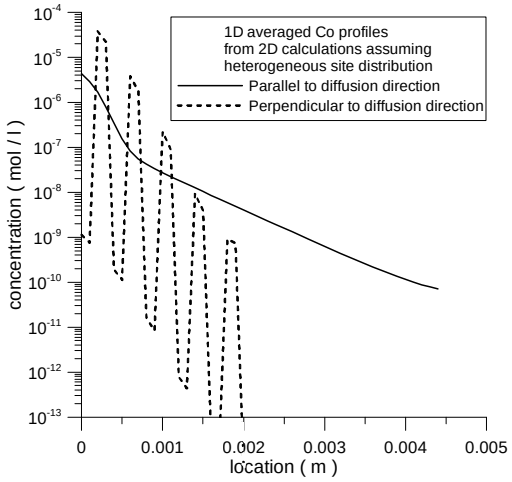

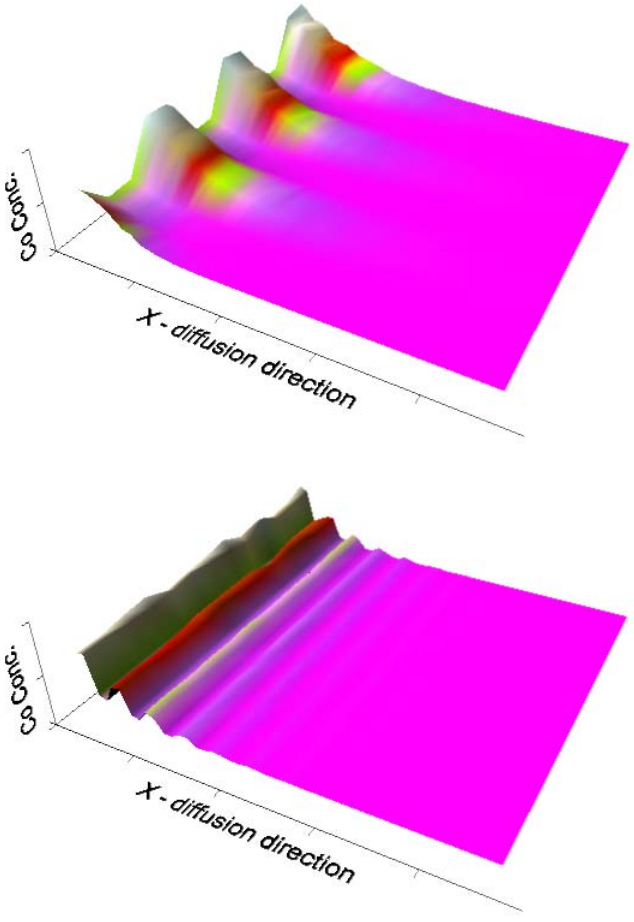

Fig. 3.6: *1D Co concentration profiles (top) as would be measured in the in-diffusion experiments by the abrasive peeling technique derived from 2D simulations with inhomogeneous sorption site density distributions: parallel (middle) and perpendicular (bottom) to the diffusion direction of tracer in-diffusion.*

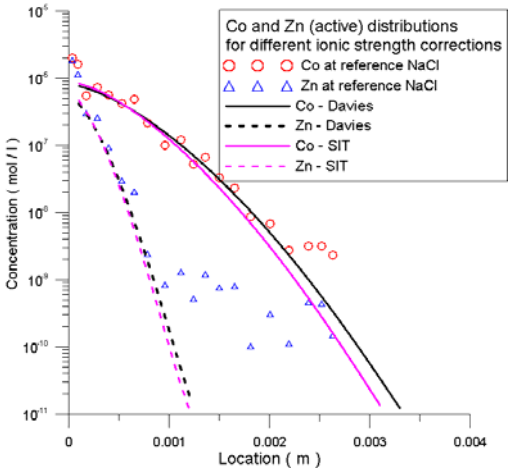

Fig. 3.7: *Calculated Co and Zn profiles using two different models for activity coefficients (Davies and SIT). The samples were pre-equilibrated with the artificial porewater for 6 month prior to the diffusion experiments.*

In-diffusion experiments were performed at three different ionic strengths (1, 0.3 and 0.03 M NaCl). The measurements showed a slightly reduced penetration depth in the in-diffusion tracer profiles at higher ionic strengths (see Chapter 7). For high ionic strengths the Davies model for activity coefficients is no longer appropriate, and a SIT activity coefficient model has been included in MCOTAC following HUMMEL (2009). SIT data for NaCl solutions were taken from THOENEN (2012). The results are shown in Fig. 3.7. The activity coefficient models predict different profiles already for an ionic strength of 0.3 M. With the Davies model the tracers were predicted to migrate further into the sample than with the SIT model. These differences originate from the formulation of the surface complexation reactions which require Na and Cl concentrations to be charge neutral in the reactive transport calculations (PFINGSTEN et al., 2011). For a given set of transport parameters, both activity coefficient models predict a deeper penetration of the tracers into the sample at higher ionic strengths, contrary to the experimental observations.

Future modelling activities will focus on the effect of the longer pre-equilibration time on the tracer in-diffusion profiles. Since the artificial clay porewater used in the long-term experiments was prepared according to equilibrium concentrations of Na, K, Ca,

Mg, Sr, Cl, SO_4^{2-}, CO_3^{2-} and pH, the leaching of other elements present in the clay sample/porewater can not be excluded, especially Fe and Mn. A potential mismatch in pH between the artificial porewater in the reservoir and the in situ clay porewater may occur and influence the Zn and Co diffusion/sorption processes in the clay sample. Sorption competition between Zn, Co, Fe, Mn and surface protonation reactions can also be expected, as well as Fe fronts within the clay sample. These possibilities should be assessed in advance of further in-diffusion experiments.

3.4 Understanding transport and sorption mechanisms

3.4.1 Cement/clay interfaces: porosity and structural changes and their relation to transport properties

Cement and concrete materials will be used as engineered barriers in radioactive waste repositories and will come directly into contact with the clay-rich host rocks. The geochemical difference between cements and clays leads to chemical alternations at their interfaces which need to be quantified in order to assess the potential influence on the long-term safety of the disposal sites. The project "Evolution of cement/clay interfaces" (PhD student Amir Shafizadeh) is aimed at the simultaneous monitoring of mineral dissolution/precipitation and porosity changes which are expected to occur at cement/clay interfaces using complementary experimental techniques, and relating these changes to the transport parameters at the interface (diffusion coefficients, accessible porosity).

A diffusion cell has been developed to accommodate an interface sample consisting of a small (5 mm diameter, 5 mm length) clay plug (montmorillonite) and a small hardened cement paste plug (OPC) of the same size. This cell allows bulk diffusion coefficients to be estimated from standard through-diffusion measurements with a tracer such as HTO. This cell can be transferred to the neutron tomography station ICON at SINQ/PSI to image the tracer movement. This will potentially allow local diffusion properties to be estimated near the interfaces of the samples which can be related to the observed structural changes.

The first neutron images of a saturated cement-clay interface have been acquired (Fig. 3.8). Preliminary tests indicate that the cell design needs to be improved in order to sustain the high swelling pressure of the clay without adversely affecting the neutron imaging capabilities. Several such optimized cells and sample holders will be built and filled with interface samples. These will then be stored at an elevated temperature in order to speed up the mineralogical reactions. Structural changes will be examined by X-ray diffraction, X-ray fluorescence, micro-XRD and FIB/SEM methods on thin sections prepared from the samples. The results obtained will be used in reactive transport modelling codes to improve the predictions on long-term repository behaviour.

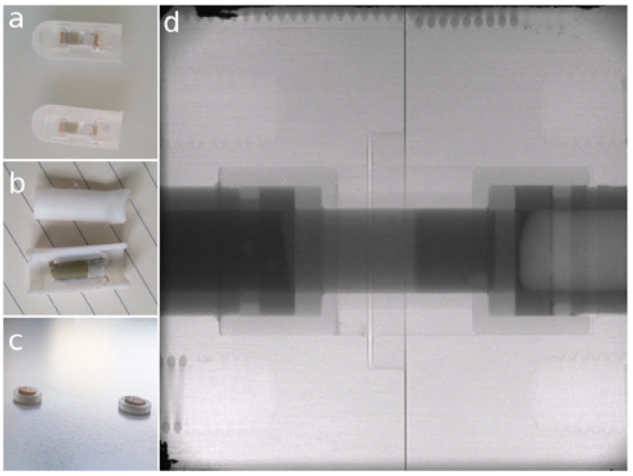

Fig. 3.8: *Sample holder for cement-clay interface investigations and a neutron image obtained at SINQ/PSI (a) Cross section of the sample after sawing the sample preserved in epoxy-resin with a diamond-saw which caused damage to the interface. (Clay, left; and cement, right). (b) Cut-away view of a second sample showing that the high swelling pressure of the montmorillonite has pushed the central part of the sample out as shown in (c). A neutron test image (d) promises good resolution for the water content measurements based on this setup.*

3.4.2 Ab initio simulations of aluminium substitutions in C-S-H

Within a postdoc sub-project "Thermodynamic equilibrium in C(-A)-S-H from molecular simulations" (L. Pegado), which is a part of a SNF-funded Sinergia project "Stable phase composition in novel cementitious materials: C(-A)-S-H (Calcium-(Aluminium)-Silicate-Hydrate)", the influence of aluminium substitutions on alkali and alkali earth ion sorption by C-S-H phases is being investigated using periodic Density Functional Theory (DFT) calculations. The emphasis of the simulations is on the preferential positions and the relative energies of different Al-Si substitutions. The C-S-H phase is being modelled based on a single structural layer-module of the natural mineral tobermorite (TAYLOR, 1993), $[Ca_4Si_6O_{14}(OH)_4]\cdot 2H_2O$, with so-called silicate "dreierketten" chains of alternating one bridging and two pairing tetrahedra on both surfaces.

By comparing the energy of a tobermorite "plate" with a single Al substitution in a bridging or in a pairing position, it was found that the former is more stable by 18 Kcal/mol. The study was extended to configurations with two Al substitutions; both in bridging positions, or both in pairing positions, or one in each, and including substitutions in the same or different "dreierketten" chains (next nearest and second next nearest neighbours). The simulations indicate that the system becomes more unstable with increasing Al pairings. It appears that there are no major correlations in the location of the Al for a given combination (e.g. two bridging Al). There is therefore strong computational evidence that Al in C-S-H phases sits preferentially in bridging positions, in agreement with experimental information (YU et al., 1999, PARDAL et al., 2012). The picture does not change even in the case where one Al is in a pairing position in the "end of a chain" i.e. adjacent to a missing bridging tetrahedron ("defect").

3.5 Benchmarking of coupled codes

Benchmarking of transport codes is an important activity which supports the credibility of the numerical simulations. It is essential for reactive transport codes describing complex geochemical interactions and/or radionuclide migration in the vicinity of a nuclear waste repository or in laboratory experiments.

3.5.1 Reactive transport modelling of natural analogues

To cross-benchmark geochemical setups and reactive transport simulation approaches against experimental data, and other transport codes, the group is participating in the Grimsel LCS (Long Term Cement Studies) project. Within this project the Maqarin natural analogue is being investigated in terms of the long-term changes occurring in rocks in contact with a hyperalkaline solution. Several modelling teams have applied state-of-the-art geochemical models to re-appraise the earlier simulations of STEEFEL & LICHTNER (1998). In the approach taken here (in collaboration with H. Shao UFZ Leipzig) the geochemical setup for the rock mineralogy and the porewater was calibrated to match measurements from the Maqarin site (SHAO et al., 2012). The setup includes several clay and zeolite minerals, considers cation exchange processes, and a state-of-the-art model for cement phases. Similar to the earlier calculations of STEEFEL & LICHTNER (1998), who used a much simpler geochemical model, pore clogging occurred after several hundred years at a distance of 5 - 10 mm from the surface in contact with the hyper alkaline solution. The cause of the pore clogging was a massive precipitation of ettringite and C-S-H minerals. Sensitivity studies performed by varying the intrinsic diffusion coefficient, the exponential factor in Archie's relation, and the mineral surface area available for dissolution and precipitation, showed that the dissolution of clay minerals controlled the availability of Al which was needed for ettringite and C-S-H phase precipitation. Thus, the initial amount of clay minerals and their dissolution rates controlled the spatial and temporal evolution of porosity changes. The simulations revealed that neither cation exchange processes, nor the formation of zeolite minerals, strongly influenced the geochemical evolution of the system.

3.5.2 OpenGeoSys consortium and co-operation with UFZ-Leipzig

Within the co-operation agreement between the Helmholtz Centre for Environmental Research (UFZ, Leipzig, Germany) and LES, the Richard's flow module has been added into the OpenGeoSys-GEMS coupling. With this module it has become possible to simulate geochemical reactions in partially saturated media. Furthermore, the coupled OpenGeoSys-GEMS version was parallelized with a hybrid algorithm based on MPI and OMP threads. This enables a much more effective simulation of 2D/3D systems on current high performance computers.

In October 2012 the OpenGeoSys version 5.3.05 was published. This version contains the GEMS3K V3 source code which was published in October 2012 after several years of development under the LGPL license. On the 11th October 2012 an OpenGeoSys community meeting took place in Leipzig where the new OpenGeoSys-GEMS version was presented. On the same day the OpenGeoSys steering board met in which Georg Kosakowski represented the LES. On the 12th October 2012 the first meeting of a network of PhD students working in the field of reactive transport took place at the Division for Reactive Transport of the Helmholtz Centre Dresden-Rossendorf. PhD students from HZDR, UFZ and PSI presented their work. In particular, a strong exchange is expected in the framework of the PhD project on "Reactive transport benchmark for coupled codes" (PhD student Jenna Poonoosamy, started in October 2012).

3.5.3 Fluid-rock interaction modelling: Geothermal electrolyte solutions thermodynamic model and computational fitting framework development

In June 2012, PhD student Ferdinand Hingerl (GEOTHERM project supported by the Competence Center Environment and Sustainability, the Paul Scherrer Institut and the Swiss Ministry of Energy) successfully defended his PhD thesis at the ETH, Zürich. Within his PhD project, Ferdinand Hingerl developed an activity model for geothermal aqueous multi-electrolyte solutions rEUNIQUAC (revised Extended Universal QUAsi-Chemical activity model) and a stand-alone module for the GEMS-code, GEMSFIT, which is a versatile computational tool for fitting thermodynamic models. The rEUNIQUAC has been applied to model the long-term permeability evolution of geothermal reservoirs.

The rEUNIQUAC activity model provides excess thermodynamic properties of aqueous binary solutions over a wide range of temperatures, from 298 to up to 573 K, and for concentrations up to 5 M (or saturation if the solubility is smaller than 5 M) under saturated water vapor conditions. Compared to the original EUNIQUAC, it implements a stricter treatment of long-range electrostatic interactions, an improved temperature dependence on the UNIQUAC parameters, and an empirical parameter for strongly associating electrolytes. The model is comparable to the standard Pitzer model in terms of accuracy, but requires less parameters and employs a simpler temperature dependence. In contrast to the Pitzer model, rEUNIQUAC does not require the addition of associated species, even in highly non-ideal systems containing complexing electrolytes.

The stand-alone computational module GEMSFIT is the first open-source implementation of a generic thermodynamic fitting tool coupled to a chemical equilibrium solver which uses the direct Gibbs energy minimization approach. GEMSFIT provides the most common tools for statistical analysis which allows a thorough evaluation of the fitted parameters, and it has a generic interface to a PostgreSQL database to access measurement data. Results from parameter regression, as well as from statistical analysis, can be visualized and directly printed to various graphical formats. Usage of the code is facilitated by a graphical user interface which assists in setting up GEMSFIT input files. Using GEMSFIT, an internally consistent set of rEUNIQUAC parameters has been created for the binary electrolyte systems NaCl-H_2O, KCl-H_2O, $CaCl_2$-H_2O, $MgCl_2$-H_2O, HCl-H_2O, NaOH-H_2O, KOH-H_2O, Na_2SO_4-H_2O, K_2SO_4-H_2O and $MgSO_4$-H_2O. The fitted parameters cover temperatures up to 573 K and a maximum concentration of 5 M. Furthermore, Ferdinand Hingerl has successfully fitted anhydrite solubility in a NaCl-H_2O solution from 373 to 573 K (Fig. 3.9), which demonstrates that rEUNIQUAC has the potential to be applied to mixed-electrolyte solutions, even if they contain highly complexing solutes.

Recent benchmarking studies performed by ANDRE et al. (2006) demonstrated that slight differences in activity coefficients, thermodynamic equilibrium constants and kinetic models can result in significant differences in the predicted mineral assemblages. Motivated by these discrepancies, Ferdinand Hingerl has investigated thermodynamic activity models (e.g. Pitzer, rEUNIQUAC) and associated computational fitting frameworks suitable for the description of fluid-rock interactions in Enhanced Geothermal Systems.

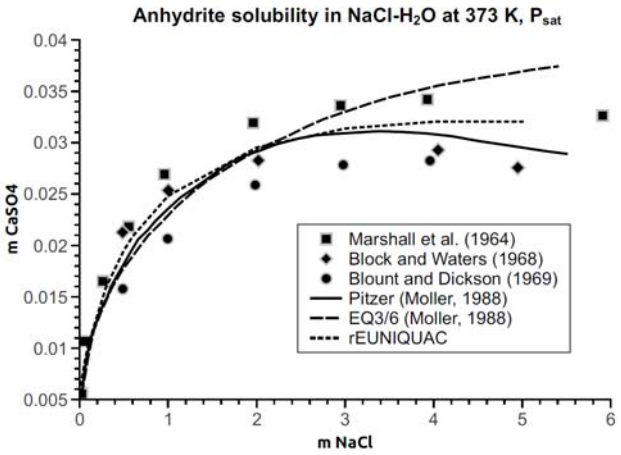

Fig. 3.9: *Predicted and measured solubilities of anhydrite in the system NaCl-$CaSO_4$ at 373 K, P_{sat} (from HINGERL, 2013).*

3.6 References

ANDRÉ, L., SPYCHER, N., YU, T., PRUESS, K., VUATAZ, F.-D. (2006)
Comparing FRACHEM and TOUGHREACT for reactive transport modeling of brine-rock interactions in Enhanced Geothermal Systems (EGS). Proceedings of the 31st Workshop on Geothermal Reservoir Engineering, Stanford University, 350–358.

BERNER, U., KULIK, D.A., KOSAKOWSKI, G. (2012)
Influence of a low-pH cement liner on the near-field of a repository for spent fuel and high-level radioactive waste. Phys. Chem. Earth, submitted.

CHURAKOV, S.V. & GIMMI, TH. (2011)
Up-scaling of molecular diffusion coefficients in clays: a two-step approach. J. Phys. Chem. C 115, 6703-6714.

HINGERL, F. (2013)
Geothermal electrolyte solutions: thermodynamic model and computational fitting framework development. Thesis, ETH Zürich, (in prep.).

HUMMEL, W. (2009)
Ionic strength corrections and estimation of SIT ion interaction coefficients. PSI Technical Report TM-44-09-01.

KOSAKOWSKI, G., BERNER, U. (2012)
The evolution of clay rock/cement interfaces in a cementitious repository for low and intermediate level radioactive waste. Phys. Chem. Earth, submitted.

PARDAL, X., BRUNET, F., CHARPENTIER, T., POCHARD, I., NONAT, A. (2012)
^{27}Al and ^{29}Si solid-state NMR characterization of calcium-aluminosilicate-hydrate. Inorg. Chem. 51, 1827-1836.

PFINGSTEN, W., BRADBURY, M.H., BAEYENS, B. (2011)
The influence of Fe(II) competition on the sorption and migration of Ni(II) in MX-80 bentonite. Appl. Geochem. 26, 1414-1422.

SHAO, H., KOSAKOWSKI, G., BERNER, U., KULIK, D.A., MÄDER, U.K., KOLDITZ, O. (2012)
Reactive transport modeling of the clogging process at Maqarin natural analogue site. Phys. Chem. Earth, submitted.

STEEFEL, C., LICHTNER, P. (1998)
Multicomponent reactive transport in discrete fractures - II: Infiltration of hyperalkaline groundwater at Maqarin, Jordan, a natural analogue site. J. Hydrology 209(1-4), 200–224.

TAYLOR, H.F.W. (1993)
Nanostructure of C-S-H: Current status. Adv. Cem. Based. Mater. 1, 38–46.

THOENEN, T. (2012)
SIT database for NaCl solutions. Priv. comm.

VAN LOON, L.R., SOLER, J.M., MUELLER, W., BRADBURY, M.H. (2004)
Anisotropic diffusion in layered argillaceous rocks: A case study with Opalinus clay. Environ. Sci. Technol. 38, 5721-5728.

YU, P., KIRKPATRICK, R.J., POE, B., MCMILLAN, P.F., CONG, X.D. (1999)
Structure of calcium silicate hydrate (C-S-H): Near-, mid-, and far-infrared spectroscopy. J. Am. Ceram. Soc. 82, 742-748.

4 CLAY SORPTION MECHANISMS

B. Baeyens, M.H. Bradbury, R. Dähn, M. Marques Fernandes, A. Schaible, D. Soltermann (PhD), N. Ver (guest scientist)

4.1 Overview

One of the main activities in the Clay Sorption Mechanisms group in 2012 was directly related to Stage 2 of the Sectoral Plan (SGT-E2). This work comprised of the following topics.

- Sorption data bases (SDBs) for the different host rocks (Opalinus Clay, "Brauner Dogger", Effingen Member, Helvetic Marl), the underlying confining units, and for MX-80 bentonite were developed and documented (Nagra NTB 12-04) for the provision safety analyses for SGT-E2.

- The results on the comparison of sorption measurements on Opalinus Clay, "Brauner Dogger" Effingen Member and MX-80 bentonite with blind predictions made using the same methodology developed to derive the SDBs have been compiled and reported (Nagra NTB 12-05).

Mechanistic sorption studies on clay minerals are an on-going activity and involved the following issues:

- Estimates of the influence of competitive sorption on the sorption values in the SDB for MX-80 have been modelled using the 2SPNE SC/CE sorption model.

- The results obtained using the "bottom-up" sorption modelling approach were compared with sorption measurements on Boda Claystone (Boda) samples. This work was carried out in the framework of the Swiss-Hungarian co-operation project SH/2/11/7.

- The Fe(II) clay interaction investigations were carried out on a synthetic iron-free montmorillonite using a combined wet chemistry, sorption modelling and spectroscopic approach (PhD project).

XAS investigations were carried out in support of the Fe(II) clay interaction PhD project, and on metal uptake by argillaceous rocks, i.e. Boda and Opalinus Clay (Swiss-Hungarian co-operation project).

The joint research project between the Hungarian Academy of Sciences and the Paul Scherrer Institut focussed on wet chemistry investigations on the Boda Claystone. A guest scientist (N. Ver) from the Centre for Energy Research (Budapest) spent 6 months working in LES.

4.2 Activities in support of the Sectoral Plan

4.2.1 Sorption data bases for SGT-E2

In Stage 2 of the Sectoral Plan, four host rock types have been identified as being potentially suitable for constructing radioactive waste repositories, namely, Opalinus Clay (SF/HLW, ILW), and "Brauner Dogger", Effingen Member and Helvetic Marl (L/ILW) (NAGRA, 2008). Sorption data bases for all of these host rocks are required for the planned Provisional Safety Analyses including all of the bounding porewater and mineralogical composition combinations. In addition, SDBs are needed for the rock formations lying below the Opalinus Clay host rock formations (lower confining units) and for the compacted bentonite backfill in a SF/HLW repository. Since for any one rock type there may be as many as three mineralogical compositions and four porewater chemistries which need to be considered for a radionuclide vector consisting of 32 radionuclides, directly measuring the sorption data required for this number of possible combinations is not feasible.

The methodology to derive sorption data bases has been described in detail by BRADBURY et al. (2010), and is based on sorption edge measurements on illite (and montmorillonite), the hypothesis that 2:1 type clay minerals are the dominant sorbents, and on the application of a series of so called conversion factors which take into account the different radionuclide speciation in the different porewaters. A Lab→Field conversion factor was applied to convert sorption data measured in dispersed systems (batch

experiments) to intact rock under in situ conditions. This methodology to develop sorption data bases has been applied to the argillaceous rocks and compacted bentonite taking into account the mineralogical and porewater composition ranges defined. In a few cases the mineralogy of the rock type was too low in clay mineral content to apply this approach. For these types of rocks SDBs were nevertheless developed, but based on a methodology in which calcite was considered to be the main sorbing phase. A report has been prepared summarising all of the SDBs required for the Provisional Safety Analyses for SGT-E2 (BAEYENS et al., 2012a).

4.2.2 Sorption measurements on host rocks

The methodology for generating SDBs as described in section 4.2.1 is relatively new, and a means of creating confidence in its application and in the robustness and reliability of the sorption values derived was required. An extensive exercise in which blind predictions of sorption values were compared with ones measured on the selected host rocks and MX-80 bentonite was carried out.

Sorption isotherms were measured for metals with valences from I to VI, i.e. Cs(I), Co(II), Ni(II), Eu(III), Th(IV) and U(VI), for a range of host rock mineralogies and their corresponding porewater chemistries. A total of 37 sorption isotherm data sets were measured. For each of these isotherms a prediction was made of the sorption at trace concentrations using the SDB derivation methodology. A comparison between measured ($R_{d,meas}$) and predicted ($R_{d,pred}$) values for each case was then made. Table 4.1 gives a summary of the results for the different host rocks and for MX-80 bentonite. For the cases where the ratios $R_{d,pred}/R_{d,meas}$ are >1, the sorption values are over predicted, whereas for ratios <1 they are under predicted.

From the information presented here, and other recent studies, e.g. BRADBURY & BAEYENS (2010, 2011), there is now a substantial body of evidence which strongly supports the approach and methodology for developing SDBs for argillaceous rocks and bentonite described in BRADBURY et al. (2010). It can be concluded that the SDBs for argillaceous rocks, and bentonite, can be used with confidence and that the values have a high degree of reliability. The results of this work are documented in a Nagra technical report (BAEYENS et al., 2012b)

4.3 Mechanistic sorption investigations

4.3.1 Estimates of the influence of competition on the sorption values in the SDB for MX-80 bentonite

The bentonite porewater of a deep geological repository for high-level waste contains dissolved impurities from many sources (stable element inventories in the porewater/bentonite, corrosion products, etc.) and radionuclides. These elements/ radionuclides can potentially compete with one another for the available sorption sites which may result in a reduction in the sorption of radionuclides. For the near-field system the influence of sorption competition cannot be determined directly by experiment. (The system is too complex and varied). However, there is experimental and modelling evidence that competitive sorption occurs between elements of the same valence and similar hydrolysis behaviour i.e (II) with (II), (III) with (III) and (IV) with (IV), but not between (II), (III) and (IV) (BRADBURY & BAEYENS, 2005a).

Estimates of the potential reduction in sorption due to competitive processes can be assessed by using a sorption model such as the 2SPNE SC/CE model (BRADBURY & BAEYENS, 1997). A case study was set up in which the solubility data in bentonite porewater was considered (BERNER, 2002), Table 4.2.

Table 4.1: *Sorption values measured at trace concentrations for host rocks and MX-80 bentonite, and the predictions based on illite and montmorillonite sorption data (BAEYENS et al., 2012b).*

Rock	Location	Sample	Radio-nuclide	$R_{d,\,pred}$ ($m^3\ kg^{-1}$)	$R_{d,\,meas}$ ($m^3\ kg^{-1}$)	$\frac{R_{d,pred}}{R_{d,meas}}$
OPALINUS CLAY	Mont Terri	BGP-1-C11 (pH = 6.3)	Cs(I)	1.7	2.8	0.6
			Ni(II)	0.72	0.25	2.9
			Eu(III)	1.0	6.3	0.16
			Th(IV)	8.7	20	0.44
		BGP-1-C11 (pH ~ 8)	Cs(I)	0.71	1.0	0.7
			Ni(II)	1.9	6.3	0.3
			Eu(III)	29	63	0.5
			Th(IV)	158	63	2.5
			U(VI)	0.10	0.13	0.8
		DI-A0-3.2	Cs(I)	2.5	1.6	1.6
			Co(II)	0.74	0.4	1.9
	Benken	BEN-636	Cs(I)	1.2	0.7	1.7
	Schlattingen	SLA-938	Cs(I)	3.0	2.5	1.2
			Co(II)	1.3	1.6	0.8
			Ni(II)	2.0	7.6	0.3
			Eu(III)	30	63	0.5
			Th(IV)	162	79	2.1
BRAUNER DOGGER	Clay-rich sequence	BEN-482	Cs(I)	1.6	0.9	1.8
			Co(II)	2.1	1.6	1.3
			Ni(II)	1.8	2.5	0.3
			Eu(III)	20	100	0.2
			Th(IV)	49	50	1.0
	Sandy-limestone sequence	SLA-795	Cs(I)	0.17	0.16	1.1
			Ni(II)	0.17	0.20	0.9
EFFINGEN MEMBER	Calcareous marl sequence	OFT-619	Cs(I)	1.2	0.4	3
			Co(II)	1.0	0.3	3.3
			Ni(II)	0.74	0.16	4.6
			Eu(III)	17	63	0.3
			Th(IV)	74	79	0.9
			U(VI)	0.038	0.013	2.9
	Limestone sequence	OFT-492	Cs(I)	0.4	0.4	1.0
			Ni(II)	0.3	0.16	1.9
BENTONITE	-	MX-80	Cs(I)	0.015	0.02	0.8
			Ni(II)	1.4	0.32	4.4
			Eu(III)	49	13	3.8
			Th(IV)	204	79	2.6
			U(VI)	0.06	0.025	2.4

Table 4.2: *Maximum concentrations (in mol L^{-1}) of elements in the porewater of a bentonite near-field of a high level waste repository (BERNER, 2002).*

BIVALENT		TRIVALENT		TETRAVALENT	
Metal	max. conc.	Metal	max. conc.	Metal	max. conc.
Cd	2×10^{-5}	Pm	5×10^{-7}	Zr	2×10^{-9}
Co	3×10^{-5}	Eu	5×10^{-7}	Hf	2×10^{-9}
Ni	3×10^{-5}	Ho	5×10^{-7}	Sn	10^{-8}
Fe	4.3×10^{-5}	Ac	10^{-6}	Th	7×10^{-7}
Pb	2.0×10^{-6}	Pu	5×10^{-8}	U	3×10^{-9}
		Am	10^{-6}	Np	5×10^{-9}
		Cm	10^{-6}		
∑(II)	1.25×10^{-4}	∑(III)	4.55×10^{-6}	∑(IV)	7.22×10^{-7}

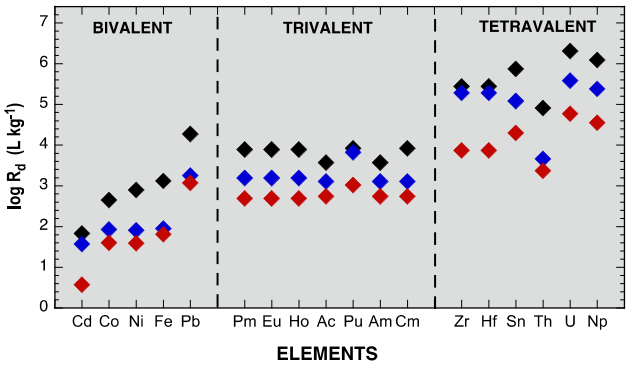

Fig. 4.1: *Sorption values for the MX-80 bentonite at trace concentrations (◆), at maximum concentrations (◆) (Table 4.2), and taking into account competitive effects (◆).*

In a first step, calculations were made in the MX-80 bentonite porewater/mineral system to produce sorption values for each element individually at trace concentration (black symbols, Fig. 4.1) and at the maximum equilibrium concentration given in Table 4.2 (blue symbols, Fig. 4.1). In a second step, for each group of elements i.e. bi-, tri- and tetravalent, sorption values for each element within the same group were calculated simultaneously with all of the others at the corresponding (equilibrium) concentrations given in Table 4.2 (red symbols, Fig. 4.1). The calculations were carried out with the surface complexation constants given in BRADBURY & BAEYENS (2005b). For the elements where no measurements were available, the linear free energy relationship was used to derive the constants. For the tetravalent elements only the sorption on the strong sites was considered since no data are available for the weak sites.

The sorption model calculations indicate that the influence of competition on trace element sorption values is to reduce them by approximately one order of magnitude for bi- and trivalent elements, and two orders of magnitude (max.) for tetravalent elements. For the bivalent and trivalent elements at high equilibrium concentrations, reductions in sorption values due to competition are relatively small because sorption is occurring predominantly on the weak sites which do not saturate. For the tetravalent elements, the reductions are larger because sorption on weak sites is not considered. The results in Fig. 4.1 indicate that in almost all cases the sorption remains significant due to uptake on the montmorillonite "weak sites" which have a high capacity for the bivalent and trivalent elements, and because the tetravalent elements are still sorbing predominantly on the strong sites (low solubilities, $< 10^{-6}$ M).

4.3.2 Modelling Boda Claystone sorption measurements: "Bottom up" approach

The "bottom-up" modelling approach is based on the premise that radionuclide uptake in complex mineral/groundwater systems can be quantitatively predicted from a knowledge and understanding of the mechanistic sorption processes on single minerals, in particular clay minerals, and the models developed to describe them. This approach has been successfully applied to Opalinus Clay and MX-80 bentonite (BRADBURY & BAEYENS, 2011) and the aim was to test the method on Boda samples.

Sorption isotherms for Cs(I), Ni(II), Co(II), Eu(III), Th(IV) and U(VI) were measured on Boda in a synthetic porewater. The isotherms were calculated using the 2SPNE SC/CE model and the PSI/Nagra 07/12 TDB (THOENEN, 2012), assuming that only the free metal ion and hydrolysed species were sorbing. These values were then scaled by a factor of 0.50, the clay mineral fraction in Boda. The results of the blind predictions (solid lines) for the Cs(I), Ni(II), Co(II),

Eu(III), Th(IV) and U(VI) isotherms measurements on Boda (symbols) are shown in Fig. 4.2.

From the results shown in Fig. 4.2 it is clear that Boda exhibits sorption properties which are comparable with other argillaceous rocks such as Opalinus Clay (BRADBURY & BAEYENS, 2011). The Cs(I) sorption was predicted well with the generalised Cs sorption model (BRADBURY & BAEYENS, 2000), however without frayed edge sites (FES). The FES sites may be blocked with stable Cs (slow desorption kinetics) or absent in the case of the 2:1 type clay minerals identified in Boda i.e. an illite/muscovite mineral. The blind predictions made using the 2SPNE SC/CE sorption model for Ni(II)/Co(II) and Th(IV) were good at equilibrium concentrations below 10^{-7} M and 10^{-8} M, respectively. At higher concentrations the model under predicted the sorption which may be due to surface induced precipitation effects. The sorption of Eu(III) and U(VI) were generally under predicted. For Eu(III) and U(IV) ternary carbonato surface complexes should probably be included in the model, based on the existence of such ternary complexes in montmorillonite systems (MARQUES FERNANDES et al., 2008, 2010, 2012). However, no data are currently available for illite.

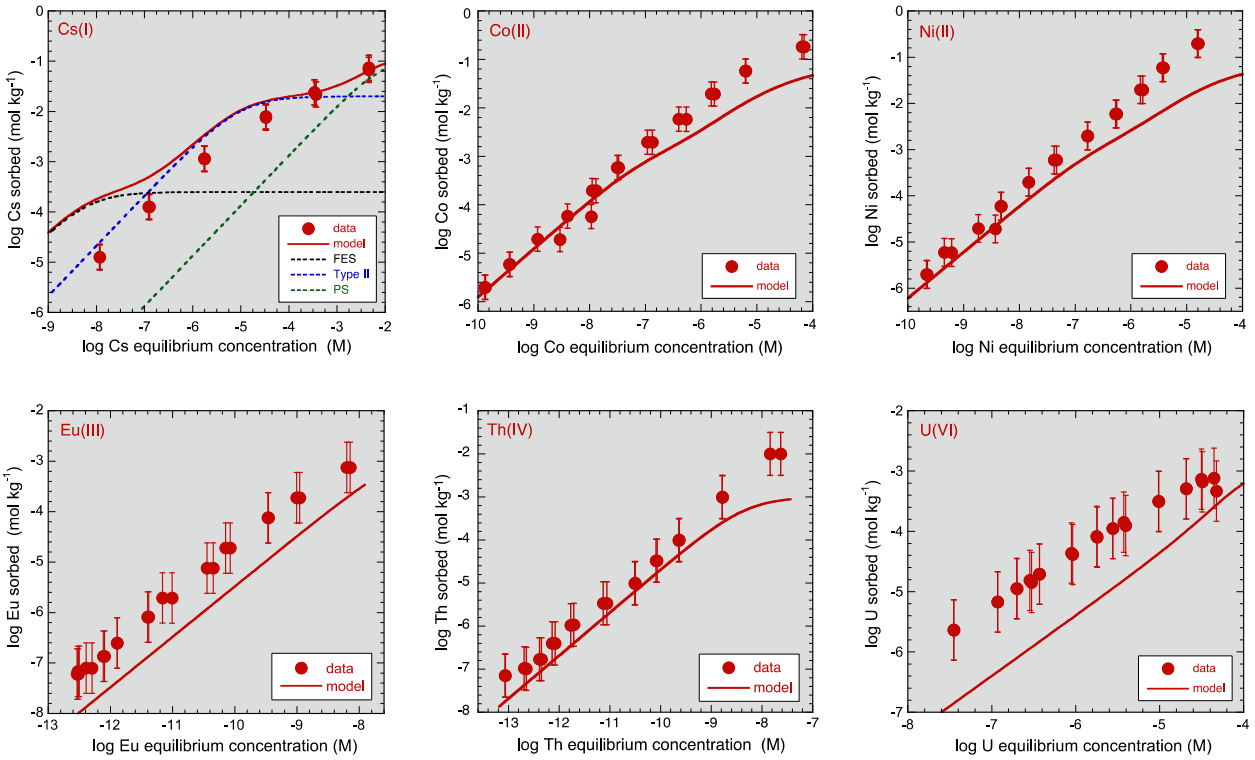

Fig. 4.2: *Sorption isotherms on Boda Claystone: Experimental results and modelling.*

4.3.3 Macroscopic and spectroscopic investigations of Fe(II)/montmorillonite interactions (PhD project)

Within the framework of the PhD thesis entitled "The influence of Fe(II) on clay properties, the sorption of Fe(II) on clays, and competitive sorption investigations: a combined macroscopic and microscopic study" EXAFS and Mössbauer spectroscopy, combined with macroscopic sorption experiments and modelling were applied to investigate the sorption mechanism of Fe(II) on a homo-ionic Na synthetic iron free montmorillonite (Na-IFM) i.e. a montmorillonite without any structural iron. Batch sorption experiments were performed to measure the Fe(II) uptake on Na-IFM at trace concentrations as a function of pH, and as a function of sorbate concentration at pH 6.7, under anoxic conditions (O_2 < 0.1 ppm). The uptake of Fe(II) at trace concentration (~10^{-7} M) on Na-IFM (Fig. 4.3a) shows a strong dependency on pH in the range 4 to 8, which is typical for the sorption of bivalent transition metals (BRADBURY & BAEYENS, 2005b). The Fe sorption isotherm on Na-IFM at pH 6.7 in 0.3 M $NaClO_4$ exhibits a clear non-linear behaviour (Fig. 4.3b).

Both types of sorption data sets could be successfully modelled with the 2SPNE SC/CE model using the same set of surface complexation reactions and constants. The cation exchange (CE) selectivity coefficient K_c was estimated from the edge data at low pH, yielding a *log* K_c of 0.8 ± 0.1. The pH dependent Fe(II) uptake above pH 4 was fitted in terms of Fe(II) bound on strong surface hydroxyl groups ($\equiv S^SOFe^+$) at clay edges using *log* ^SK = 1.9 ± 0.3. To fit the sorption isotherm one additional surface complex on the weak edge sites, $\equiv S^WOFe^+$, with a *log* ^WK = -2.0 ± 0.3 was required. The predicted constants from the linear free energy relationships between the surface complexation constants and the associated hydrolysis constants of bivalent metals i.e. *log* $^SK_{LFER}$ = 0.8 ± 1.0, *log* $^WK_{LFER}$ = -2.7 ± 1.6 (BRADBURY & BAEYENS, 2005b), are in broad agreement with the modelled ones, increasing the credibility and reliability of the sorption model and the assumption that Fe(II) is the sorbing species. The sorption model for Fe(II) was used to define the experimental conditions for the preparation of EXAFS and Mössbauer samples for which the Fe(II) was predominantly sorbed onto either the "strong" or the "weak" sites. Four samples with different Fe loadings (low 1.7 and 2.7 mmol kg^{-1}; high 12.3 and 17.0 mmol kg^{-1}) were prepared and investigated.

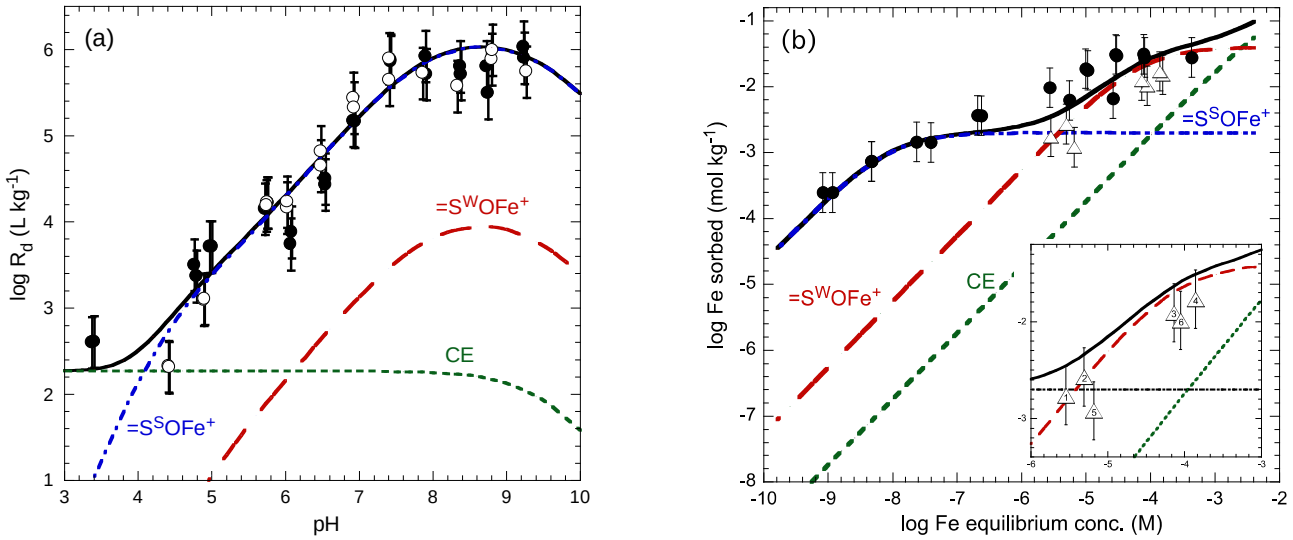

Fig. 4.3: *(a) Sorption edge data of Fe(II) on synthetic Na-IFM (symbols) in 0.1 M $NaClO_4$. (b) Fe(II) sorption isotherm data on Na-IFM at pH 6.7 in 0.3 M $NaClO_4$. The Fe(II) loadings used in the EXAFS/Mössbauer measurements were analyzed by ICP-OES (open triangles). The continuous lines are the best-fit curves obtained using the 2SPNE SC/CE sorption model. The contributions of the Fe surface species to the overall sorption are illustrated by the different broken curves. (strong sites: $\equiv S^SOFe^+$; weak sites: $\equiv S^WOFe^+$; cation exchange: CE).*

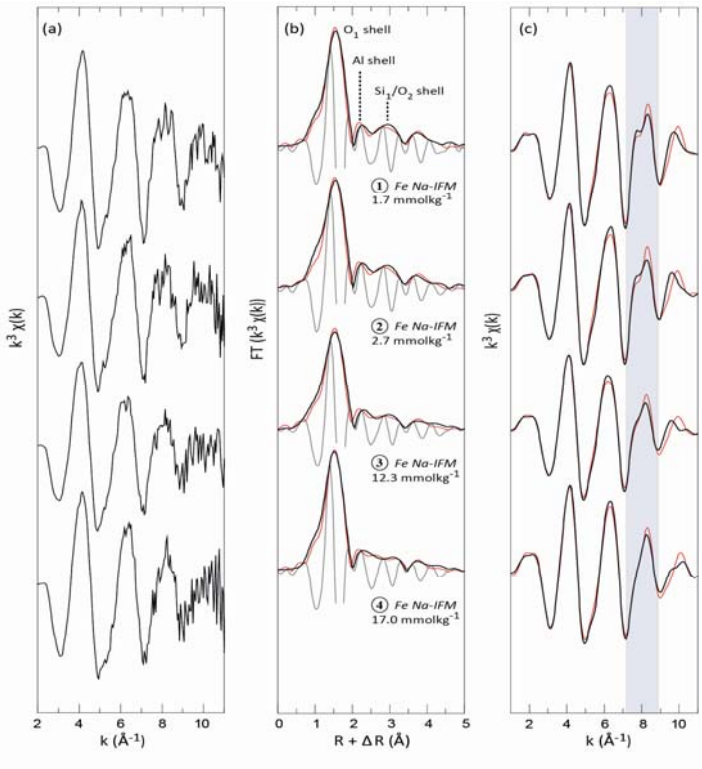

Fig. 4.4: *(a) k^3-weighted Fe K-edge EXAFS spectra obtained for Fe sorbed on synthetic Na-IFM, (b) the corresponding RSFs and, (c) the least-squares fit of FT^{-1} EXAFS data. The red line represents the fit of the real and imaginary parts.*

The k^3-weighted EXAFS spectra of the four Fe loaded Na-IFM samples showed a multi-frequency wave shape indicating that Fe atoms were surrounded by more than one neighbouring shell, and consequently, that outer-sphere complexation (cation exchange) was not the predominant uptake mode (Fig. 4.4a). In the corresponding radial structure functions (RSFs) there was a backscattering peak (Fe-O contribution) at R+ΔR = 1.54 Å, which was essentially invariant with increasing Fe loading (Fig. 4.4b). Beyond the first shell further RSF peaks in the R+ΔR range between 2 and 4.5 Å were present, which can be attributed to Fe-Al, Fe-Si, long Fe-O, and long Fe-Si-tetrahedral backscattering pairs. These peaks in the RSFs were less pronounced in the spectra for higher Fe loadings, suggesting either a higher disorder or a decrease in coordination numbers. The FT^{-1} data in the range of R+ΔR from 1 to 4.5 Å showed a splitting of the EXAFS oscillation at ~8 $Å^{-1}$ at low metal loading, indicating slight structural differences between the samples (Fig. 4.4c). With increasing loading the prominence of this feature decreased. The structural parameters derived from EXAFS measurements were characteristic of bivalent metals located in the octahedral sheets of a 2:1 phyllosilicate (SCHLEGEL et al., 2001; DÄHN et al., 2011). Data analysis indicated that the structural environment of the sample with the lowest metal loading consisted of different shells: 4.0±0.6 O at 2.01±0.01 Å, 2.3±1.0 Al at 3.04±0.05 Å and 3.4±1.4 Si at 3.20±0.03 Å. The obtained coordination numbers and distances for the Fe-Si backscattering pairs agree well with the structural parameters derived for Zn sorbed on the edge sites of STx-1 montmorillonite (DÄHN et al., 2011) except that in the case of the Zn study an additional short Zn-Si distance at ~3.1 Å was observed. This difference can be attributed to the different symmetries of the synthetic and the natural montmorillonite. Whereas most of natural montmorillonites are cis vacant (c2 symmetry), the synthetic montmorillonite used in this study was trans vacant (c2/m symmetry). The c2/m symmetry has a much more regular crystal structure, whereas

the c2 montmorillonite structure is corrugated, causing a greater difference in Si-distances. It seems, therefore, that sorption to trans-symmetric octahedral positions prevailed. With increasing Fe loading the Fe-Al and Fe-Si distances sequentially increased, i.e. $R_{Fe\text{-}Al}$ = from 3.04 Å to 3.09 Å, and $R_{Fe\text{-}Si}$ = from 3.20 Å to 3.25 Å (sample 1 to 4). This finding is consistent with the hypothesis that iron complexes at the high loadings (weak sites) exhibit a stronger structural disorder and are less well crystallographically defined than iron sorbed at low loadings (strong sites) (DÄHN et al., 2011). Mössbauer spectroscopy measurements confirmed that Fe was predominantly present as Fe(II) on the Na-IFM surface.

4.4 XAS investigations of Ni(II) and Zn(II) uptake by argillaceous rocks

The joint research project between the Hungarian Academy of Sciences (Centre for Energy Research) and the PSI/LES aims at investigating uptake of the metals by argillaceous rocks by a combined wet chemistry, geochemical modelling and spectroscopic approach. In 2012 EXAFS was used to investigate the uptake of bivalent metals by argillaceous rocks.

The uptake of Ni(II) and Zn(II) on two types of argillaceous rocks, the Boda Claystone (Boda) from Hungary and the Opalinus Clay (OPA) from Switzerland, was investigated. Zn was chosen because of the lower detections limits and a better signal to noise ratio in the Fe rich rock matrix. Clay minerals are important components in such rock types and can often make up 50 or more wt.% of the total mass. They are considered to be the predominant phases responsible for metal uptake in such complex natural systems. Therefore, as reference samples, Ni and Zn treated illite samples were used. The samples and references were prepared at pH ~7.0 in an 0.1 M $NaClO_4$ background electrolyte and at metal loadings varying from 15 to 42 mmol kg^{-1}.

The EXAFS measurements were performed at the Strahl X at the Hamburger Synchrotron Strahlungslabor (HASYLAB/DESY) in fluorescence mode. The k^3-weighted K-edge Zn-EXAFS spectra and the RSFs are shown in Fig. 4.5. The spectra of the Zn/illite samples are characteristic for the formation of inner-sphere complexes. On the contrary, the spectra of Zn/"real rock" samples (OPA and Boda) showed the presence of Zn-Zn backscattering pairs at ~2.7 Å (R+ΔR) in the RSF, indicating the precipitation of Zn solid phases, even though the initial Zn concentrations were below the solubility limits of Zn-hydroxide phases. The EXAFS analysis for Ni treated samples (not shown) indicated a similar uptake behaviour to Zn. Hence, under the given experimental conditions the uptake of these metals is not primarily controlled by sorption on the clay fraction in Boda and OPA, and can explain the mismatch between the experimental Ni(II) sorption isotherm on Boda, and the predicted curve (Fig. 4.2). These findings suggest that Ni/Zn solubility limiting phases are formed in these argillaceous rock/ groundwater systems which are currently not included in the thermodynamic data bases.

Additional EXAFS measurements were performed at the 11-2 beamline at the Stanford Synchrotron Radiation Laboratory (SSRL) in order to investigate much more dilute samples. Beamline 11-2 offers a high photon flux generated by a wiggler and the availability of a 30-element solid-state detector. These combined features make this beamline unique in the world, and offers the possibility of measuring ultra-dilute samples. In order to investigate whether the formation of inner-sphere complexes prevail in the Boda and OPA system at low loadings, Zn samples with a metal loading of ~2 mmol kg^{-1} (Boda) and ~5 mmol kg^{-1} (OPA) were prepared. The k^3-weighted EXAFS spectra of both systems were, to within the typical error margins associated with EXAFS data, the same (Fig. 4.6). However, any further more detailed data processing requires that the structural Zn (both Boda and OPA contain ~2 mmol kg^{-1} Zn) needs to be analysed with EXAFS. Despite this, both EXAFS spectra exhibit typical features for incorporated and/or sorbed species (DÄHN et al., 2011). Based on this similarity, and the absence of any features characteristic of Zn precipitation, it was concluded that inner-sphere complexation is the predominant uptake mode at these low metal loadings. The measurements made so far in this study demonstrate that the Zn treated Boda and OPA samples show a similar uptake behaviour, e.g. sorption and precipitation at low and high loadings, respectively.

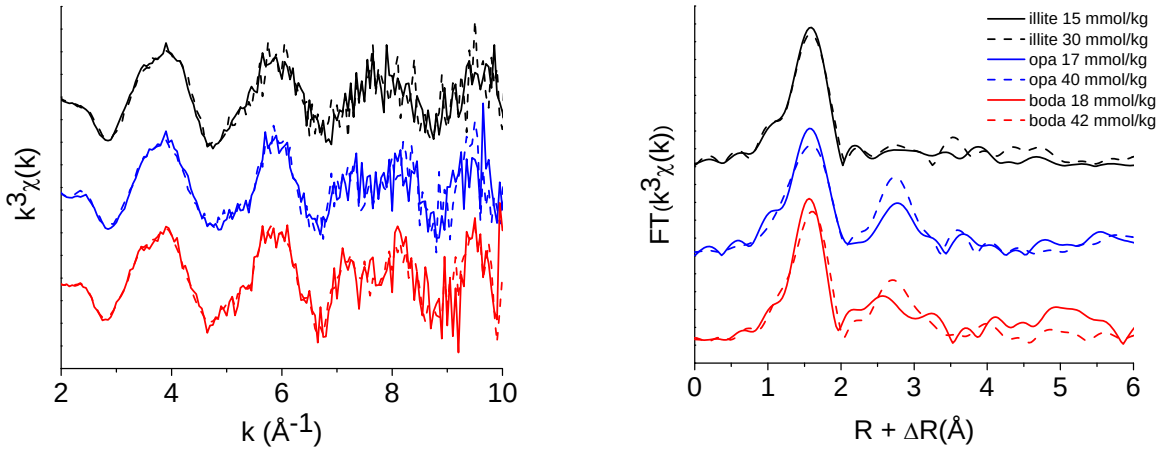

Fig. 4.5: *k^3-weighted Zn K-edge EXAFS spectra and the corresponding RSFs for illite, OPA and Boda at two different Zn loadings.*

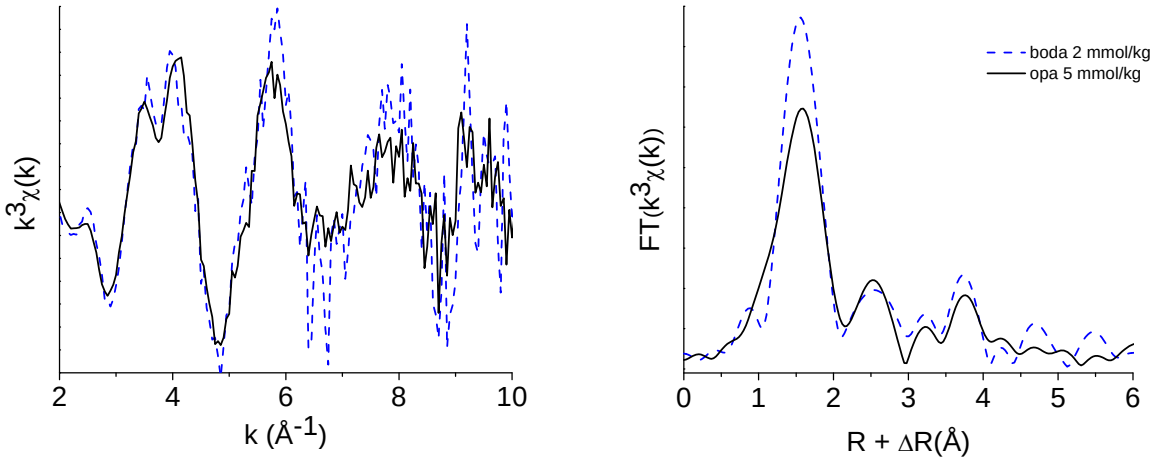

Fig. 4.6*: k^3-weighted Zn K-edge EXAFS spectra and corresponding RSFs of Boda and OPA samples with Zn loadings of ~2 mmol kg^{-1} and ~5 mmol kg^{-1}, respectively.*

4.5 References

BAEYENS, B., THOENEN, T., BRADBURY, M.H., MARQUES FERNANDES, M. (2012a)
Sorption data bases for the host rocks and lower confining units and bentonite for provisional safety analyses for SGT-E2. Nagra NTB 12-04 (in press).

BAEYENS, B., MARQUES FERNANDES, M., BRADBURY, M.H. (2012b)
Comparison between host rock and bentonite sorption measurements and predictions using the SDB approach applied in the provisional safety analyses for SGT-E2. Nagra NTB 12-05 (in press).

BERNER, U. (2002)
Project Opalinus Clay: Radionuclide concentration limits in the near-field of a repository for spent fuel and vitrified high-level waste. PSI Bericht Nr. 02-22, and Nagra Technical Report NTB 02-22.

BRADBURY, M.H., BAEYENS, B. (1997)
A mechanistic description of Ni and Zn sorption on Na-montmorillonite. Part II: Modelling. J. Contam. Hydrol. 27, 223-248.

BRADBURY, M.H., BAEYENS, B. (2000)
A generalised sorption model for the concentration dependent uptake of Cs by argillaceous rock. J. Contam. Hydrol. 42, 141-163.

BRADBURY, M.H., BAEYENS, B. (2005a)
Experimental measurements and modeling of sorption competition on montmorillonite. Geochim. Cosmochim. Acta 69, 4187-4197.

BRADBURY, M.H., BAEYENS, B. (2005b)
Modelling the sorption of Mn(II), Co(II), Ni(II), Zn(II), Cd(II), Eu(III), Am(III), Sn(IV), Th(IV), Np(V) and U(VI) on montmorillonite: Linear free energy relationships and estimates of surface binding constants for some selected heavy metals and actinides. Geochim. Cosmochim. Acta 69, 875-892.

BRADBURY, M.H., BAEYENS, B. (2010)
Comparison of the reference Opalinus Clay and MX-80 bentonite sorption databases used in the Entsorgungsnachweis with sorption databases predicted from sorption measurements on illite and montmorillonite. PSI Bericht Nr. 10-09 and Nagra Technical Report NTB 09-07.

BRADBURY, M.H., BAEYENS, B. (2011)
Predictive sorption modelling of Ni(II), Co(II), Eu(III), Th(IV) and U(VI) on MX-80 bentonite and Opalinus Clay: A "bottom-up" approach. Appl. Clay Sci. 52, 27-33.

BRADBURY, M.H., BAEYENS, B., THOENEN, T. (2010)
Sorption data bases for generic Swiss argillaceous, crystalline and calcareous rock systems. PSI Bericht Nr. 10-03.

DÄHN, R., BAEYENS, B., BRADBURY, M.H. (2011)
Investigation of the different binding edge sites for Zn on montmorillonite using P-EXAFS - The strong/weak site concept in the 2SPNE SC/CE sorption model. Geochim. Cosmochim. Acta *75*, 5154-5168.

MARQUES FERNANDES, M., BAEYENS, B., BRADBURY, M.H. (2008)
The influence of carbonate complexation on lanthanide/actinide sorption on montmorillonite. Radiochim. Acta 96, 691-698.

MARQUES FERNANDES, M., STUMPF, T., BAEYENS, B., WALTHER, C., BRADBURY, M.H. (2010)
Spectroscopic identification of ternary Cm−carbonate surface complexes. Environ. Sci. Technol. 44, 921-927.

MARQUES FERNANDES, M., BAEYENS, B., DÄHN, R., SCHEINOST, A.C., BRADBURY, M.H. (2012)
U(VI) sorption on montmorillonite in the absence and presence of carbonate: A macroscopic and microscopic study. Geochim. Cosmochim. Acta 93, 262-277.

NAGRA (2008)
Begründung der Abfallzuteilung, der Barrierensysteme und der Anforderungen an die Geologie. Bericht zur Sicherheit und technischen Machbarkeit. Nagra Technical Report NTB 08-05.

SCHLEGEL, M.L., MANCEAU, A., CHARLET, L., HAZEMANN, J.L. (2001)
Adsorption mechanisms of Zn on hectorite as a function of time, pH, and ionic strength. Am. J. Sci. 301, 798-830.

THOENEN, T. (2012)
The PSI/Nagra Chemical Thermodynamic Data Base 12/07: Compilation of updated and new data with respect to the PSI/Nagra Chemical Thermodynamic Data Base 01/01. PSI Internal Report TM-44-12-06.

5 CEMENT SYSTEMS

E. Wieland, J. Tits, A. Laube, D. Kunz, Ph. Schaub (postdoc), J. Schenzel (postdoc), H. Rojo (guest scientist)

5.1 Overview

Cementitious materials are foreseen to be used in the planned deep geological repositories for low-level and short-lived intermediate-level (L/ILW) as well as long-lived intermediate-level (ILW) radioactive waste in Switzerland. The research programme carried out by the group "Cement Systems" aims at strengthening the credibility of the sorption values used in performance assessment (PA) for predicting radionuclide release from the cementitious near-field into the host rock and improving knowledge on the chemical processes in the near-field of the planned cement-based repositories.

The main lines of research in 2012 were:

- Development of up-dated sorption data bases (SDBs) for the Provisional Safety Assessments (PSAs) within the framework of the Sectoral Plan.
- Development of analytical methods for the identification of ^{14}C-organic compounds released during the anaerobic corrosion of steel.
- Wet chemistry experiments and spectroscopic investigations on the interaction of actinides (U(VI), Np(IV/V/VI)) with hardened cement paste (HCP) and calcium silicate hydrate (C-S-H) phases.
- In situ characterisation of alkali-silicate-aggregate reaction (ASR) products formed at the interface between aggregate and cement paste using synchrotron-based micro X-ray diffraction.

The development of an analytical methodology for identifying ^{14}C-organic compounds released during the anaerobic corrosion of activated steel is partially financed by Swissnuclear. Specific tasks within the Swissnuclear project are being developed in PSI internal co-operations (Dr. I. Günther-Leopold – Hot laboratory; Dr. D. Schumann – Laboratory for Radiochemistry and Environmental Chemistry), and with external partners (Prof. G. Schlotterbeck – FHNW Muttenz; PD Dr. S. Szidat – Bern University).

Dr. J. Schenzel (postdoc) joined LES on July 1st, 2012. Her research activities will focus on the development of the analytical techniques required for identifying and quantifying ^{14}C-organic compounds in the framework of the Swissnuclear financed project.

Dr. H. Rojo (guest scientist) joined LES on November 4th, 2012. Her research activities will focus on Se and Tc uptake mechanisms on cement minerals under reducing conditions. This project is partially financed by the Verbundprojekt "Immorad" (Grundlegende Untersuchungen zur Immobilisierung langlebiger Radionuklide durch die Wechselwirkung mit endlagerrelevanten Sekundärphasen; co-ordinator: Dr. Th. Stumpf (KIT-INE)).

The studies on U(VI) uptake by cementitious materials using time-resolved laser fluorescence spectroscopy are being carried out in the framework of a co-operation with Dr. Th. Stumpf (KIT-INE) and Prof. C. Walther (Hannover University).

Characterisation studies of the ASR products were carried out in co-operation with Dr. A. Leemann (Empa) and Dr. P. Pattison (EPFL and ESRF/SNBL).

5.2 Activities in support of the Sectoral Plan: Development of a cement sorption data base

PSAs carried out within the framework of the Sectoral Plan require further updates of the existing cement sorption data bases (SDBs) since hardened cement paste (HCP) is considered to be the most important sorbing material present in the cementitious near-field of L/ILW and ILW repositories controlling radionuclide migration from the near-field into the host rock. Development of the current SDBs was based on procedures reported in earlier SDB work (BRADBURY & SAROTT, 1994; BRADBURY & VAN LOON, 1996; WIELAND & VAN LOON, 2002). The sorption values recommended in the updated SDBs were either selected on the basis of data from in-house experimental studies and/or literature data.

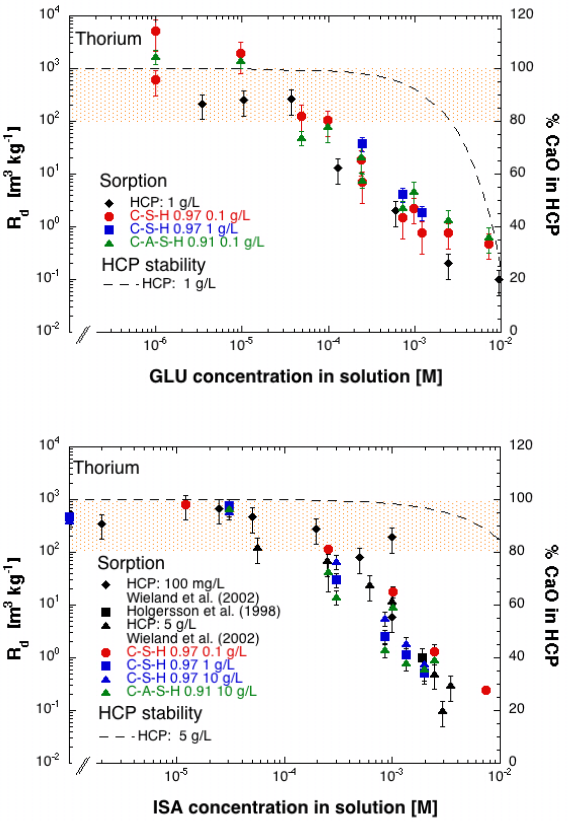

Fig. 5.1: *Distribution ratios (R_d) of Th on HCP and C-S-H phases in the presence of GLU and ISA at pH = 13.3 (left scale). Broken lines: Calculated stability limit of HCP due to the dissolution of the HCP through the formation of Ca-ISA or Ca-GLU complexes expressed in terms of % CaO present in HCP (right scale; WIELAND et al., 2002). Shaded area: Estimated uncertainty range of the distribution ratio.*

The values selected in the earlier SDBs were revised if new information and/or data justified changes to, or re-appraisals of, the existing values (WIELAND, 2012).

In the updated SDBs emphasis was placed on assessing the influence of internal geochemical processes such as carbonation caused by the generation of CO_2 during the course of the degradation of organic waste materials, the dissolution of metallic waste materials, and external geochemical processes such as cement degradation caused by the interaction of inflowing groundwater (saline and non-saline) from the host rock. Furthermore, sorption reductions caused by the presence of complexing ligands such as iso-saccharinic (ISA) and gluconic (GLU) acids in the near-field were estimated on the basis of in-house results. For example, Fig. 5.1 shows the influence of ISA and GLU on Th(IV) sorption which is negligibly small at ISA concentrations $\leq 10^{-4}$ M and GLU concentrations $\leq 2.0\times10^{-5}$ M. Above these threshold concentrations, however, Th(IV) uptake by HCP and C-S-H phases was found to decrease with increasing GLU or ISA concentrations. Sorption reduction caused by the presence of GLU and ISA in due to the different waste types was based on the estimated ISA and GLU concentrations in the near-field.

5.3 Formation of ^{14}C containing organic compounds during anaerobic steel corrosion

Carbon-14 in the form of low molecular weight (LMW) organic compounds such as methane, ethane etc., or oxidized hydrocarbons, such as alcohols, aldehydes, carboxylic acids, can potentially form during the anaerobic corrosion of steel in a cementitious near-field. If such ^{14}C-organics form, they can be major contributors to the annual dose released from an L/ILW repository. Although the ^{14}C inventory in the repository is known, the chemical speciation of ^{14}C in the cementitious near-field upon liberation from activated steel is only poorly known. More detailed quantification of the ^{14}C source term, however, requires information on the chemical nature of any ^{14}C containing organic compounds formed and on their long-term chemical stability under the reducing, alkaline conditions in a cementitious near-field.

In 2012 analytical approaches were developed which allowed volatile and dissolved LMW organic compounds (number of carbon atoms, C ≤ 5) to be identified and quantified, namely, gas chromatography (GC) coupled with ion mass spectrometry (MS) for the volatile LMW organics, and high performance ion exclusion chromatography (HPIEC) coupled with ion mass spectrometry (MS) and conductivity detection (CD) for oxidized hydrocarbons. Development of the gas phase analysis was undertaken at the Institute of Chemistry and Bioanalytics (ICB) of the Fachhochschule Nordwest-

schweiz (FHNW, Muttenz, Prof. G. Schlotterbeck) in the framework of a LES-ICB co-operation.

The GC-MS method developed for the analysis of volatile organics in iron-water systems at different pH values is based on head-space injection and is focused on the identification and quantification of small-chain, aliphatic hydrocarbons. The linearity of the method was demonstrated, and the limits of detection (LOD) and quantification (LOQ) were determined (Table 5.1).

Spectra of a calibration sample and a corrosion sample are shown in Fig. 5.2. The corrosion samples were prepared by immersing iron powder in either acidic (pH 3) or alkaline (pH 13) solutions. Unexpectedly high levels of gaseous hydrocarbons were observed already after one day of equilibration at both pH values, which prompted a reduction in the amount of iron used in further experiments. The final tests showed that volatile hydrocarbons will form during the anoxic corrosion of iron under acidic and alkaline conditions in accord with the results of DENG et al. (1997).

Table 5.1: *Calibration of the GC-MS method for various volatile organics and the determination of the volatile organic compounds in two corrosion samples (5 g Sigma iron powder in HCL (Sample 1) or NaOH (Sample 2) after a 1 day reaction time). Note that both iron samples showed concentrations of hydrocarbons significantly above the concentrations used in the calibration. LOD = limit of detection; LOQ = limit of quantification with* $LOQ \cong 3 \times LOD$.

Compound	Methane (µM)	Ethane (µM)	Ethene (µM)	Propane (µM)	Ethine (µM)	Propene (µM)	Butane (µM)
Calibration (min)	0.020	0.020	0.020	0.019	0.020	0.020	0.021
Calibration (max)	2.453	2.536	2.549	2.435	2.544	2.490	2.614
LOD	0.025	0.068	0.009	0.049	0.005	0.007	0.029
LOQ	0.063	0.203	0.026	0.146	0.016	0.021	0.086
Sample 1	19.70	8.32	4.21	5.76	n.d	5.48	3.56
Sample 2	9.37	3.80	2.78	2.06	n.d	3.83	1.02

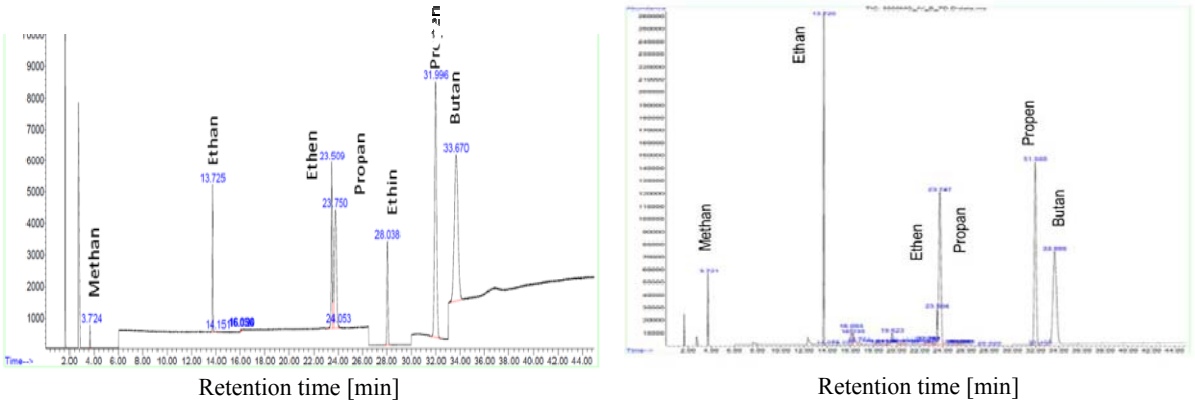

Fig. 5.2*: GC-MS-spectrum of a calibration standard (left) and an iron-water sample (right).*

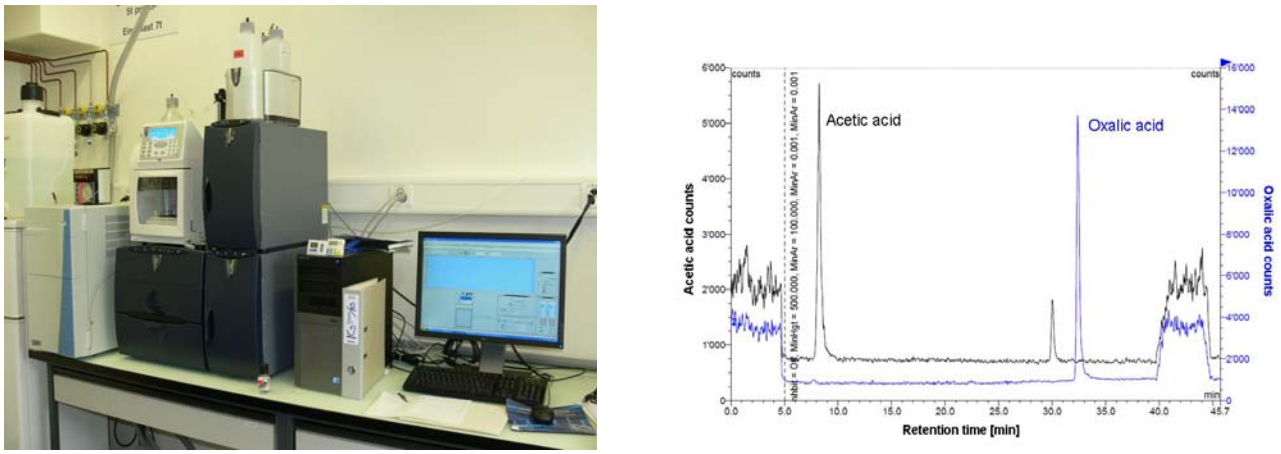

Fig. 5.3: *HPIEC-MS equipment (left) and chromatogramme for acetic acid and oxalic acid (right). The HPIEC systems consists of a IonPac AS11-HC column (Dionex, Sunnyvale, CA, USA), a GP 50 gradient pump, an EG 40 eluent generator, an AS 50 auto-sampler coupled to a CD 25 conductivity detector, and a MSQ™ Plus (Thermo Fisher, Sunnyvale, CA, USA) MS electrospray (ESI) operated in the negative ionization mode*

.

In addition, an analytical approach was developed in 2012 which allowed carboxylic acids to be identified and quantified using HPIEC-MS (Fig. 5.3). Separation of selected mono- and dicarboxylic acids was achieved with gradient elution using a NaOH eluent concentration ranging between 1 mM and 30 mM. An example of separation and MS detection is shown for acetic acid and oxalic acid (Fig. 5.3).

A first series of batch-type corrosion experiments using different types of iron powders (Sigma, BASF OM, and BASF HQ powders produced by the reduction of $Fe(CO)_5$ with hydrogen) were carried out with the aim of determining the identity of those oxidized LMW hydrocarbons which could form during iron corrosion. Note that the same Sigma iron powder was used as in the afore mentioned corrosion studies carried out to identify the volatile hydrocarbons released during anaerobic corrosion. The iron powders were pre-treated with 1.0 M HCl, rinsed with Ar-purged water, dried at 100°C under N_2 atmosphere and finally stored in the glovebox under a N_2 atmosphere prior to use. The formation of LMW organics was monitored under acidic conditions (pH 3) over a period of 42 days. After appropriate periods of time, four reaction vials (20 mL serum vials sealed with Teflon septa) were analysed: three vials contained 5.0 g of the iron powders and one control flask contained no iron. The vials were shaken end-over-end on a rotor in a dark incubator at 20 °C in the glovebox.

After sampling, the supernatant solutions were purified prior to analysis using an OnGuard® II Ag/H cartridge (Dionex: Part of Thermo Fisher, Sunnyvale, CA, USA) which traps the interfering chloride anions, and, in addition, reduces the high concentrations of alkaline earth and transition metals. Quantification of the selected carboxylic acids was achieved by applying deuterated forms of the compound being analysed as internal standards, which additionally compensated for matrix effects. Significant concentrations of acetic acid (199.6-308.4 µM, Fig. 5.4a) and formic acid (36.7-72.3 µM; data not shown) were detected in all of the analysed experiments containing iron powders already after 5 min of reaction time. The concentrations tended to decrease over time. Further compounds such as malonic acid, oxalic acid (Fig. 5.4b), and valeric acid, were detected at trace levels.

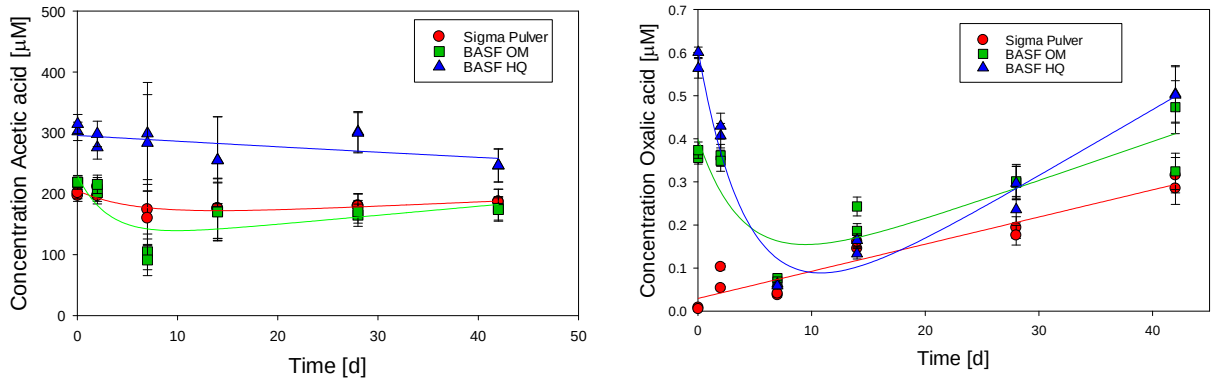

(a) (b)

Fig. 5.4: *Time dependent concentrations of (a) acetic acid, and (b) oxalic acid in the corrosion batch experiment using low CO_2 containing water acidified with 0.001 M HCl. The solid lines are given only to guide the eye.*

The high initial concentrations of acetic- and formic acid, along with the presence of other carboxylic acids at trace concentrations, was tentatively assigned to the oxidative pre-treatment of the iron powders using HCl in which the carbon released due to iron dissolution was oxidised. In an additional experiment, where no pre-treated powders were used, the initial concentrations of acetic and formic acid were much lower (7.3 and 28.3 µM). Pre-treatments with HCl will not be used further. Future studies will focus on corrosion experiments in hyperalkaline cement porewaters, bentonite porewater and Opalinus Clay groundwater.

5.4 Immobilization of actinides by cementitious materials

5.4.1 Uptake of Np by TiO_2, C-S-H phases and HCP under alkaline conditions

Speciation studies carried out in collaboration with KIT/INE showed that neptunium exists in the tetravalent state under reducing conditions, and in the pentavalent and hexavalent states under anoxic and oxidising conditions, respectively, in the alkaline pH range (GAONA et al. 2012a). Furthermore, the formation of anionic Np(VI) hydroxy species ($NpO_2(OH)_3^-$ and $NpO_2(OH)_4^{2-}$) was found to significantly limit the stability field of Np(V) under hyperalkaline conditions.

In the past year batch sorption experiments with Np(IV/V/VI) were carried out with the aim of determining the influence of pH and the Ca concentration on the uptake processes. TiO_2 was also used as a sorbent because the oxide is stable under alkaline conditions and surface complexation is considered to be the dominant uptake mechanism (TITS et al. 2012). The hydrolysis of Np(IV/V/VI) was found to have an effect on the uptake process. Furthermore, it was observed that the presence of Ca significantly enhanced NpO_2^+ and NpO_2^{2+} sorption onto TiO_2, presumably due to the formation surface-stabilized $NpO_2(OH)_xCa_y$ complexes. The sorption behaviour of Np(IV/V/VI) on C-S-H phases with different C:S ratios was found to be very similar to that observed on TiO_2. Uptake of Np(IV) by C-S-H phases was observed to be strong and independent of pH and aqueous Ca concentration, while Np(V/VI) uptake decreased with increasing pH and increased with increasing Ca concentration (TITS et al. 2012).

Sorption kinetic measurements were carried out with Np(IV) and Np(V) on fresh HCP at pH 13.3 and on a degraded HCP at pH 12.5. The HCP was prepared from a sulfate-resisting Portland cement CEM I 52.5 N HTS (Lafarge, France), which is currently in use for the conditioning of radioactive waste in Switzerland. The experiments were carried out using the short-lived ^{239}Np isotope ($t_{1/2}$ = 2.355 days) and 10^{-2} M hydrazine (N_2H_4) as a redox buffer to maintain reducing conditions.

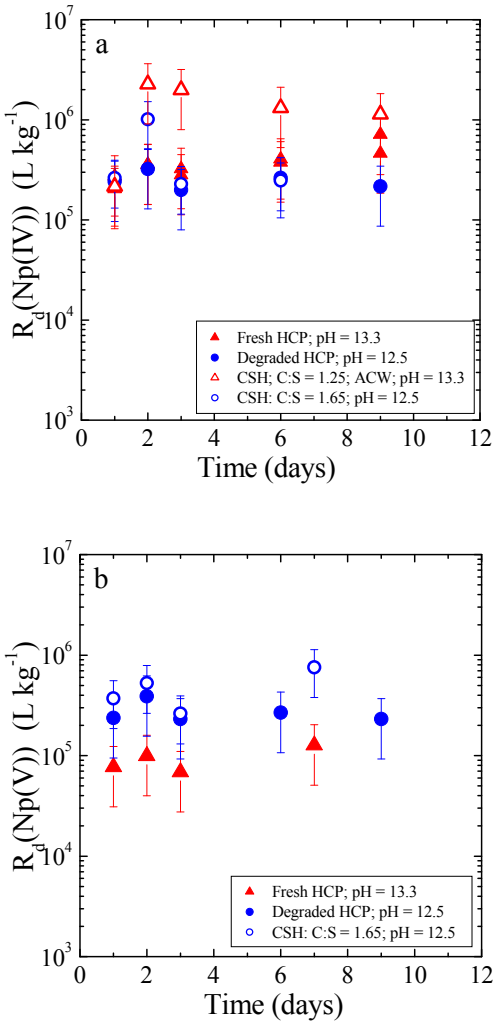

Fig. 5.5: *Np(IV) (a) and Np(V) (b) sorption kinetics on fresh HCP (pH = 13.3) and degraded HCP (pH = 12.5). Comparison with sorption kinetics on C-S-H phases in ACW (C:S = 1.25; pH = 13.3) and in absence of alkalis (C:S = 1.65; pH = 12.5). The total Np concentration was 1.5×10^{-10} M. S/L = 10^{-4} kg L^{-1}.*

The uptake of Np(IV) and Np(V) by HCP was found to be very similar to that previously observed on C-S-H phases with high C:S ratios under the same conditions. (Note that C-S-H phases are the most important constituent of HCP controlling the immobilisation of actinides.) The sorption of Np(IV) and Np(V) was found to be fast and within the uncertainty of the results, constant over time, with R_d values ranging between 7×10^4 and 2×10^6 L kg^{-1} (Fig. 5.5). The uptake of Np(IV/V) by HCP is thus strong. The large scatter in the data is a consequence of the strong interaction of Np with colloidal HCP material. The latter material remains in solution after centrifugation due to incomplete phase separation or small amounts of Np loaded HCP colloids are re-suspended during the sampling of the supernatant solution. The wet chemistry data agree with the conclusions drawn from earlier EXAFS studies that C-S-H phases are the component in HCP controlling the Np(IV/V) uptake (GAONA et al., 2011, GAONA et al., 2012b).

5.4.2 Luminescence spectroscopy investigations of U(VI) uptake processes

The investigations on the U(VI) uptake by cementitious materials using luminescence spectroscopy were continued in collaboration with KIT/INE. In previous studies it was observed that the luminescence broadband spectra of U(VI) taken up by cementitious materials exhibited strong red shifts compared to U(VI) species in alkaline solutions, suggesting changes in the ligand field due to strong changes in the local geometry of the oxygen atoms surrounding the U metal cation (TITS et al., 2011). Additional measurements have been carried out on U(VI) loaded C-S-H phases using direct laser excitation at cryogenic temperatures (~20 K) instead of broadband laser excitation. In the case of broadband excitation, the spectrum of U(VI) in poorly ordered environments, such as amorphous C-S-H phases, consisted of three to five broad bands resulting from the superposition of many narrower fluorescence emission bands attributable to the relaxation of slightly different non-interacting U(VI) luminescence centers (Fig. 5.6a). This gave rise to the observed broadening of the emission peaks, which strongly limited detailed analysis of the spectra (Fig. 5.6b).

A much better spectral resolution was obtained by selectively probing small spectral sub-samples of the U(VI) luminescence centers at varying excitation wavelengths (λ_{ex}) using a tuneable laser as a narrow-band, monochromatic light source (direct laser excitation, Fig. 5.6c). The sub-samples of U(VI) centers directly excited at varying λ_{ex} exhibited a much higher luminescence intensity (resonance peak) than the indirectly excited centers at higher wavelengths, which resulted in a much better spectral resolution (Fig. 5.6b).

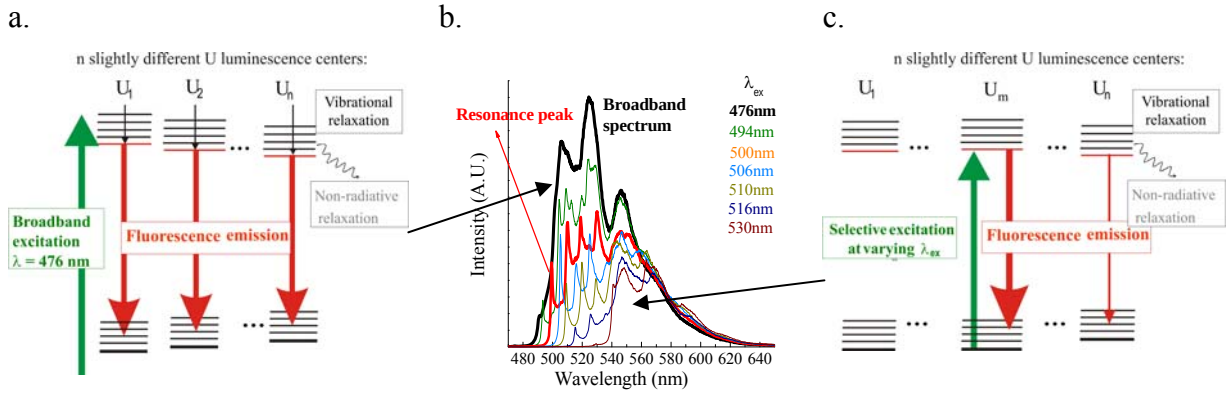

Fig. 5.6: *Broadband excitation and direct excitation of U(VI) sorbed onto an amorphous C-S-H phase. a) Energy diagram of broadband excitation. b) Broadband (λ_{ex} = 476 nm (=21'008 cm^{-1})) and narrow band (selective excitation) spectra. c) Energy diagram of selective excitation at varying wave lengths.*

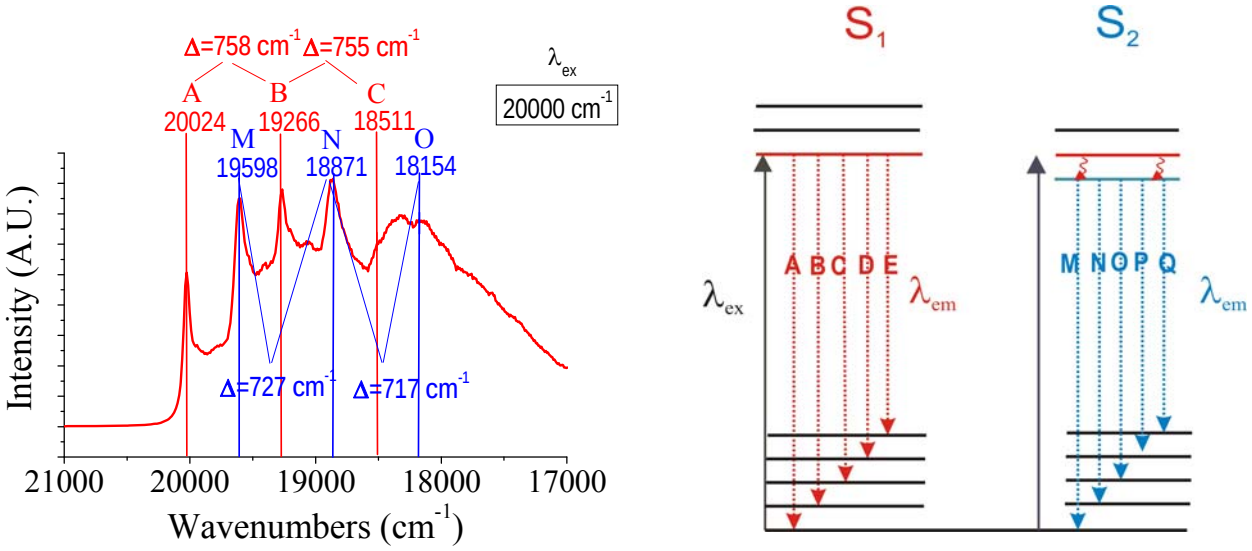

Fig. 5.7: *Narrow band spectrum of U(VI) sorbed onto a C-S-H phase (C:S = 1.07) in ACW at pH = 13.3. λ_{ex} = 500 nm (20'000 cm^{-1}). A, B, C (red) and M, N, O (blue) indicate two different sets of emission bands attributable to the two U(VI) sorbed species S_1 and S_2. Transitions A and M correspond to the electronic transitions (v_E) from the 1st excited state to the ground state of species S_1 and S_2, respectively. All other transitions correspond to transitions to various vibrational levels of the ground state (v_S).*

Luminescence spectroscopy measurements were conducted on TiO_2, on a C-S-H phase and on HCP, all of which had the same U(VI) loadings of 10^{-2} mol kg^{-1}, using both broadband laser excitation and direct laser excitation. (The reason for including TiO_2 in the measurements is the same as given above in section 5.4.1.) Fig. 5.7 shows a narrow-band spectrum of U(VI) sorbed on a C-S-H phase recorded after direct excitation at a wavelength of 500 nm. Two sets of emission bands (A,B,C and M,N,O) were detected, which belong to two different types of U(VI) sites (S_1 and S_2). Note that the second type of site (S_2) is directly excited to the 2nd level of excited state from which it relaxes rapidly and non-radiatively to the 1th level of excited state. The pronounced red-shift (i.e. lower wave numbers) of the spectrum of species S_2 (i.e. from $v_E(2)$ = 20'500 cm^{-1} for the uranyl aquo ion (TITS et al., 2011) to 19'598 cm^{-1}) is indicative of a

strong crystal field effect, suggesting incorporation of U(VI) into the C-S-H structure.

In Fig. 5.8 direct excitation spectra of U(VI) sorbed on TiO_2, C-S-H and HCP are compared. The spectrum for U(VI) sorbed on TiO_2 is poorly resolved due to energy transfer to neighbouring, non-excited U(VI) centers (distance < 10 nm), with a slightly lower excitation energy. The significantly higher surface area of the C-S-H phases, together with the possible incorporation of U(VI) into the C-S-H structure, results in a separation of the U(VI) luminescence centers in the solid. As a consequence, the energy transfer to neighbouring, non-excited U(VI) centers, is strongly reduced, giving rise to the observed improvement in spectral resolution. The luminescence spectrum of U(VI) sorbed on HCP exhibits two sets of emission bands very similar to those found for C-S-H phases, indicating the presence of two types of U(VI) sorbed species in HCP. The first species ($\nu_E(1)$) is identical to that observed for TiO_2, indicating the formation of a U(VI) surface complex. The strong red-shift of the spectrum suggests that the 2nd species ($\nu_E(2)$) corresponds to U(VI) incorporated into the C-S-H structure rather than adsorbed onto the C-S-H surface.

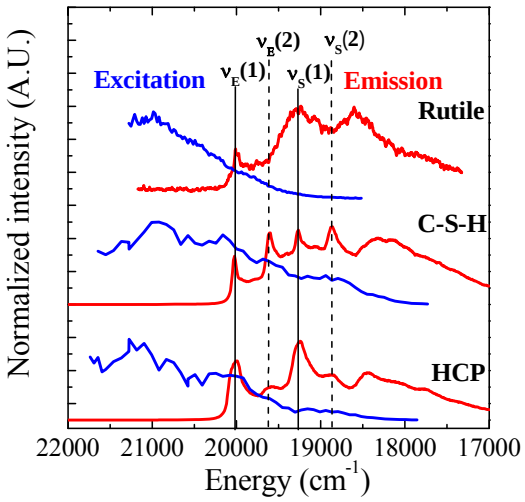

Fig. 5.8: *Luminescence spectra of U(VI) sorbed onto TiO_2, C-S-H phase (C:S = 1.07) and HCP in ACW at pH = 13.3 (red). U(VI) loadings = 10^{-2} mol kg^{-1}. The excitation spectra (blue) correspond to the integrated fluorescence emission intensities at the given excitation energy.*

5.5 X-ray micro-diffraction investigation of alkali-silicate-aggregate reaction (ASR) products

The aim of the X-ray micro-diffraction (micro-XRD) project is to develop a method for in situ phase characterization on a micro-scale in cementitious materials and at interfaces between cementitious materials and the host rock. Micro-XRD measurments complement the chemical information obtained by conventional analytical methods (e.g. SEM-EDX, XRF) with structural information.

A micro-XRD study was carried out with the aim of identifying the product(s) formed during the course of ASR reactions in concrete. The ASR is one of the most important deterioration mechanisms in concrete systems, leading to substantial damage of structures all over the world. For example, over 400 structures, including several alpine dams, are affected in Switzerland. The reaction between amorphous or crystalline SiO_2 (in aggregates) and the alkaline pore solution of concrete (pH 13.0-13.5) leads to a volume expansion causing severe damage to concrete structures. As the reaction proceeds relatively slowly, damage only appears after years to decades. The mechanism of the ASR leading to the volume increase is presently unclear. In order to understand the ASR, it is essential to know the compositions and crystal structures of the reaction products. While the chemical compositions analyzed with EDX are well documented, the mineralogy is poorly known, and the structures are difficult to study because the crystals are micron sized. The micro-XRD technique was applied to determine the crystal structure of the reaction products formed in micro-cracks within concrete aggregates (Fig. 5.9). Two types of samples were prepared from an approximately 40-year old, ASR damaged railway bridge: 1) micro-particles (sizes <100 µm) extracted from ASR veins, and 2) thin sections prepared with a thickness of about 20 µm for in situ investigations.

Synchrotron-based micro-XRD experiments were carried out at three facilities using different beam sizes: i) the 2-ID-D beamline, Advanced Photon Source (APS), Argonne National Laboratory, Argonne IL, USA; beam size: ~0.25×0.30 μm^2; ii) the micro-XAS beamline, Swiss Light, Source (SLS), PSI Villigen; beam size: ~1.0×1.0 μm^2; iii) the

Swiss-Norwegian beamline (SNBL), ESRF, Grenoble, France; minimum beam size: ~60×60 μm^2.

Rotational scans were performed on both sample types. However, in the case of the thin sections the rotational range was limited to about +/–45°. Diffraction data collected with the smallest beam size at APS showed partially single-crystal like Bragg intensities, while with the larger beam size, the diffraction patterns only showed (sometimes slightly structured) powder rings (Fig. 5.10a). Thus, the sizes of the crystallites of the reaction products lie in the sub-micron range. Powder patterns (Fig. 5.10b) from different points along the vein, and in different veins, were found to be identical, indicating a homogenous distribution of an invariant crystal structure of the reaction product. Fingerprint-matching using crystallographic databases were not successful in identifying the phase, indicating that the structure had not yet been determined. Several possible structural models of the ASR phase were developed in collaboration with the Laboratory of Crystallography at EPFL Lausanne and A. Arakcheeva (Phase Solutions Ltd., Lausanne). The preliminary structural model shown in Fig. 5.10c was developed solely from the analysis of the powder diffraction pattern. To corroborate this structural model requires further detailed modeling and analysis of the measured single crystal diffraction data.

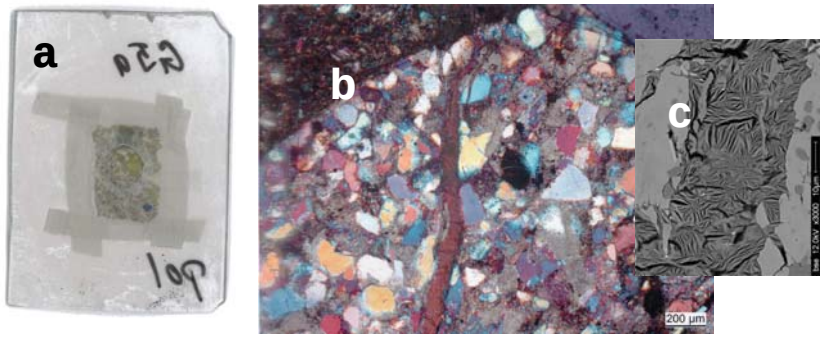

Fig. 5.9: *a) Thin section of an ASR damaged concrete on an acrylic carrier (vertical edge length: 3.5 cm), b) optical micrograph in cross-polarized light of an aggregate showing an ASR induced micro-vein (red-brown vertical feature), c) SEM-BSE picture of the vein filled with the analyzed reaction product.*

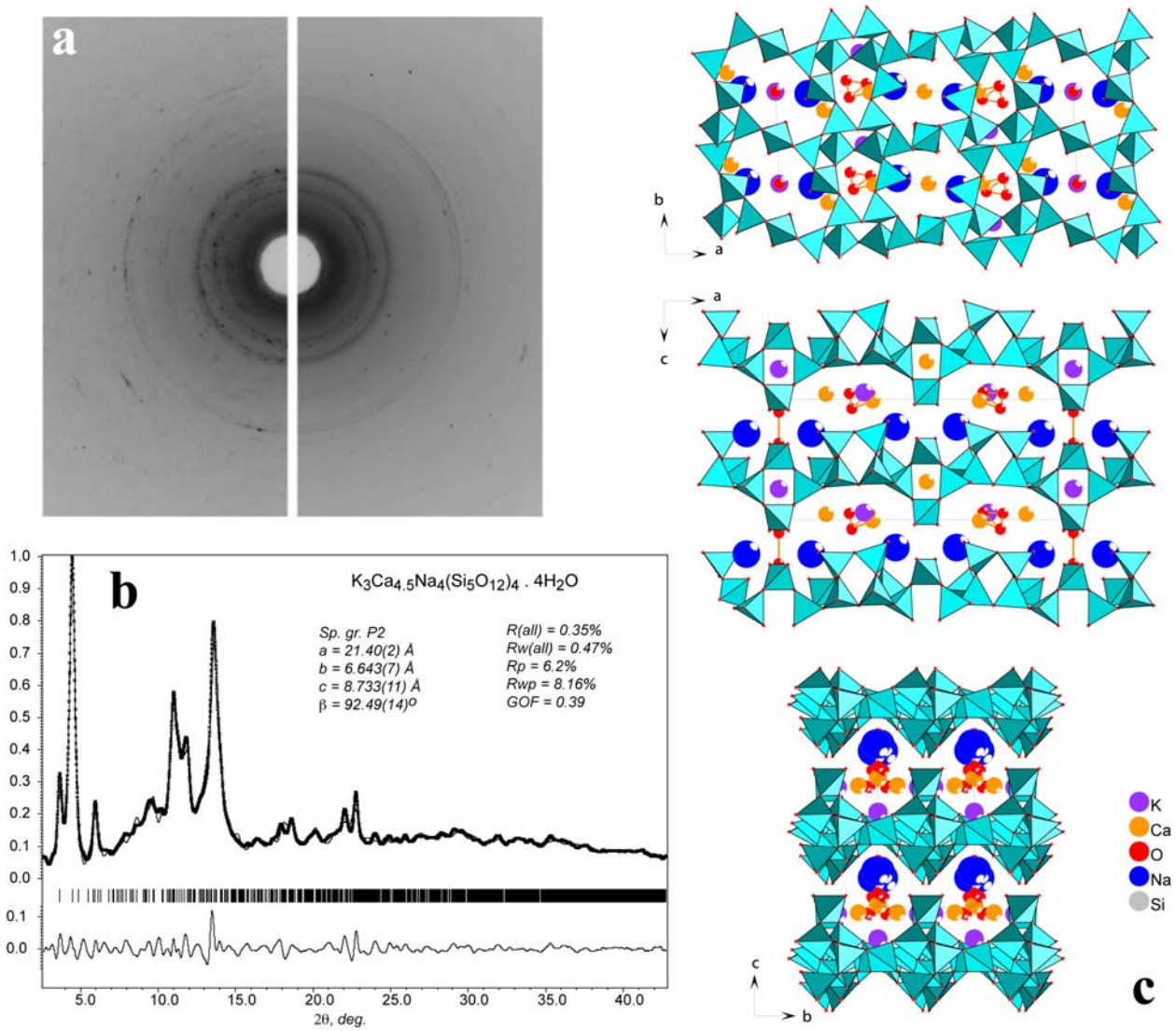

Fig. 5.10: *a) Micro diffraction pattern of the ASR product taken at beamline 2-ID-D, APS, Argonne. Left half – individual diffraction frame showing single crystal characteristics; right half – integration over a rotational range of +/–45° used for powder analysis, b) Comparison of the experimental (thin line) and the modelled (thick line) 1d powder diffraction pattern (wavelength: 0.6931 Å), c) Proposed model of the corresponding layered silicate structure. The chemical composition given agrees with EDX analysis.*

5.6 References

BRADBURY, M.H., SAROTT, F.A. (1994)
Sorption databases for the cementitious near-field of a L/ILW repository for performance assessment. PSI Bericht Nr. 95-06 and Nagra Technical Report NTB 93-08.

BRADBURY, M.H., VAN LOON, L.R. (1996)
Cementitious near-field sorption data bases for performance assessment of a L/ILW repository in a Palfris marl host rock, CEM-94 Update I, June 1997. PSI Bericht Nr. 98-01 and Nagra Technical Report NTB 96-04.

DENG, B.L., CAMPBELL, T.J., BURRIS, D.R. (1997)
Hydrocarbon formation in metallic iron/water systems. Environ. Sci. Technol. 31, 1185-1190.

GAONA, X., DÄHN, R., TITS, J., SCHEINOST, A.C., WIELAND, E. (2011)
Uptake of Np(IV) by C-S-H phases and cement paste: An EXAFS study, Environ. Sci. Technol. 45, 8765-8771.

GAONA, X., TITS, J., DARDENNE, K., LIU, X., ROTHE, J., DENECKE, M.A., WIELAND, E., ALTMAIER, M. (2012a)
Spectroscopic investigations of Np(V/VI) redox speciation in hyperalkaline TMA–(OH,Cl) solutions. Radiochim. Acta 100, 759-770.

GAONA, X., WIELAND, E., TITS, J., SCHEINOST, A., DÄHN, R. (2012b)
Np(V/VI) redox chemistry in cementitious systems: XAFS investigations on the speciation under anoxic and oxidizing conditions. Appl. Geochem. (in press).

HOLGERSSON, S., ALBINSSON, Y., ALLARD, B., BORÉN, H., PAVASARS, I. (1998).
Effects of gluco-isosaccharinate on Cs, Ni, Pm and Th sorption onto, and diffusion into cement. Radiochim. Acta 82, 393-398.

TITS, J., GEIPEL, G., MACÉ, N., EILZER, M., WIELAND, E. (2011)
Determination of uranium(VI) sorbed species in calcium silicate hydrate phases: A laser-induced luminescence spectroscopy and batch sorption study. J. Colloid Interface Sci. 359, 248-256.

TITS, J., GAONA, X., LAUBE, A., WIELAND, E. (2012)
Neptunium(IV/V/VI) sorption behaviour under hyperalkaline conditions: Comparative batch sorption studies on titanium dioxide and calcium silicate hydrates. Appl. Geochem. (in prep.)

WIELAND, E., TITS, J., DOBLER, J.P., SPIELER, P. (2002)
The effect of alpha-isosaccharinic acid on the stability of, and Th(IV) uptake by hardened cement paste. Radiochim. Acta 90(9-11), 683-688.

WIELAND, E., VAN LOON, L.R. (2002)
Cementitious near-field sorption database for performance assessment of an ILW repository in Opalinus clay. PSI Bericht Nr. 03-06 and Nagra Technical Report NTB 02-20.

WIELAND, E. (2012)
Sorption data base for the cementitious near-field of L/ILW and ILW repositories for performance assessment. Nagra Technical Report. (in prep.)

6 COLLOID CHEMISTRY

C. Degueldre, S. Frick

6.1 Overview

The aim of the colloid sub-program is to understand the role of colloids in the migration of radionuclides in the geosphere. The colloid properties studied are concentration, size distribution and behavior under safety relevant conditions. This report summarizes the activities over the past year within the framework of the Grimsel colloid project: "Colloid Formation and Migration" (CFM). The focus continues to remain on colloid generation using single particle counting (SPC) as a characterisation technique.

6.2 Activities in the CFM project

The Colloid Formation and Migration (CFM) project is conducted in the framework of Phase VI of the research program of the Grimsel Test Site (GTS), Switzerland. GTS Phase VI runs from 2004 to 2013 and is dedicated to repository-relevant (i.e. large-scale, long-term) in situ experiments. In February and March 2012, a tracer test involving the injection of a radionuclide-colloid cocktail was conducted in the MI shear zone at the GTS, as part of the CFM project. The colloids were derived from Febex bentonite. The tracer test, designated as test 12-02, involved the injection of a tracer cocktail into the borehole interval CFM 06.002i2 and extraction from a surface packer on the main access tunnel wall approximately 6.1 m from the injection interval. The test configuration is depicted in Fig. 6.1.

This tracer test was conducted in a weak dipole flow field in which the tracer cocktail was injected at a target flow rate of approximately 0.35 mL/min while water was being continuously extracted at a rate of 25 mL/min from the "Pinkel" channel at the surface packer on the tunnel wall (Fig. 6.1). The test was initiated by introducing the tracer cocktail into a flow loop circulating through the injection interval at a relatively high rate to keep the interval well mixed while maintaining a near constant net injection flow rate into the shear zone. The volume of the vessel containing the tracer cocktail was 2.25 L, and the volume of the injection flow loop was 1.0 L, so the entire injection circuit volume was 3.25 L once the tracer vessel was plumbed into the system. This arrangement resulted in an exponentially-decaying source term in the shear zone as the tracers were slowly bled out of the injection circuit.

The identity, masses, and concentrations of the tracers in the injection cocktail are listed in Table 6.1, as well as the reported fractions of each radionuclide that were initially partitioned to the bentonite colloids in the cocktail. The dilution of the 2.25 L of cocktail into the 3.25 L total volume of the injection circuit is accounted for in the tracer concentrations given in Table 6.1. The normalized tracer concentrations (concentrations divided by injection mass) in the water extracted from the "Pinkel" channel surface packer as a function of time are shown in Fig. 6.2. All the data shown in Fig. 6.2 should be considered preliminary; particularly the actinide concentrations which were measured by ICP-MS at KIT, because they were generally close to the detection limits. The ^{22}Na, ^{137}Cs and ^{133}Ba concentrations were measured by gamma spectrometry at both LES and KIT, and were found to be in excellent agreement. The Amino-G acid concentrations were measured in the field using an inline fluorimeter and were found to be in good agreement with offline measurements.

The colloid concentrations were measured in the field using a mobile laser-induced breakdown detection (LIBD) system operated by KIT personnel. Offsite colloid measurements were also conducted by LES using a the SPC. The general trends in the LIBD and SPC data were in good agreement (Fig. 6.3). The SPC data are not normalized, but are rather multiplied by an appropriate constant to yield approximately the same normalized concentrations as the LIBD data.

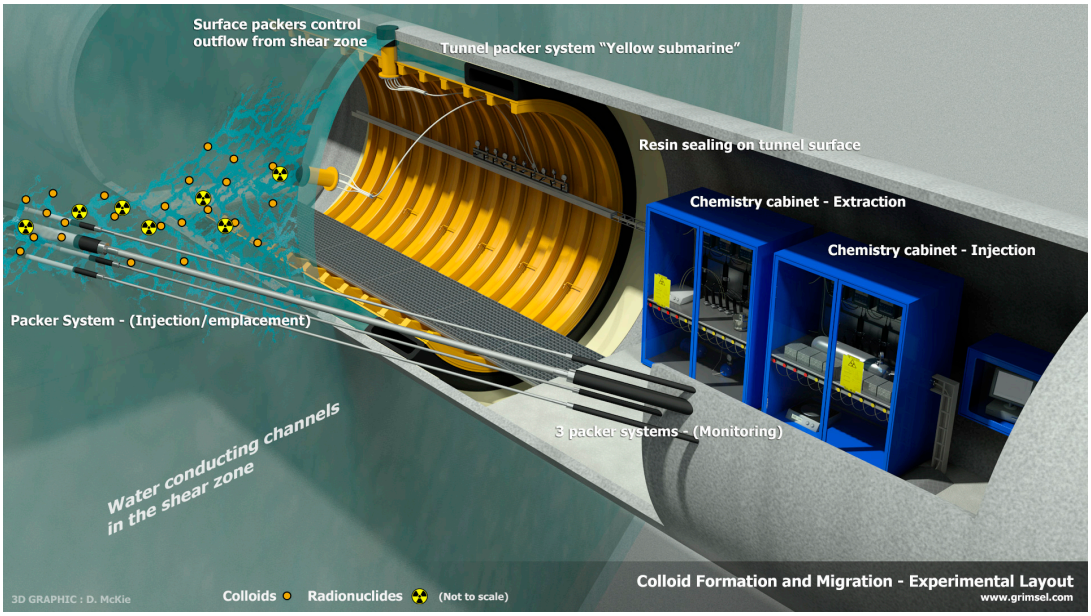

Fig. 6.1: *Schematic illustration of the CFM field test zone and instrumentation.*

Table 6.1*: Tracer injection masses, concentrations (in 3.25 L), and fractions partitioned to colloids in the CFM tracer test 12-02. Radionuclide masses are calculated from activities.*

Tracer or Radionuclide	Injection Mass mg	Injection Concentration, mg/L	Fraction Partitioned to Colloids
Amino G Acid (AGA)	3706	1140	0
Bentonite Colloids	228, 150 ± 5600	70, 200 ± 1700	N/A
^{22}Na	0.0045	0.00139	0-0.03
^{133}Ba	0.268	0.082	0.24-0.34
^{137}Cs	0.499	0.153	0.97
^{243}Am	0.038	0.118	1.0
^{242}Pu	1.267	0.39	1.0

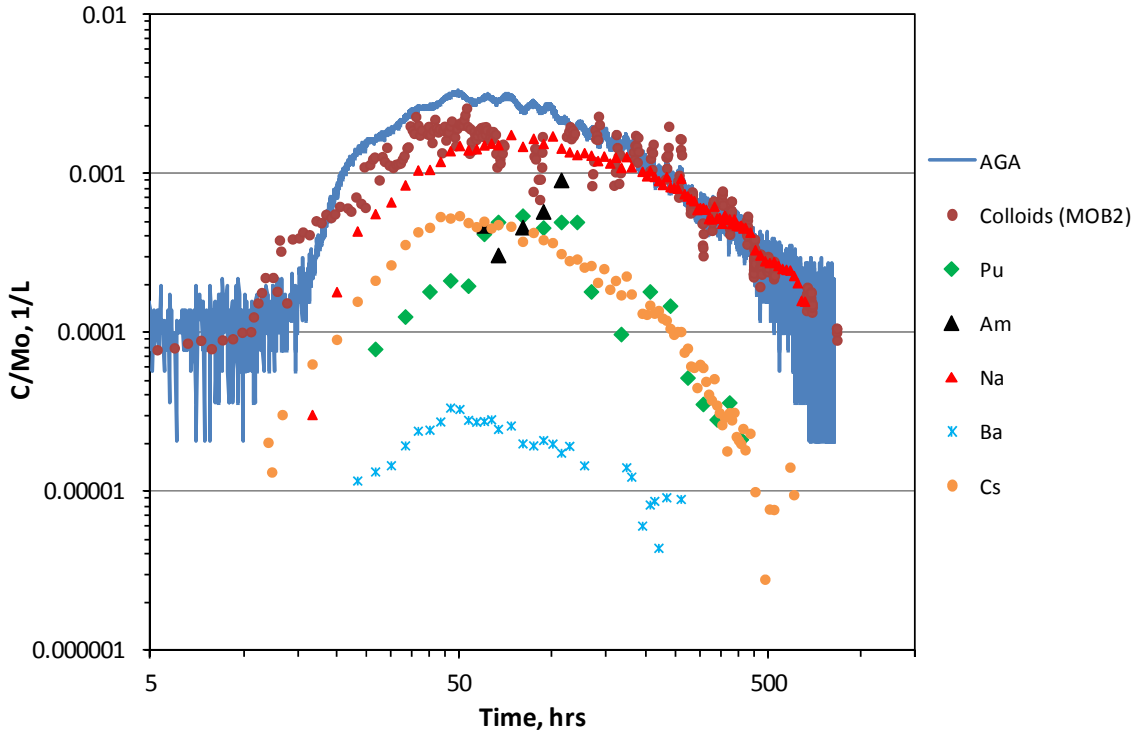

Fig. 6.2: *Normalized breakthrough curves of all tracers in CFM tracer test 12-02.*

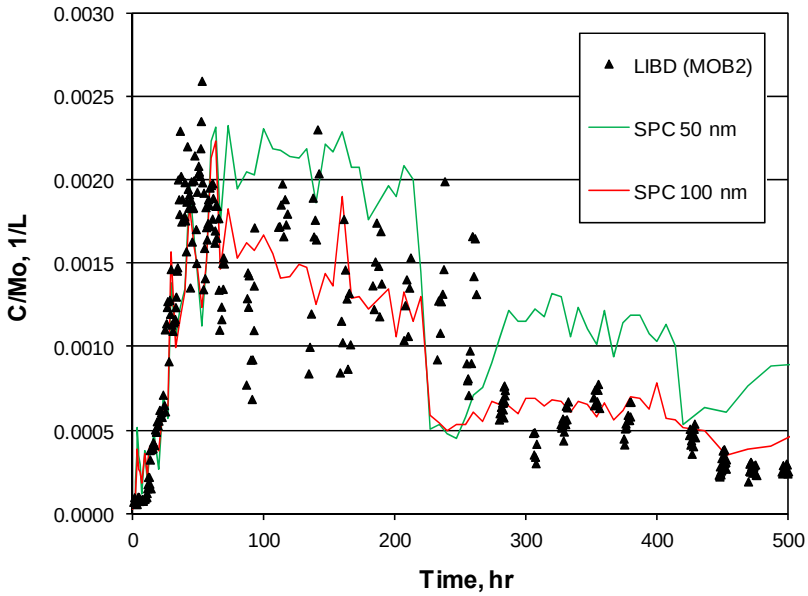

Fig. 6.3*: Comparison of the colloid breakthrough curves in the tracer test 12-02 from the mobile LIBD system (MOB2) operated by KIT at the Grimsel Test Site and the LES single particle counter (50-100 and 100-150 nm channels).*

6.3 Other colloid activities

The co-operation with CIEMAT is continuing in a very productive manner. The main aim is to optimise the radio-analytical effort required to measure colloid breakthrough curves in the CFM experiment at the GTS. Colloid labeling was discussed, and it was decided that ^{64}Ge could be used. Since ^{64}Ge decays to ^{64}Ga, α β^+ emitter, it can be used for breakthrough tests (in the lab and in situ) and detected by liquid scintillation counting and by Positron Emission Tomography (PET) during core breakthrough tests allowing a 3D reconstruction of the colloid pathway in laboratory experiments. The PET analysis is foreseen to be carried out at CIEMAT. In close co-operation with the colloid sub-project, a Spanish student is studying the interaction of colloids with Ga to better understand the PET tracer labeling.

6.4 Future work

The application of the advances made in groundwater colloid sciences over the last decade allowed colloid data to be derived for the hydro-geochemical systems in the argillaceous rock formations proposed by Nagra in the framework of the Sectoral Plan. A publication is foreseen which will include groundwater colloid concentration results from field experiments ranging from dilute systems to salty groundwater systems, a comparison of colloid concentration results with laboratory batch experiments, and the results of colloid adhesion tests (attachment factor values). The study will be completed by calculations of colloid concentrations in the relevant systems using the suspension pseudo-equilibrium model derived recently (DEGUELDRE et al., 2009). This field/lab and model study will provide the required colloid data for the formations being investigated by Nagra.

6.5 Reference

DEGUELDRE, C., AEBERHARD, PH, KUNZE, P., BESSHO, K. (2009)
Colloid generation/elimination dynamic processes: Toward a pseudo-equilibrium? Colloids Surf. A 337, 117-126.

7 DIFFUSION PROCESSES

L.R. Van Loon, M.A. Glaus, W. Müller, S. Frick, S. Dale, H. Wang (PhD), M. Bestel (PhD)

7.1 Overview

The foci of the activities in the Diffusion Processes Group are i) understanding the diffusion mechanism(s) of radionuclides in compacted argillaceous materials and ii) measuring diffusion parameters (effective diffusion coefficients and rock capacity values) which can be used in safety assessment studies.

Within the framework of the Sectoral Plan (SGT) the diffusion measurements with HTO, $^{36}Cl^-$ and $^{22}Na^+$ on the potential host rocks Helvetic Marls, "Brauner Dogger" and Effingen Member were completed. Additional measurements, with the same radionuclies, on fresh samples of Opalinus Clay and "Brauner Dogger" from the deep borehole at Schlattingen, were performed. The measurements were used to confirm/check the validity of the extended Archie's relation covering a wide range of porosities for estimating effective diffusion coefficients to be used in safety assessment studies. Also, the effect of ionic strength on diffusion was studied using samples of Opalinus Clay. The results of the measurements have been summarised in a technical report together with a compilation of effective diffusion coefficients for the different Swiss host rocks currently under investigation. This diffusion data base will be used in the Provisional Safety Assessment (PSA) analyses for SGT-E2.

In the framework of the EU CatClay project, diffusion measurements with $^{60}Co(II)$, $^{65}Zn(II)$ and $^{152}Eu(III)$ on OPA were performed using a filter-free in-diffusion technique. The ionic strength of the saturating/contacting solutions was varied in order to test whether surface enhanced diffusion is an important process or not. The first results showed a small effect of ionic strength on the diffusion of both $^{65}Zn(II)$ and $^{60}Co(II)$, indicating that sorption enhanced difffusion might play a role. The modelling of the results is ongoing. Strong effects were observed in diffusion experiments with $^{85}Sr^{2+}$ in Na-exchanged compacted illite samples.

A new type of diffusion cell with a thin membrane interface between the compacted sample and the contacting solution was developed and tested successfully for the measurements with illite.

The TRAPHICCS programme on pure clay minerals was continued. A study of the in-diffusion of U(VI) in compacted montmorillonite was designed to investigate the influence of speciation on radionuclide transport. Within the project on the diffusion of radioelements sorbing by cation exchange on clay minerals, the diffusion studies of Cs^+ on illite were essentially finished during the present report period.

Two PhD projects on reactive transport were started in close co-operation with the Transport Mechanisms Group.

Two new PhD proposals concerning the transport of small organic molecules in compact clay systems and the behaviour of anions in argillaceous rocks were successful, and both projects will start in 2013.

7.2 Activities in support of the Sectoral Plan

Diffusion measurements with HTO, $^{36}Cl^-$ and $^{22}Na^+$ in potential host rocks such as Effingen Member, Helvetic Marls and "Brauner Dogger" were completed and modelled. All of the data could be described by an extended Archie's relation. New measurements with HTO and $^{36}Cl^-$ on fresh samples of Opalinus Clay and "Brauner Dogger" from the deep borehole at Schlattingen have been finished. The experiments with $^{22}Na^+$ are still ongoing. All of the measured diffusion coefficients are in good agreement with values estimated using the extended Archie's relation (e-Archie). Based on these very consistent results, the e-Archie relation was used to compile a diffusion data base for the PSAs within the framework of SGT-E2 (VAN LOON, 2012).

A remarkable observation is the fact that the anion accessible porosity measured with $^{36}Cl^-$ is ca. 50% of the total porosity in the cases of Opalinus Clay, Effingen Member and "Brauner Dogger". For Helvetic Marl, this value decreased to ca. 12% of the total porosity.

The study on the effect of water chemistry on the anion accessible porosity indicated that, in the case of OPA, no significant effect of ionic strength was observed on the anion accessible porosity. This observation could not be explained by the current knowledge based on anion exclusion effects in

bentonite (VAN LOON et al., 2007). A new project on this topic will be started in co-operation with the University of Bern, the University of New Brunswick (Canada) and the Nuclear Waste Management Organisation of Canada (NWMO) in order to further the understanding of anion diffusion behaviour in clay rocks (VAN LOON et al., 2012).

7.3 CatClay

The contribution of LES to WP3 in the CatClay project is to perform and interpret the diffusion results of Sr, Zn and Eu in a complex matrix such as Opalinus Clay. In 2012, diffusion measurements of ^{60}Co(II), ^{65}Zn(II) and ^{152}Eu(III) were performed on Opalinus Clay samples from the Mont Terri Rock Laboratory. The effect of ionic strength on diffusion was studied. To this end, samples were pre-equilibrated with OPA porewater containing different amounts of NaCl resulting in ionic strength values between 0.17 M and 1.07 M. After a 6 month pre-equilibration time, the solutions were spiked with ^{60}Co(II), ^{65}Zn(II) and ^{152}Eu(III). After 17 days of in-diffusion, the experiments with ^{60}Co(II) and ^{65}Zn(II) were stopped, and the diffusion profile measured. In the case of ^{152}Eu(III), the diffusion experiment was stopped after 3 month.

Figs. 7.1 and 7.2 show the diffusion profiles for ^{60}Co(II) and ^{65}Zn(II), and ^{152}Eu(III) respectively for the three different porewater compositions. The pH of all solutions was 7.9.

The diffusion parameters used to model the profiles are summarised in Table 7.2. The parameters derived for ^{152}Eu(III) are preliminary and associated with large uncertainties.

It is clear from the diffusion profiles that the sorption of the different elements follows the sequenc: R_d(Eu) > R_d(Zn) > R_d(Co). Further, it can be seen that the ionic strength has an effect on the diffusion of Co and Zn; the lower the ionic strength of the porewater, the larger the penetration depth. This might be an indication of sorption enhanced diffusion. In the case of ^{152}Eu(III), this effect was not observed. The first modelling attempts were performed using a semi-infinite diffusion model assuming aqueous phase diffusion (VAN LOON & EIKENBERG, 2005). All of the profiles showed features characteristic of linear sorption e.g. no front sharpening. Both the sorption value, and the effective diffusion coefficient, had to be modified in order to model the profiles at the three different ionic strength values (Table 7.1). Modelling with reactive transport codes (MCOTAC, PHREEQC3) is ongoing.

The scope of LES's contribution to WP2 in the CatClay project includes diffusion experiments with a Na-conditioned illite at a bulk-dry density of 1700 kg m^{-3}. Through-diffusion experiments with $^{85}Sr^{2+}$ at pH 5 and pH 9 and different background electrolyte concentrations were finished in the present reporting period. The results obtained at both pH values show typical features of sorption enhanced diffusion, namely, large effective diffusion coefficients compared to those of tritiated water, and a trend towards increasing effective diffusion coefficients with decreasing background electrolyte concentration. In agreement with batch sorption measurements on illite suspensions, the R_d values measured from tracer retardation at pH 9 were larger than at pH 5.

For the diffusion measurements foreseen for ^{60}Co(II), ^{65}Zn(II) and ^{152}Eu(III) on compacted illite, a new type of diffusion cell was developed and tested in which the problems of tracer sorption on filters, and the diffusive resistance of the filters, were avoided. The tests on the prototype cells were carried out using $^{85}Sr^{2+}$ and ^{60}Co(II) tracers. In contrast to the experiments with Opalinus Clay, a mechanical confinement of the compacted illite sample is necessary.

Figure 7.3 shows a schematical view of this diffusion cell. For small samples, confinement by an organic polymeric membrane with a thickness of ~100 µm was sufficient to withstand the swelling pressure of the compacted illite. A series of these diffusion cells are being produced, and the planned experiments will start at the beginning of 2013.

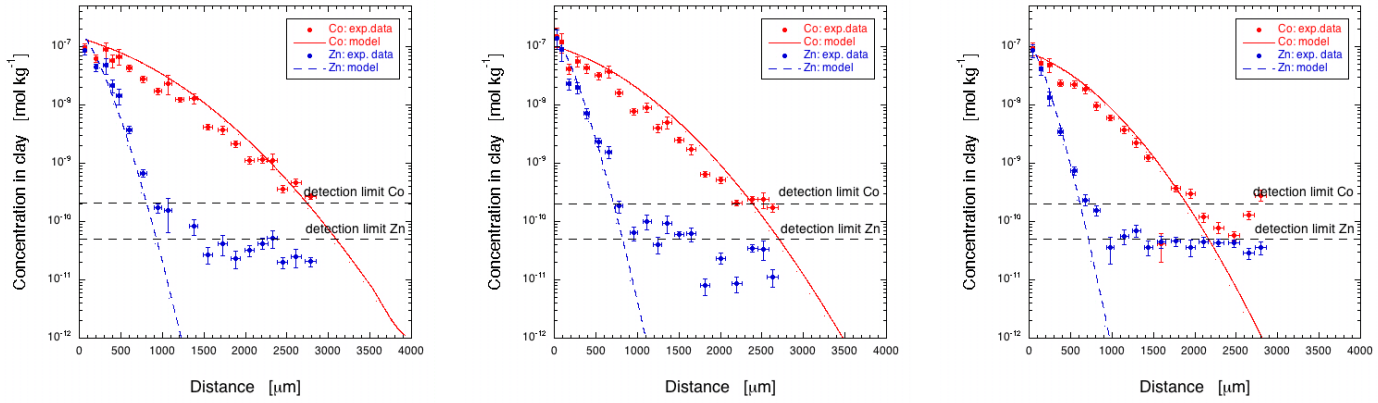

Fig. 7.1: *Diffusion profiles of ^{60}Co(II) and ^{65}Zn(II) in OPA after 17 days diffusion time for three different ionic strengths (left: 0.17 M; middle: 0.4 M; right: 1.07 M). The profiles can be described with one effective diffusion coefficient and a rock capacity factor assuming linear sorption.*

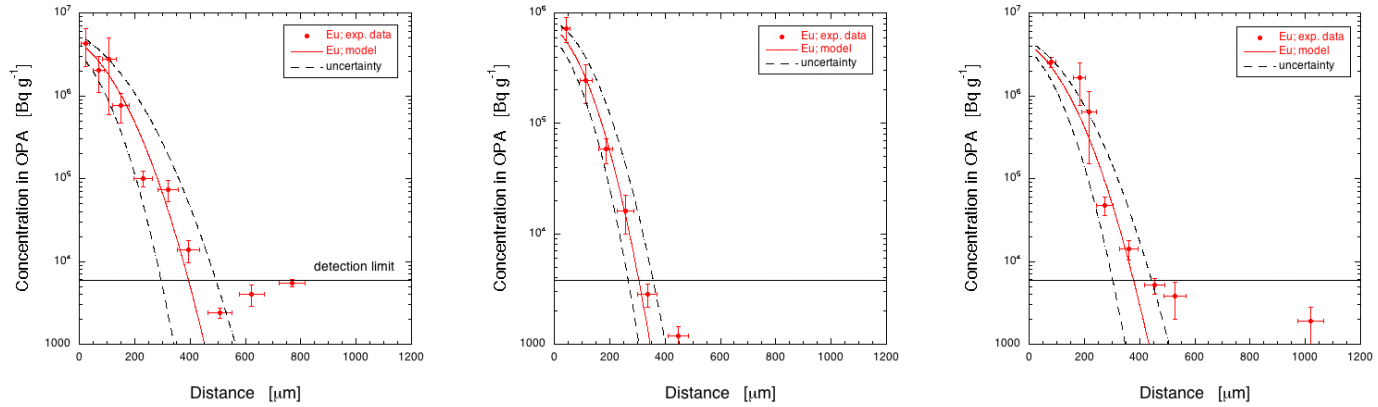

Fig. 7.2: *Diffusion profiles of ^{152}Eu(III) in OPA after 117 days diffusion time for three different ionic strengths (left: 0.17 M; middle: 0.4 M; right: 1.07 M). The profiles can be described with one effective diffusion coefficient and a rock capacity factor assuming linear sorption.*

Table 7.1: *Overview of the diffusion parameters used to model the diffusion profiles of ^{60}Co(II), ^{65}Zn(II) and ^{152}Eu(III) in OPA. The data for ^{152}Eu(III) are only indicative and are associated with large uncertainties.*

I	^{60}Co(II)		^{65}Zn(II)		^{152}Eu(III)	
	D_e [m^2 s^{-1}]	K_d [ml g^{-1}]	D_e [m^2 s^{-1}]	K_d [ml g^{-1}]	D_e [m^2 s^{-1}]	K_d [ml g^{-1}]
0.17 M	1.2×10^{-10}	220	1.4×10^{-10}	2000	1.0×10^{-11}	10’000
0.40 M	7.0×10^{-11}	180	9.0×10^{-11}	2000	6.0×10^{-11}	60’000
1.07 M	4.0×10^{-11}	130	5.0×10^{-11}	1800	3.0×10^{-11}	30’000

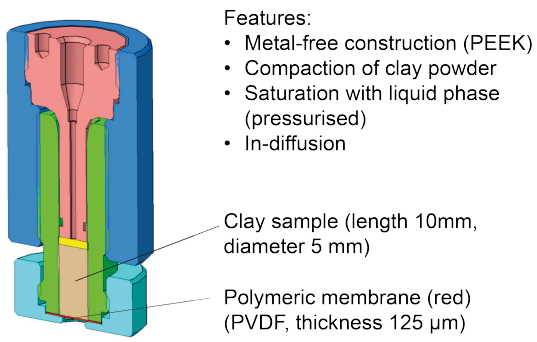

Fig. 7.3: *Cross sectional view of the "membrane-confined diffusion cell". The compacted illite sample has a diameter of ~5 mm.*

7.4 Dynamics of water in compacted montmorillonite (PhD project: Martina Bestel)

The transport of water and ions in compacted montmorillonite takes place in (i) m scale macropores, and in (ii) nm scale interlayer pores. It strongly depends on the distribution of porewater between these two pore types. The two water populations (interlayers, macropores) have been quantified in montmorillonite as a function of total water content using fixed window scan measurements (FWS) on a backscattering neutron spectrometer SPHERES at FRM II (Munich). This equipment measures the amount of immobile hydrogen in the samples as a function of temperature. For this purpose, use was made of the fact that water in the interlayers is partly bound to internal surfaces and interlayer cations, and thus can be significantly undercooled, whereas the water in the macropores shows a bulk-like behaviour, i.e. it freezes at approximately 273 K. The water distribution in several Na montmorillonite and two Cs montmorillonite samples was directly measured. Fig. 7.4 shows the amount of interlayer water as a function of total water in the sample. In Na montmorillonite, at low water contents, almost all of the water is absorbed in the interlayer (up to ~0.2 g water/g dry clay, Fig. 7.4), and beyond this value the macropores start to fill.

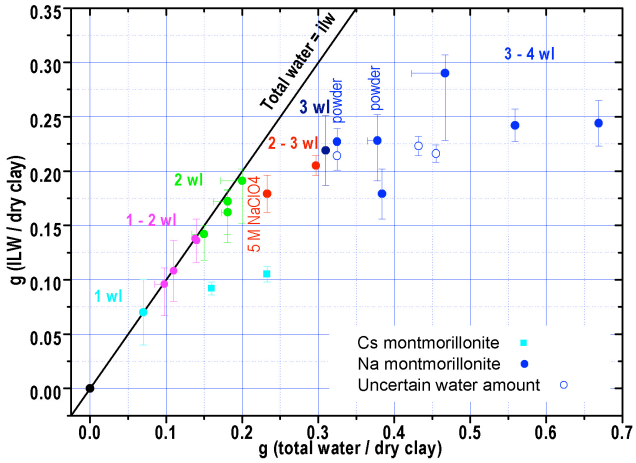

Fig. 7.4: *Amount of interlayer water as a function of total water in Na- and Cs-montmorillonite.*

The local diffusion coefficients, and the activation energy for the diffusion of H_2O in Na montmorillonite with 1, 2, 3 and 4 water layers in the interlayer, were measured using quasi-elastic neutron scattering (QENS). On the time scale of the QENS measurements, two distinct water populations exist, and the signals coming from them are treated additively.

7.5 Micro-heterogeneous systems (PhD project: Hao Wang)

In 2012, the new laser ablation cell was further developed and some applications in various research fields such as material science, geology and biology were tested. An ETH logo (in gold) was overlaid with a PSI logo (in silver) using a Laser Induced Forward Transfer Technique (Fig. 7.5a). (A SEM image is shown in Fig. 7.5b.) Two complementary techniques, SR-microXRF (Synchrotron Radiation micro X-Ray Fluorescence, Figs. 7.5c and 7.5e) and LA-ICPMS (Laser Ablation – Inductively Coupled Plasma Mass Spectrometry, Figs. 7.5d and 7.5f), were used to scan over the superimposed logos to reveal the individual logos in gold and silver. These techniques show that the chemical composition images are in good agreement, and that the spatial resolution of LA-ICPMS is approaching that of the SR-microXRF.

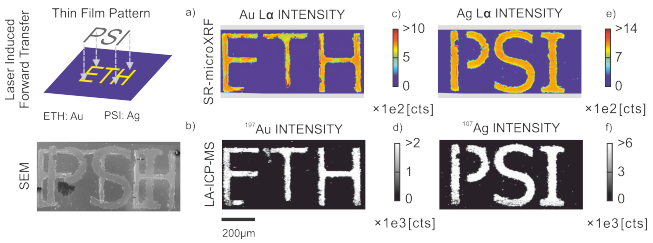

Fig. 7.5: *Test imaging case of a metal thin film micro-pattern by both LA-ICPMS (Laser Ablation – Inductively Coupled Plasma Mass Spectrometry) and SR-microXRF (Synchrotron Radiation micro X-Ray Fluorescence).*

7.6 Transport phenomena in compacted clay systems (TRAPHICCS)

While diffusion data for strongly sorbing elements in compacted clay minerals has been available for a few decades (e.g. SATO et al., 1992; TORSTENFELT et al., 1982), the interpretation of these results is based on apparent diffusion coefficients (D_a) only. Important issues such as possible differences between compacted and dispersed clay systems, or the influence of speciation on transport have not been answered. Transition elements, lanthanides and actinides are often present as negatively charged complexes (carbonate complexes for example) under the relevant porewater conditions. Whether these complexes are transported as such in the nano pores near the negatively charged surfaces of the clay minerals/rocks remains an open question.

First diffusion experiments addressing such questions were carried out in a compacted Na-montmorillonite sample using hexavalent uranium as the diffusing element in a carbonate containing background electrolyte buffered at pH ~9. Speciation calculations using the PSI/Nagra 12/07 TDB (THOENEN, 2012) showed that negatively charged uranyl complexes dominate under the chosen conditions, irrespective of whether mixed-metal species, such as $[Ca(UO_2)(CO_3^{2-})_3]^{2-}$ are included in the calculations or not. The results of experiments carried out under different background electrolyte concentrations showed a trend of increasing effective diffusion coefficients (D_e) and rock capacity factors (α) with increasing salinity (see Table 7.2). The diffusion of hexavalent uranium can thus be characterised as being somewhat "anion-like". Parameter fitting was done using a single-species transport model with a constant α. The experimental data could be fitted well with such a simple model. This could be indicative of the tracer distribution between the solid and the clay pore solution being independent of time and space, and in particular, being independent of the concentration of the diffusing species.

Table 7.2: *Best-fit parameters for the in-diffusion of ^{233}U at various background electrolyte concentrations in Na-montmorillonite compacted to a bulk dry density of ~1600 kg m^{-3}. Total concentrations of carbonate and Ca^{2+} were ~1 mM, and the pH was between 8.6 and 9.0. The relative uncertainties in the best-fit parameters are of the order of 20 %.*

Electrolyte	D_e [m^2 s^{-1}]	α [–]	D_a [m^2 s^{-1}]	R_d [dm^3 kg^{-1}]
0.1 M $NaClO_4$	7.5×10^{-15}	2.5	3.0×10^{-15}	1.3
0.5 M $NaClO_4$	1.4×10^{-13}	3.0	4.7×10^{-14}	1.6
1.0 M $NaClO_4$	2.0×10^{-13}	3.2	6.3×10^{-14}	1.7
3.0 M $NaClO_4$	2.7×10^{-13}	4.1	6.6×10^{-14}	2.3

Another approach to obtain diffusion parameters would be to estimate D_e values from bulk water diffusion coefficients and to calculate R_d values using the 2SPNE SC/CE sorption model (BRADBURY & BAEYENS, 2005) and the solution/sorbing species given in MARQUES FERNANDES et al. (2012) in which uranium calcium hydroxy carbonate complexes are considered to form in solution, and uranium hydroxo- and carbonato species are considered to sorb. A comparison of the data measured at 0.5 M $NaClO_4$ with a blind prediction using this methodology (D_e= 1x10^{-11} m^2 s^{-1}; α=137) is shown in Fig. 7.6. It can be clearly seen that the blind prediction made on the above basis is in strong disagreement with the experimental data, both qualitatively and quantitatively. The only feature that is reflected more or less correctly is the penetration depth. This can be explained by the over estimation of both D_e and α in the blind prediction, resulting in a D_a value of more or less the correct order of magnitude.

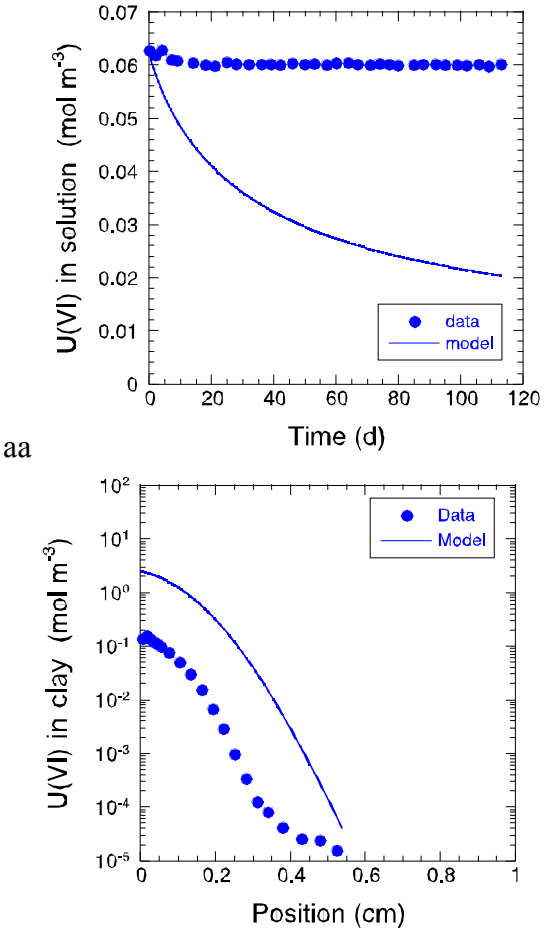

Fig. 7.6: *Comparison between experimental results (top: reservoir concentration; bottom: tracer profile in the clay) obtained for a background electrolyte concentration of 0.5 M $NaClO_4$ and a blind prediction based on a "pore diffusion model".*

The discrepancy between predicted and measured D_e and α value highlights the importance of the independent measurement of these two parameters instead of a simple measurement of D_a values. Otherwise, no significant progress in the process-based understanding of the diffusion of both weakly and strongly sorbing radioelements can be realised. However, the present experiments leave some open questions concering the interpretation of the best-fit parameters. Changes in the accessibility of binding sites, or changes in chemical equilibria in the confined nano pores of a compacted clay mineral, are just two such questions. As a next step similar experiments using ^{14}C labelled carbonate are planned in order to clarify the question whether U(VI) diffuses as carbonate complexes or not.

Another focus of the experiments carried out in the framework of the TRAPHICCS programme was in-diffusion measurements of $^{134}Cs^+$ in illite. Two series of experiments were carried out. In the first series, a fully Na-exchanged illite was used with trace concentrations of $^{134}Cs^+$. In the second series the illite was pre-equilibrated with stable Cs^+ in order to saturate the frayed-edge sites and generate a constant distribution of Cs^+ between the solid and the liquid phase. The $^{134}Cs^+$ tracer solution contained a stable Cs^+ carrier. The main features in the results obtained were (i) much stronger sorption of $^{134}Cs^+$ in the first series and (ii) rather large D_e values showing a clear dependence on the external background electrolyte concentration. Almost no difference in D_e values between the first and the second series was observed. Under the premise that the collapsed interlayers in illite are inaccessible to Cs^+, these observations can be interpreted in terms of the pore space between the illite particles being the main transport pathway, and that this porosity has similar properties to the hydrated interlayers of montmorillonite. Currently, similar experiments are running with a fully Na-exchanged illite and a $^{134}Cs^+$ tracer solution containing a background of stable ^{133}Cs. Profile measurements of K^+ and Cs^+ in these samples will provide additional information on whether or not the competition between these cations has an impact on the transport behaviour of Cs^+. Low Cs^+ concentrations can be measured in the presence of large salt background levels using in-house high-performance cation exchange chromatography in combination with a new mass spectrometric detector. The sensitivities are two orders of magnitude lower than conventional conductometric detection.

7.7 Porosity changes in porous media

Repository systems have several interfaces where there are strong chemical gradients. The most striking example is the cement-clay interface. Due to dissolution-precipitation reactions occurring at these interfaces, porosity changes can result in changes in the transport properties of solutes and gases. In order to achieve a better understanding of dissolution-precipitation reactions and their effect on solute transport, two new project were started in 2012. The projects are a co-operation between the Transport Mechanisms Group, the Diffusion Processes Group and the University of Bern. More information on these projects is given in Chapter 3.

7.8 Transport of small organic molecules in dense clay systems

The PhD proposal for the elucidation of structure–transport relationships for small molecular weight organic compounds in Opalinus Clay and clay minerals was accepted, and a suitable candidate for this work has been chosen. Mobile high-pressure infiltration equipment was obtained by courtesy of the Rock-Water Interaction Group of the University of Bern and moved to PSI where the first tests will start before the end of 2012.

7.9 References

BRADBURY, M.H., BAEYENS, B. (2005)
Modelling the sorption of Mn(II), Co(II), Ni(II), Zn(II), Cd(II), Eu(III), Am(III), Sn(IV), Th(IV), Np(V) and U(VI) on montmorillonite: Linear free energy relationships and estimates of surface binding constants for some selected heavy metals and actinides. Geochim. Cosmochim. Acta 69, 875–892.

MARQUES FERNANDES, M., BAEYENS, B., DÄHN, R., SCHEINOST, A.C., BRADBURY, M.H. (2012)
U(VI) sorption on montmorillonite in the absence and presence of carbonate: A macroscopic and microscopic study. Geochim. Cosmochim. Acta 93, 262–277.

SATO, H., ASHIDA, T., KOHARA, Y., YUI, M., SASAKI, N. (1992)
Effect of dry density on diffusion of some radionuclides in compacted sodium bentonite. J. Nucl. Sci. Technol. 29, 873–882.

THOENEN, T. (2012)
The PSI/Nagra Chemical Thermodynamic Data Base 12/07: Compilation of updated and new data with respect to the PSI/Nagra Chemical Thermodynamic Data Base 01/01. PSI Technical Report TM-44-12-06

TORSTENFELT, B., KIPATSI, H., ANDERSSON, K., ALLARD, B., OLOFSSON, U. (1982)
Transport of actinides through a bentonite backfill. Mater. Res. Soc. Symp. Proc. 11, 659–668.

VAN LOON, L.R., EIKENBERG, J. (2005)
A high-resolution abrasive method for determining diffusion profiles of sorbing radionuclides in dense argillaceous rocks. Appl. Radiat. Isotopes 63, 11-21.

VAN LOON, L.R., GLAUS, M.A., MÜLLER, W. (2007)
Anion exclusion effects in compacted bentonites: towards a better understanding of anion diffusion. Appl. Geochem. 22, 2536-2552.

VAN LOON, L.R. (2012)
Effective diffusion coefficients and porosity values for argillaceous rocks and bentonite: measured and estimated values for provisional safety analyses for SGT-E2. Nagra Technical Report NTB 12-03.

VAN LOON, L.R., HOBBS, M., AL, T., MÄDER, U. (2012)
Anion accessibility in low porosity argillaceous rocks (ANPOR). PhD proposal, Paul Scherrer Institut, Villigen, Switzerland.

8 PUBLICATIONS

8.1 Peer reviewed journals

AIMOZ L., KULIK D.A., WIELAND E., CURTI E., LOTHENBACH B.[1], MÄDER U.[2] (2012)
Thermodynamics of AFm-(I_2,SO_4) solid solution and its end-members in aqueous media. Appl. Geochem. 27(10), 2117-2129
doi: 10.1016/j.apgeochem.2012.06.006.
[1] Empa, Dübendorf, Switzerland
[2] University of Bern, Switzerland

AIMOZ L., TAVIOT-GUÉHO C.[1], CHURAKOV S.V., CHUKALINA M.[2], DÄHN R., CURTI E., BORDET P.[3], VESPA M.[4] (2012)
Anion and cation order in iodide-bearing Zn/Mg-Al layered double hydroxides. J. Phys. Chem. C. 116(9), 5460-5475
[1] Institut de Chimie de Clermont-Ferrand, France
[2] Institute of Microelectronics Technology, Russia
[3] Institut Néel, Université Joseph Fourier, France
[4] Dutch−Belgium Beamline, ESRF, France

AIMOZ L., WIELAND E., TAVIOT-GUÉHO C.[1], DÄHN R., VESPA M.[2], CHURAKOV S.V. (2012)
Structural insight into iodide uptake by AFm phases. Environ. Sci. Technol. 46, 3874–3881
doi: 10.1021/es204470e
[1] Institut de Chimie de Clermont-Ferrand, France
[2] Institute for Transuranium Elements, Germany

ALTMANN S.[1], TOURNASSAT C.[2], GOUTELARD F.[3], PARNEIX J-C.[4], GIMMI TH., MAES N.[5] (2012)
Diffusion-driven transport in clayrock formations. Appl. Geochem. 27(2), 463–478
doi: 10.1016/j.apgeochem.2011.09.015
[1] Andra, Châtenay-Malabry Cedex, France
[2] BRGM, Orléans, France
[3] CEA Saclay, Gif-sur-Yvette, France
[4] ERM, Poitiers, France
[5] SCK•CEN, Mol, Belgium

CHURAKOV S.V., DÄHN R. (2012)
Zinc adsorption on clays inferred from atomistic simulations and EXAFS spectroscopy. Environ. Sci Technol. 46, 5713-5719
doi: 10.1021/es204423k

CURTI E., AIMOZ L., KITAMURA A. (2012)
Selenium uptake onto natural pyrite. J. Radioanal. Nucl. Chem.
doi: 10.1007/s10967-012-1966-9

DEGUELDRE C., BENEDICTO A.[1] (2012)
Colloid generation during water flow transients. Appl. Geochem. 27, 1220-1225
[1] CIEMAT, Madrid, Spain

DILNESA, B.Z.[1], LOTHENBACH B.[1], RENAUDIN G.[2], WICHSER A.[1], WIELAND E. (2012)
Stability of monosulfate in the presence of iron. J. Amer. Ceram. Soc. 95, 3305-3316
[1] Empa, Dübendorf, Switzerland
[2] Université d'Auvergne Clermont-FD, Clermont-Ferrand, France

GAONA X., TITS J., DARDENNE K.[1], LIU X.[1], ROTHE J.[1], DENECKE M.A.[1], WIELAND E., ALTMAIER M.[1] (2012)
Spectroscopic investigations of Np(V/VI) redox speciation in hyperalkaline TMA–(OH,Cl) solutions. Radiochim. Acta 100, 759-770
[1] KIT-INE, Karlsruhe, Germany

GAONA X., KULIK D. A., MACÉ N.[1], WIELAND E. (2012)
Aqueous-solid solution thermodynamic model of U(VI) uptake in C-S-H phases. Appl. Geochem. 27, 81-95
[1] CEA Saclay, Gif-sur-Yvette, France

GORSKI C.A.[1], AESCHBACHER M.[2], SOLTERMANN D., VOEGELIN A.[1,2], BAEYENS B., MARQUES FERNANDES M., HOFSTETTER T.B.[1,2], SANDER M.[2] (2012)
Redox properties of structural Fe in clay minerals: 1. Electrochemical quantification of electron-donating and -accepting capacities of smectites. Environ. Sci. Technol. 46, 9360-9368
[1] Eawag, Dübendorf, Switzerland
[2] ETH, Zürich, Switzerland

HAYEK M., KOSAKOWSKI G., JAKOB A., CHURAKOV S.V. (2012)
A class of analytical solutions for multidimensional multicomponent diffusive transport coupled with precipitation-dissolution reactions and porosity changes. Water Res. Research 48, W03525

KOLDITZ O.[1,2], BAUER S.[3], BILKE L.[1], BÖTTCHER N.[2], DELFS J. O.[1], FISCHER T.[1], GÖRKE U.J.[1], KALBACHER T.[1], KOSAKOWSKI G., MCDERMOTT C. I.[4], PARK C. H.[6], RADU F.[1,8], RINK K.[1], SHAO H.[5], SHAO H.B.[1], SUN F.[1,2], SUN Y.[1,2] , SINGH A. K.[1], TARON J.[1], WALTHER M.[2], WANG W.[1], WATANABE N.[1,2], WU Y.[1,9], XIE M.[7], XU W.[5], ZEHNER B.[1] (2012)
OpenGeoSys: an open-source initiative for numerical simulation of thermo-hydro-mechanical/chemical (THM/C) processes in porous media. Environ. Earth Sci. 67(2), 589-599
[1] Helmholtz Centre for Environmental Research UFZ, Germany
[2] Technische Universität Dresden, Germany, [3] University of Kiel, Germany, [4] University of Edinburgh, UK, [5] BGR, Germany, [6] KIGAM, Korea, [7] GRS, Germany, [8] University of Erlangen, Germany, [9] Ocean University of China

LOTHENBACH B.[1], LE SAOUT G.[1], BEN HAHA M.[1], FIGI R.[1], WIELAND E. (2012)
Hydration of low-alkali CEM III/B-SiO_2 cement (LAC). Cem. Concr. Res. 42, 410-423
[1] Empa, Dübendorf, Switzerland

MARQUES FERNANDES M., BAEYENS B., DÄHN R., SCHEINOST A.C.[1], BRADBURY M.H. (2012)
U(VI) sorption on montmorillonite in the absence and presence of carbonate: A macroscopic and microscopic study. Geochim. Cosmochim. Acta 93, 262-277
[1] Helmholtz Zentrum Dresden-Rossendorf, Dresden, Germany

ORLOV A., KULIK D.A., DEGUELDRE C., OLIVER L. (2012)
Thermodynamic modelling of the processes in a boiling water reactor to buildup the magnetic corrosion product deposits. Corr. Sci. 64, 28-36
doi: http://dx.doi.org/10.1016/j.corsci.2012.06.022

THIEN B., GODON N.[1], BALLESTERO A.[1,2], GIN S.[1], AYRAL A.[2] (2012)
The dual effect of Mg on the long-term alteration rate of AVM nuclear waste glasses. J. Nucl. Mat. 427, 297-310
[1] CEA Marcoule, Bagnols sur Cèze, France
[2] Université de Montpellier II et IEM, Montpellier, France

WABER H.N.[1], GIMMI TH., SMELLIE J.A.T.[2] (2012)
Reconstruction of palaeoinfiltration during the Holocene using porewater data (Laxemar, Sweden). Geochim. Cosmochim. Acta 94, 109-127
[1] University of Bern, Switzerland
[2] Conterra AB, Stockholm, Sweden

WITHAM F.[1], BLUNDY J.D.[1], KOHN S.C.[1], LESNE P.[1], DIXON J.E.[2], CHURAKOV S.V., BOTCHARNIKOV R.[3] (2012)
SolEx: A model for mixed COHSCl-fluid solubilities and exsolved gas compositions in basalt. Comput. Geosci., 45, 87-97
[1] University of Bristol, Bristol, UK
[2] University of South Florida, St. Petersburg, USA
[3] Universität Hannover, Hannover, Germany

WANG H.A.O., GROLIMUND D., VAN LOON L.R., BARMETTLER K.[1], BORCA C.N., AESCHLIMANN B.[1], GÜNTHER D.[1] (2012).
High spatial resolution quantitative imaging by cross-calibration using laser ablation inductively coupled plasma mass spectrometry and synchrotron micro-X-ray fluorescence technique. Chimica 66, 223-228
[1] ETH, Zürich, Switzerland

8.2 Publications in books

MARQUES FERNANDES M., BAEYENS B., BEAUCAIRE C.[1] (2012)
Chapter 8: Radionuclide retention at mineral-water interfaces in the natural environment. In: Radionuclide behaviour in the natural environment: Science, implications and lessons for the nuclear industry. (Eds. Poinssot C. & Geckeis H.) Woodhead Publishing Limited, 261-301
[1] CEA Saclay, Gif-sur-Yvette, France

VAN LOON L.R., GLAUS M.A., FERRY C.[1], LATRILLE C.[1] (2012)
Chapter 12: Studying radionuclide migration on different scales: the complementary roles of laboratory and in situ experiments. In: Radionuclide behaviour in the natural environment: Science, implications and lessons for the nuclear industry. (Eds. Poinssot C. & Geckeis H.) Woodhead Publishing Limited, 446 – 482
[1] CEA Saclay, Gif-sur-Yvette, France

8.3 Conference proceedings

CHURAKOV S.V. (2012)
Crystal chemistry of C-S-H phases from atomistic simulations. In: GDCh-Monographie Band 45, Eds. Winnefeld, F., Deschner, F. GDCh-Fachgruppe Bauchemie 2012, 74-85
ISBN- 978-3-936028-72-0

8.4 Conference/workshops presentation

BERNER U., KOSAKOWSKI G., KULIK D.A.
An adaptable thermodynamic model for clay materials. 5th International Meeting on "Clays in Natural and Engineered Barriers for Radioactive Waste Confinement", 22–25 October 2012, Montpellier, France

BESTEL M., JURÁNYI F., VAN LOON L.R., GLAUS M.A., GIMMI TH., DIAMOND L.W.[1]
Water diffusion in Na-montmorillonite as a function of water/clay ratio. 10th International Conference on Quasielastic Neutron Scattering (QENS 2012), 30 September – 4 October 2012, Nikko, Japan
[1] University of Bern, Switzerland

BRADBURY M.H., BAEYENS B., MARQUES FERNANDES M.
Estimates of the influence of competition on the sorption values in the SDB of MX-80 Bentonite. 5th International Meeting on "Clays in Natural and Engineered Barriers for Radioactive Waste Confinement", 22-25 October 2012, Montpellier, France

CARMELIET J.[1,2], DEROME D.[2], DERLUYN D.[2], GUYER R.[3], CHURAKOV S.V.
Sorption and crystallisation induced deformation: from molecular dynamics to macroscopic modeling. Cryspom III, 4-7 September 2012, Tróia, Portugal
[1] ETH, Zürich, Switzerland
[2] Empa, Dübendorf, Switzerland
[3] LANL/University of Nevada, USA

CURTI E., LEUPIN O.X.[1]
Release of uranium from nuclear waste: dissolution kinetics, chemical constraints and diffusive transport. International Workshop on Uranium Biogeochemistry: Transformations and Applications, 11-16 March 2012, Monte Verità, Ascona, Switzerland
[2] Nagra, Wettingen, Switzerland

DÄHN R., OSÁN J.[1], BREITNER D.[1], SAJÓ I.[1], MARQUES FERNANDES M., BAEYENS B., TÖRÖK S.[1]
X-ray microspectroscopic investigations of Ni(II) uptake by argillaceous rocks of the Boda Claystone Formation in Hungary. Goldschmidt 2012 Conference, 24-29 June 2012, Montreal, Canada
[1] Centre for Energy Research, Budapest, Hungary

DÄHN R., BAEYENS B., BRADBURY M.H.
P-EXAFS investigations of Zn uptake by montmorillonite. The strong and weak sites concept in the 2SPNE SC/CE sorption model. 5th International Meeting on "Clays in Natural and Engineered Barriers for Radioactive Waste Confinement", 22–25 October 2012, Montpellier, France

FRASCA B.[1], GROLIMUND D., VAN LOON L.R., LEUPIN O.X.[2], WANG H.A.O., SAVOYE S.[3], MICHELOT J.-L.[1]
Fate of selenium: a microspectroscopic study of an oxyanion migration through Opalinus Clay and Toarcian argillite. 5th International Meeting on "Clays in Natural and Engineered Barriers for Radioactive Waste Confinement", 22-25 October 2012, Montpellier, France
[1] UMR "IDES" CNRS–Université de Paris-Sud, Orsay, France
[2] Nagra, Wettingen, Switzerland
[3] CEA Saclay, Gif-sur-Yvette, France

GIMMI TH., JAKOB A.
Assessing conceptual errors and parameter errors of a transport model used for analysing a field diffusion experiment. EGU 2012, General Assembly, 22-27 April, 2012, Vienna, Austria. Geophysical Research Abstracts, Vol. 14, EGU2012-9340

GLAUS M.A., VAN LOON L.R.
Diffusive behaviour of charged metal ion complexes in compacted montmorillonite. 5th International Meeting on "Clays in Natural and Engineered Barriers for Radioactive Waste Confinement", 22–25 October 2012, Montpellier, France

GLAUS M.A., JAKOB A., VAN LOON L.R.
How to measure effective diffusion coefficients of strongly sorbing radiotracers? 5th International Meeting on "Clays in Natural and Engineered Barriers for Radioactive Waste Confinement", 22–25 October 2012, Montpellier, France

HAYEK M., KOSAKOWSKI G., JAKOB A., CHURAKOV S.V.
Benchmarking of numerical codes against analytical solutions for multidimensional multicomponent diffusive transport coupled with precipitation-dissolution reactions and porosity changes. EGU 2012, General Assembly, 22-27 April, 2012, Vienna, Austria. Geophysical Research Abstracts, Vol. 14, EGU2012-2650

HINGERL F.F., WAGNER T. [1], KULIK D.A., KOSAKOWSKI G., DRIESNER T.[1]
Development of a new activity model for complex mixed-salt solutions from ambient to geothermal conditions. EGU 2012, General Assembly, 22-27 April, 2012, Vienna, Austria. Geophysical Research Abstracts, Vol. 14, EGU2012-5332
[1] ETH, Zürich, Switzerland

JOSEPH C.[1], VAN LOON L.R., JAKOB A., STEUDTNER R.[1], SCHMEIDE K.[1], SACHS S.[1], BERHARD G.[1]
Do elevated temperatures and organic matter influence the U(VI) diffusion through argillaceous rocks? 5th International Meeting on "Clays in Natural and Engineered Barriers for Radioactive Waste Confinement", 22–25 October 2012, Montpellier, France
[1] Helmholtz-Zentrum Dresden-Rossendorf, Dresden, Germany

KOSAKOWSKI G., BERNER U.
Reactive transport calculations on the geochemical near-field evolution of a SF/HLW repository. 5th International Meeting on "Clays in Natural and Engineered Barriers for Radioactive Waste Confinement", 22–25 October 2012, Montpellier, France

KOSAKOWSKI G[1]., KULIK D.A., SHAO H.[1]
OpenGeoSys-GEMS: Hybrid parallelization of a reactive transport code with MPI and threads. EGU 2012, General Assembly, 22-27 April, 2012, Vienna, Austria. Geophysical Research Abstracts, Vol. 14, EGU2012-2642
[1] Helmholtz Centre for Environmental Research UFZ, Germany

KULIK D.A., THIEN B., CURTI E.
Partial-equilibrium concepts to model trace element uptake. Goldschmidt 2012 Conference, 24-29 June 2012, Montreal, Canada

LOTHENBACH B.[1], DILNESA B.Z.[1,2], WIELAND E.
Fate of iron during the hydration of cements. Ibausil 2012, 12-15 September 2012, Weimar, Germany
[1] Empa, Dübendorf, Switzerland
[2] EPFL, Lausanne, Switzerland

MARQUES FERNANDES M., BAEYENS B., DÄHN R., SCHEINOST A.C.[1], BRADBURY M.H.
U(VI) sorption on montmorillonite: A macroscopic and microscopic study. "Uranium Biogeochemistry: Transformations and Applications". International Workshop, 11-16 March, 2012, Monte Verita, Ascona, Switzerland
[1] Helmholtz Zentrum Dresden-Rossendorf, Dresden, Germany

MARQUES FERNANDES M., BAEYENS B., DÄHN R., STUMPF T.[1], BRADBURY M.H.
Sorption of lanthanides and trivalent actinides on montmorillonite in the presence and absence of carbonate. Goldschmidt 2012 Conference, 23-29 June, 2012, Montreal, Canada
[1] KIT-INE, Karlsruhe, Germany

MARQUES FERNANDES M., VER N.[1], BAEYENS B.
Application of the "bottom up" approach for the predictive modelling of sorption isotherms on Hungarian Boda Clay. 5th International Meeting on "Clays in Natural and Engineered Barriers for Radioactive Waste Confinement", 22–25 October 2012, Montpellier, France
[1] Centre for Energy Research, Budapest, Hungary

MIBUS J.[1], BAEYENS B., MARQUES FERNANDES M., TRABER D.[1] (2012)
Derivation of sorption parameters for argillaceous host rocks in Switzerland. 5th International Meeting on "Clays in Natural and Engineered Barriers for Radioactive Waste Confinement", 22–25 October 2012, Montpellier, France
[1] Nagra, Wettingen, Switzerland

SCHAUB PH., WEBER TH.[1], STEURER W.[1]
Unravelling the local ~8 Å structure of Al–Cu–Co quasicrystals by the use of three-dimensional pair distribution function analysis. Jahrestagung der Deutschen Gesellschaft für Kristallographie (DGK), 12-15 March 2012, Munich, Germany
[1] ETH, Zürich, Switzerland

SCHAUB PH., WIELAND E., DÄHN R., LEEMANN A.[1]
X-ray micro-diffraction analysis of heterogenous concrete samples. Jahrestagung der Deutschen Gesellschaft für Kristallographie (DGK), 12-15 March 2012, Munich, Germany
[1] Empa, Dübendorf, Switzerland

SCHAUB PH., WIELAND E., DÄHN R., LEEMANN A.[1], ARAKCHEEVA A.[2], GROLIMUND D.
In-situ X-ray micro-diffraction analysis of reaction products in heterogeneous concrete samples. European Mineralogical Conference EMC2012, 2-6 September 2012, Frankfurt/M, Germany
[1] Empa, Dübendorf, Switzerland
[2] Phase Solutions Ltd., Lausanne, Switzerland

SHAO H.[1] , KOSAKOWSKI G., BERNER U., KULIK D.A., MÄDER U.[2], KOLDITZ O.[1]
Is the clogging process in Maqarin natural analogue controlled by accessory clay minerals? A reactive transport study with new data. EGU 2012, General Assembly, 22–27 April 2012, Vienna, Austria, Geophysical Research Abstracts, Vol. 14, EGU2012-1760-1
[1] Helmholtz Centre for Environmental Research UFZ, Germany
[2] University of Bern, Switzerland

SOLTERMANN D., MARQUES FERNANDES M., DÄHN R., BAEYENS B., BRADBURY M.H.
Investigations of Fe(II) sorption onto montmorillonite. A wet chemistry and XAS study**.** Goldschmidt 2012 Conference, 23-29 June, 2012, Montreal, Canada

SOLTERMANN D., MARQUES FERNANDES M., DÄHN R., BAEYENS B., BRENDLÉ J.[1], BRADBURY M.H.
Investigations of Fe(II) sorption onto montmorillonite**.** A wet chemistry and XAS study**.** 5th International Meeting on "Clays in Natural and Engineered Barriers for Radioactive Waste Confinement", 22–25 October 2012, Montpellier, France
[1] Université de Haute Alsace, Mulhouse, France

THIEN B., GODON N.[1], AYRAL A.[2]
The double effect of Mg on the long-term alteration rate of a nuclear waste glass. Delta-Min "Fluid-Mineral Interaction: Mechanisms of Mineral Replacement Reactions, 29 February-2 March 2012, Oviedo, Spain
[1] CEA Marcoule, Bagnols sur Cèze, France
[2] Université de Montpellier II et IEM, Montpellier, France

THIEN B., KULIK D.A., CURTI E.
Adding uptake kinetics and surface entrapment to geochemical models. Goldschmidt 2012 Conference, 24-29 June 2012, Montreal, Canada

THIEN B., KULIK D.A., CURTI, E.
Kinetics of trace element retention in minerals: Comparison of modelling approaches. Delta-Min Meeting on "Fluid-Mineral Interaction: Mechanisms of Mineral Replacement Reactions". 29 February-2 March 2012, Oviedo, Spain

TITS J., MACÉ N.[1], STUMPF T.[2], WALTHER C.[2], WIELAND E.
Immobilisation of hexavalent actinides in cementitious materials: Evidence for structural incorporation in calcium silicate hydrates. Goldschmidt 2012 Conference, 24-29 June 2012, Montreal, Canada
[1] CEA Saclay, Gif-sur-Yvette, France
[2] KIT-INE, Karlsruhe, Germany

TITS J., STUMPF T.[1], WALTHER C.[1], WIELAND E.
Investigation of the uranium(VI) speciation in cementitious environments by direct laser excitation. International Workshop on "Advanced Techniques in Actinide Spectroscopy (ATAS)", Helmholtz Zentrum Dresden, 5-7 November 2012, Rossendorf, Germany
[1] KIT-INE, Karlsruhe, Germany

TYAGI M., GIMMI TH., CHURAKOV S.V.
Modelling clay microstructures and up-scaling of effective diffusion coefficients. 5th International Meeting on "Clays in Natural and Engineered Barriers for Radioactive Waste Confinement", 22–25 October 2012, Montpellier, France

VAN LOON L.R.
On the use of an extended Archie's relation for estimating effective diffusion coefficients in low permeability rocks. 5th International Meeting on "Clays in Natural and Engineered Barriers for Radioactive Waste Confinement", 22–25 October 2012, Montpellier, France

WANG H.A.O., GROLIMUND D., BORCA C.N., SHAW-STEWART J., KARVINEN P., GÜNTHER D.[1]
High spatial resolution chemical imaging by laser ablation inductively coupled plasma mass spectrometry (LA-ICPMS) using a novel fast washout ablation cell: A comparison with synchrotron micro/nano X-ray fluorescence (SR-micro/nanoXRF). 11th European Workshop on Laser Ablation, 19–22 June 2012, Gijón, Spain
[1] ETH, Zürich, Switzerland

WANG H.A.O., GROLIMUND D., VAN LOON L.R., BORCA C.N., SHAW-STEWART J., KARVINEN P., GÜNTHER D.[1]
High spatial resolution quantitative studies by complementary techniques. SLS Symposium, 3 July 2012, PSI, Villigen, Switzerland
[1] ETH, Zürich, Switzerland

WANG H.A.O., GROLIMUND D., BORCA C.N., SHAW-STEWART J., GÜNTHER, D.[1]
A novel laser ablation cell for laser ablation inductively coupled plasma mass spectrometry (LA-ICPMS). Swiss Chemical Society (SCS) Fall Meeting, 13 September 2012, Zurich, Switzerland
[1] ETH, Zürich, Switzerland

WIELAND E., DÄHN R., GAONA X.[1], TITS J.
Immobilization of actinides in the cementitious near-field of a repository for radioactive waste. EMRS 2012 Spring Meeting, 13-18 May 2012, Strassburg, France
[1] KIT-INE, Karlsruhe, Germany

8.5 Invited talks

CHURAKOV S.V.
Crystal chemistry of C-S-H phases from atomistic simulations. (Keynote lecture) GDCh-Tagung Bauchemie, 11-12 October 2012, Empa, Dübendorf, Switzerland

CHURAKOV S.V., DÄHN R.
Zn adsorption on clays inferred atomistic simulations and EXAFS spectroscopy. 5th International Meeting on "Clays in Natural and Engineered Barriers for Radioactive Waste Confinement", 22–25 October 2012, Montpellier, France

CURTI E.
Application of radiotracers to quantify mineral recrystallization kinetics. Delta-Min Meeting on "Fluid-Mineral Interaction: Mechanisms of Mineral Replacement Reactions". 29 February-2 March 2012, Oviedo, Spain

DÄHN R.
Validation of sorption models for clay minerals using a combined EXAFS and molecular modeling approach. Glenn T. Seaborg Center, Lawrence Berkeley National Laboratory, 12 July 2012, Berkeley, USA

8.6 Others/teachings

DÄHN R.
The use of X-ray absorption spectroscopy from the bulk- to the nano-scale to study radioactive waste repository materials. School on Synchrotron Radiation Methods and their Applications in Earth Science 2012, 24-26 September 2012, Mátrafüred, Hungary

GIMMI TH.
Lecture and examinations "Fluids in the Crust", Master Course in Environmental and Resource Geochemistry, University of Bern, Fall Semester 2012

HOLLÄNDER H., ALT-EPPING P., SOLER J.M., TARON J., KOSAKOWSKI G.
ERE5.3/GMPV6.7/HS8.2.8/SSS5.22 Coupled Physical and Chemical Transformations Affecting the Performance of GeoSystems. EGU 2012, General Assembly, 22-27 April, 2012, Vienna, Austria

KOSAKOWSKI G.
Statistics in Earth Sciences. University of Tübingen, Germany, Summer Semester 2012

PFINGSTEN W.
Modelling of Processes in Soils and Aquifers: 701-1334-00L, Department for Environmental Sciences, ETH, Zurich, Spring Semester 2012

PRASSER H.-M., GÜNTHER-LEOPOLD I., HIRSCHBERG S., HUMMEL W., WILLIAMS T., ZUIDEMA P. K.
Nuclear Energy Systems. Lecture course with exercises, ETH Zurich, Spring Semester 2012

WIELAND E.
A synchrotron-based approach to study cementitious materials, immobilization processes of radioactive materials and interfaces in cement-clay systems using micro-XRF/XAS/XRD techniques. School on Synchrotron Radiation Methods and their Applications in Earth Science 2012, 24-26 September 2012, Mátrafüred, Hungary

Paul Scherrer Institut, 5232 Villigen PSI, Switzerland
Tel. +41 56 310 21 11, Fax +41 56 310 21 99
www.psi.ch